INVESTIGATING THE EFFECTS AND MECHANISMS OF HMG-CoA REDUCTASE INHIBITOR SIMVASTATIN ON THE HUMAN MYOMETRIUM

Vincent Wai Shun Pang

Thesis submitted to the University of Nottingham for the degree of Doctor of Philosophy
October 2016

Table of Contents

DECLARATION **1**

ACKNOWLEDGEMENTS **2**

PROJECT-RELATED ABSTRACTS **3**

1 INTRODUCTION **9**

1.1 Anatomy of the human uterus 9
1.2 Myometrial contractility 11
1.3 Control of intracellular Ca^{2+} 14
1.4 Voltage-operated Ca^{2+} channels 14
1.5 Receptor-operated and store-operated Ca^{2+} channels 15
1.6 K^+ channels 19
1.7 Ca^{2+}-operated K^+ channels 19
1.8 Voltage-operated K^+ channels 21
1.9 ATP-sensitive K^+ channels 21
1.10 Other ion channels 22
1.11 Contractility dysfunctions in the uterus 23
1.12 The role of cholesterol in myometrial contractility 25
1.13 The myometrial cell membrane 26
1.14 Cholesterol-lowering drugs 30
1.15 Statins and smooth muscle physiology 34
1.16 Statin pleiotropic properties 35
1.17 Maternal weight, age, and statins during pregnancy 36
1.18 Statins as a therapeutic agent in pregnancy complications 39
1.19 Aims and hypothesis 40

2 MATERIALS AND METHODS **43**

2.1 Materials 44
2.2 Informed patient consent 44
2.3 Patient demographics 46
2.4 Myometrial cell culture 47
2.4.1 Myometrial cell passage 48
2.5 Myometrial tissue contractility 49
2.5.1 Contractility transducer calibration 50
2.5.2 Myometrial tissue length tension optimisation 51
2.5.3 Assessment of myometrial tissue viability 52
2.5.4 Myometrial tissue contractility experimental conditions 54
2.6 Total cholesterol and protein assay 60
2.6.1 Amplex red® cholesterol assay protocol 61
2.6.2 BCA protein assay protocol 62
2.7 Intracellular FLUO-4AM® Ca^{2+} assay 64
2.7.1 Intracellular FLUO-4AM® Ca^{2+} assay protocol 64
2.8 FLIPR® Ca^{2+} 5 assay 66
2.8.1 FLIPR® Ca^{2+} 5 assay protocol 66
2.9 Hoechst 33342 dye tracer permeability assay 68
2.9.1 Hoechst 33342 dye tracer permeability assay protocol 68
2.10 Immunocytochemistry 70
2.10.1 α-actin and caveolin-1 protein expression by immunocytochemistry protocol 72
2.10.2 Cell fixation and non-specific blocking 72
2.10.3 Primary antibody incubation 73
2.10.4 Secondary antibody 74
2.10.5 Slide preparation for immunofluorescence imaging 75

2.11 STUDY EXPERIMENTAL DATA ANALYSIS 76
2.11.1 Analysis of tissue contractility data 76
2.11.2 Analysis of cholesterol and protein assay data 77
2.11.3 Analysis of FLOU-4AM® and FLIPR® Ca^{2+} assay data 78
2.11.4 Analysis of Hoechst 33342 tracer dye permeability data 78
2.11.5 Immunofluorescence image analysis 79

3 RESULTS AND ANALYSIS 81
3.1 DETERMINE THE CUMULATIVE EFFECTS OF SIMVASTATIN ON SPONTANEOUS MYOMETRIAL CONTRACTIONS. 81
3.1.1 Aims 81
3.1.2 Simvastatin reduced spontaneous contractions in myometrial tissues obtained from pregnant women 82
3.1.3 Simvastatin reduced spontaneous contractions in myometrial tissues obtained from non-pregnant women 84
3.1.4 Simvastatin-induced reduction of spontaneous contractions is more potent in myometrial tissues obtained from non-pregnant women 86
3.1.5 DISCUSSION 88
3.1.6 Critique and further work 89
3.2 DETERMINE THE EFFECTS OF SIMVASTATIN ON CHOLESTEROL CONCENTRATION IN THE MYOMETRIAL CELL, AND THE ROLE OF CHOLESTEROL MODULATION ON SPONTANEOUS MYOMETRIAL CONTRACTIONS 91
3.2.1 Aims 91
3.2.2 MCD increases spontaneous myometrial contraction amplitude 92
3.2.3 Simvastatin-induced reduction of spontaneous myometrial contractions does not involve cholesterol depletion 94
3.2.4 MCD co-incubation inhibits simvastatin-induced effects on spontaneous myometrial contractions 96
3.2.5 The addition of water-soluble cholesterol did not reverse simvastatin-induced reduction of spontaneous myometrial contractions 98
3.2.7 DISCUSSION 102
3.2.8 Critique and further work 103
3.3 DETERMINE THE EFFECTS OF NO INHIBITION ON SIMVASTATIN-INDUCED EFFECTS ON SPONTANEOUS MYOMETRIAL CONTRACTIONS 105
3.3.1 Aims 105
3.3.2 L-NAME-induced inhibition of eNOS partially inhibited simvastatin-induced effects on spontaneous myometrial contractions 106
3.4 DETERMINE THE PRESENCE OR ABSENCE OF THE HMG-COA REDUCTASE PATHWAY IN THE MYOMETRIUM 108
3.4.1 Aims 108
3.4.2 The addition of mevalonate or GGPP did not reverse simvastatin-induced reduction of spontaneous myometrial contractions 109
3.4.3 DISCUSSION 112
3.4.4 Critique and further work 115
3.5 DETERMINE THE EFFECTS OF SIMVASTATIN ON CA^{2+} AND K^+ ION CHANNEL ACTIVITY DURING SPONTANEOUS MYOMETRIAL CONTRACTILITY 118
3.5.1 Aims 118
3.5.4 BK channel inhibition via paxilline partially inhibits simvastatin-induced reduction of spontaneous myometrial contractions 123
3.5.5 Inhibition of SK and BK channels combined enhanced the inhibition of simvastatin-induced effects on spontaneous myometrial contractions 125
3.5.6 BayK 8644-induced VOCC activation partially inhibited simvastatin-induced reduction of spontaneous myometrial contractions 127
3.5.7 DISCUSSION 129

3.5.8 Critique and further work ... *131*
3.6 DETERMINE THE EFFECTS OF SIMVASTATIN ON BASAL AND OXYTOCIN-INDUCED $[Ca^{2+}]_i$ RELEASE IN MYOMETRIAL CELLS ... 133
3.6.1 Aims ... *133*
3.6.3 Simvastatin exposure did not alter $[Ca^{2+}]i$ in myometrial cells using the FLUO-4AM® Ca^{2+} assay ... *136*
3.6.4 Simvastatin exposure partially inhibited oxytocin-induced increase in $[Ca^{2+}]i$ in myometrial cells using the FLUO-4AM® Ca^{2+} assay ... *138*
3.6.5 Oxytocin increases $[Ca^{2+}]i$ in myometrial cells using the FLIPR® Ca^{2+} 5 assay *140*
3.6.6 MYOMETRIAL CELLS PRE-INCUBATED WITH SIMVASTATIN FOR 18-HOURS INHIBITED OXYTOCIN-INDUCED INCREASE IN $[Ca^{2+}]_i$ USING THE FLIPR® Ca^{2+} 5 ASSAY 142
3.6.7 Discussion ... *144*
3.6.8 Critique and further work ... *146*
3.7 DETERMINE THE EFFECTS OF SIMVASTATIN ON HOECHST 33342 DYE TRACER PERMEABILITY IN MYOMETRIAL CELLS ... 149
3.7.1 Aims ... *149*
3.7.2 Myometrial cells are permeable to the Hoechst 33342 dye tracer ... *150*
3.7.3 Simvastatin increased detected fluorescence in the absence of Hoechst 33342 dye tracer in myometrial cells ... *152*
3.7.4 Simvastatin exposure did not alter myometrial cell permeability to Hoechst 33342 dye tracer ... *154*
3.7.5 Discussion ... *156*
3.7.6 Critique and further work ... *157*
3.8 DETERMINE THE EFFECTS OF SIMVASTATIN ON THE EXPRESSION OF CAVEOLAE CHOLESTEROL BINDING PROTEIN CAVEOLIN-1 IN THE MYOMETRIAL CELL ... 158
3.8.1 Aims ... *158*
3.8.2 Identification of myometrial cells in culture ... *159*
3.8.3 Caveolin-1 is expressed in myometrial cells ... *160*
3.8.4 Simvastatin exposure did not alter α-actin expression in myometrial cells *161*
3.8.5 Simvastatin and MCD exposure disrupted caveolin-1 expression in myometrial cells over time ... *162*
3.8.6 Discussion ... *169*
3.8.7 Critique and further work ... *172*
4 CONCLUSIONS ... 174
5 APPENDIX ... 180
5.1 EXPERIMENTAL FORMULATIONS ... 180
5.2 EXAMPLE OF PATIENT STUDY CONSENT FORMS AND INFORMATION SHEET ... 182
6 BIBLIOGRAPHY ... 188

Declaration

I declare that this thesis is the result of my own work based on research that was undertaken at either the Academic Division of Obstetrics and Gynaecololgy, Graduate Entry Medical School, Royal Derby Hospital, the School of Veterinary Medicine and Science, Sutton Bonington, and the Queens Medical Centre, during the period of November 2009 to April 2015.



Vincent Wai Shun Pang

October 2016

Acknowledgements

Many thanks to my supervisors Dr. Raheela Khan and Dr. Cyril Rauch for their guidance and support. Both of you have been extremely patient with me during my research training. Thank you to my research colleagues at both the Sutton Bonington and QMC sites, and a special thank you to Mrs. Averil Warren for all the technical support and lab training. Furthermore, this work would not be possible without the support of the labour ward staff at the Royal Derby Hospital and the participation of the patients who gave their valuable time for this project.

I would like to thank my family who never gave up on me. Thank you **母親, 父親**, **弟弟 和 妹妹**. I would also like to thank my partner Ms. Katie Marshall, who encouraged and motivated me throughout my PhD.

This study was funded by the School of Graduate Entry Medicine and Health, University of Nottingham.

Project-related abstracts

1. V. Pang, C. Rauch, R. Khan (July 2012) **The potential therapeutic role and mechanisms of simvastatin on myometrial contractility: Simvastatin relaxes myometrial contractility independently of cholesterol inhibition** *Society for Reproduction & Fertility 2012, Edinburgh (Oral presentation).*

2. V. Pang, C. Rauch, R. Khan (April 2010) **The expression of lipid-raft markers in cultured human myometrial cells** *European Congress on Environmental Health 2010, University of Rennes, France (Poster presentation).*

3. V. Pang, C. Rauch, R. Khan (December 2011) **The effects of simvastatin on myometrial contractility and myocyte lipid-raft markers** *Royal College of Obstetricians & Gynaecologists meeting 2011, RCOG, London (Poster presentation).*

4. V. Pang, C. Rauch, R. Khan (July 2012) **The potential therapeutic role and mechanisms of simvastatin on myometrial contractility** *Physiological Society Main Meeting 2012, Edinburgh (Poster presentation).*

5. V. Pang, C. Rauch, R. Khan (July 2013) **Simvastatin inhibits human myometrial contractility by mechanisms independent of cholesterol depletion and HMG-CoA reductase inhibition** *Physiological Society IUPS 2013, Birmingham (Poster presentation).*

Abstract

Preterm birth is responsible for 28% of all early neonatal deaths worldwide (Liu et al., 2015). The primary cause of preterm birth is preterm labour, occurring in 40 – 45% of all preterm deliveries (Goldenberg et al., 2008). Current management alleviates symptoms without disease prevention, due largely to incomplete mechanistic understanding. Emerging evidence suggests a role for cholesterol in the regulation of uterine contractility (Taggart et al., 2000; Kendrick et al., 2004; Smith et al., 2005), with evidence that cholesterol-manipulation agents can affect myometrial contractions. Further research into the effects of cholesterol modulation on myometrial contractility may reveal possible new tocolytics in the treatment of preterm labour.

In this study, we determined the effects and mechanisms of simvastatin, a cholesterol-lowering drug, on the human myometrium, using myometrial biopsies obtained from term non-labouring women undergoing scheduled caesarean section delivery. Biopsies were either dissected into individual tissue strips for isometric tension recordings, or disaggregated into myometrial cells and cultured for in-vitro experiments. Myometrial biopsies were also obtained from women undergoing elective hysterectomy for benign conditions but were only prepared for isometric tension recordings. Tissue strips from non-pregnant women were used to determine the effects of simvastatin exposure on spontaneous uterine contractility only.

Firstly, the effects of independent simvastatin exposure on spontaneous myometrial contractility were assessed. This was followed by investigating the effects of cholesterol depletion and addition, using methyl-β-cyclodextrin (MCD) and water-soluble cholesterol respectively. The effects of simvastatin on myometrial cell total cholesterol concentration was also assessed. The effects of nitric oxide (NO) inhibition via Nω-nitro-L-arginine methyl ester (L-NAME), and evidence for the presence of the 3-hydroxy-3-methylglutaryl-coenzyme A (HMG-CoA) reductase pathway, by replenishment with mevalonate and geranyl-geranyl pyrophosphate (GGPP) in the presence of simvastatin were also determined. Evidence of simvastatin-induced ion channel modulation was investigated using broad inhibition of voltage-operated potassium (K^+) and calcium (Ca^{2+})-operated K^+ channels, specific inhibition of small-conductance (SK) and large-conductance (BK) Ca^{2+}-operated K^+ channels, and activation of voltage-operated Ca^{2+} channels (VOCC). In cultured myometrial cells, the effects of simvastatin exposure on intracellular oxytocin-induced Ca^{2+} release, and cell permeability to the Hoechst 33342 dye tracer molecule were investigated. Finally, changes in cholesterol-containing lipid-raft structure caveolae, via its cholesterol-binding protein caveolin-1 expression, in myometrial cells after simvastatin exposure over time was determined.

Simvastatin caused a cumulative reduction of spontaneous myometrial contractions in tissues obtained from pregnant and non-pregnant women. Co-incubation with MCD inhibited simvastatin-mediated effects, but replenishment with water-soluble cholesterol did not. Furthermore, no change in total cholesterol concentration was observed after simvastatin exposure in

myometrial cells over time. L-NAME-induced inhibition of endothelial nitric oxide synthase (eNOS) partially prevented simvastatin-mediated effects, but not replenishment with mevalonate or GGPP. Broad inhibition of voltage-operated K^+ and Ca^{2+}-operated K^+ channels inhibited simvastatin's effects on myometrial contractility. Specific inhibition of SK and BK channels, and activation of VOCCs also appeared to inhibit simvastatin-mediated effects. Furthermore, myometrial cells exposed to simvastatin overnight caused a reduction in oxytocin-induced Ca^{2+} release. However, myometrial cells showed no change in permeability to Hoechst 33342 dye tracer after simvastatin exposure. Finally, a gradual reduction in caveolin-1 expression was observed after simvastatin exposure over time.

Our findings have shown for the first time, that independent exposure to simvastatin results in the cumulative reduction of spontaneous contractions in human myometrial tissue. This effect appears to be cholesterol-independent, involving several different mechanisms not associated with inhibition of cholesterol or the HMG-CoA reductase pathway. However, these effects were observed at concentrations (3.3nM – 330μM) higher than those found in human serum (1 – 15nM) after therapeutic doses (0.1 – 1mg/kg). Additional experiments are therefore required to determine whether these effects are observed at therapeutic concentrations. Furthermore, the complexity of simvastatin's mechanisms requires further investigations before its potential as a possible tocolytic can be assessed.

Keywords: Cholesterol, contractility, myometrium, preterm birth, preterm labour, simvastatin, uterus.

Abbreviations

- 1,2-bis (aminophenoxy)-ethane-tetraacetic acid (BAPTA)
- 3-hydroxy-3-methyl-glutaryl-CoA (HMG-CoA)
- 3,3-dimethylallyl pyrophosphate (DPP)
- 4’,6-diamidino-2-phenylindole (DAPI)
- 5-pyrophosphomevalonate (5-PP mevalonate)
- Acetoxymethyl (AM)
- Adenosine diphosphate (ADP)
- Adenosine triphosphate (ATP)
- Arbitrary units (a.u.)
- Area under the curve (AUC)
- Bicinchoninic acid (BCA)
- Bovine serum albumin (BSA)
- Ca^{2+}-operated K^+ intermediate conductance channel (IK)
- Ca^{2+}-operated K^+ large conductance channel (BK)
- Ca^{2+}-operated K^+ small conductance channel (SK)
- Calcium ion (Ca^{2+})
- Calmodulin (CaM)
- Caesarean delivery (CD)
- Chloride (Cl^-)
- Cyclic GMP (cGMP)
- Cyclohexyl-(2-(3,5-dimethyl-Pyrazol-1-yl)-6-methyl-Pyrimidin-4-yl)-Amine (CyPPA)
- Diacylglycerol (DAG)
- Dimethyl sulfoxide (DMSO)
- Double distilled water (ddH_2O)
- Dulbecco’s Modified Eagle Medium (DMEM)
- Electrical cell-substrate impedance sensing (ECIS)
- Endoplasmic reticulum (ER)
- Endothelial nitric oxide synthase (eNOS)
- Enzyme-linked immunosorbent assay (ELISA)
- Farnesyl pyrophosphate (FPP)
- Fetal calf serum (FCS)
- Fluorescein isothiosyanate (FITC)
- G immunoglobulin (IgG)
- G-protein coupled receptors (GPCRs)
- Geranyl-geranyl pyrophosphate (GGPP)
- Good Clinical Practice (GCP)
- Grams (g)
- Guanosine diphosphate (GDP)
- Guanosine triphosphate (GTP)
- Horse-radish peroxidise (HRP)
- Human umbilical vein endothelial cells (HUVECs)
- Hydrogen peroxide (H_2O_2)
- Industrial methylated spirit (IMS)
- Inositol 1,4,5-triphosphate (IP_3)
- Interquartile range (IQR)

- Isopentenyl pyrophosphate (IPP)
- K^+ salt solution (KPSS)
- L-N^G-monomethyl arginine citrate (L-NMMA)
- L-N^G-nitroarginine (L-NOARG)
- Lipopolysaccharide (LPS)
- Long-lasting Ca^{2+} channel (L-type)
- Low-density lipoproteins (LDLs)
- Magnesium adenosine triphosphatase (Mg-ATPase)
- Methyl-β-cyclodextrin (MCD)
- Millinewtons (mN)
- Mitogen-activated protein kinase (MAPK)
- Myosin light chain (MLC)
- Myosin light chain kinase (MLCK)
- Myosin light chain phosphatase (MLCP)
- NG-nitro L-arginine methyl ester (L-NAME)
- Nitric oxide (NO)
- Nitric oxide synthase (NOS)
- Nitrogen (N_2)
- Paraformaldehyde (PFA)
- Phosphate buffered saline (PBS)
- Phosphatidylinositol 4,5-biphosphate (PIP_2)
- Phospholipase C enzyme (PLC)
- Physiological salt solution (PSS)
- Potassium (K^+)
- Potassium chloride (KCl)
- Preterm premature rupture of the membranes (PPROM)
- Protein kinase A (PKA)
- Protein kinase G (PKG)
- Receptor-operated Ca^{2+} channel (ROCC)
- Rubidium (Rb^+)
- Ras homolog gene A protein (RhoA)
- Revolutions per minute (rpm)
- Sarcoplasmic reticulum (SR)
- Sodium (Na^+)
- SR Ca^{2+}-ATPase (SERCA)
- Standard deviation (SD)
- Standard error of the mean (SEM)
- Tetraethylammonium (TEA)
- Transepithelial/transendothelial electrical resistance (TEER)
- Transient Ca^{2+} channel (T-type)
- Ultra-violet (UV)
- Voltage-operated Ca^{2+} channel (VOCC)

1 Introduction

1.1 Anatomy of the human uterus

The uterus is a muscular organ in the pelvic cavity, located dorsally to the urinary bladder and ventrally to the upper rectum. (Bennet, 1872). The uterus can be divided into four main regions: The fundus, corpus, cervix, and cervical canal (**See Figure 1-1**) (Krantz and Phillips, 1962).

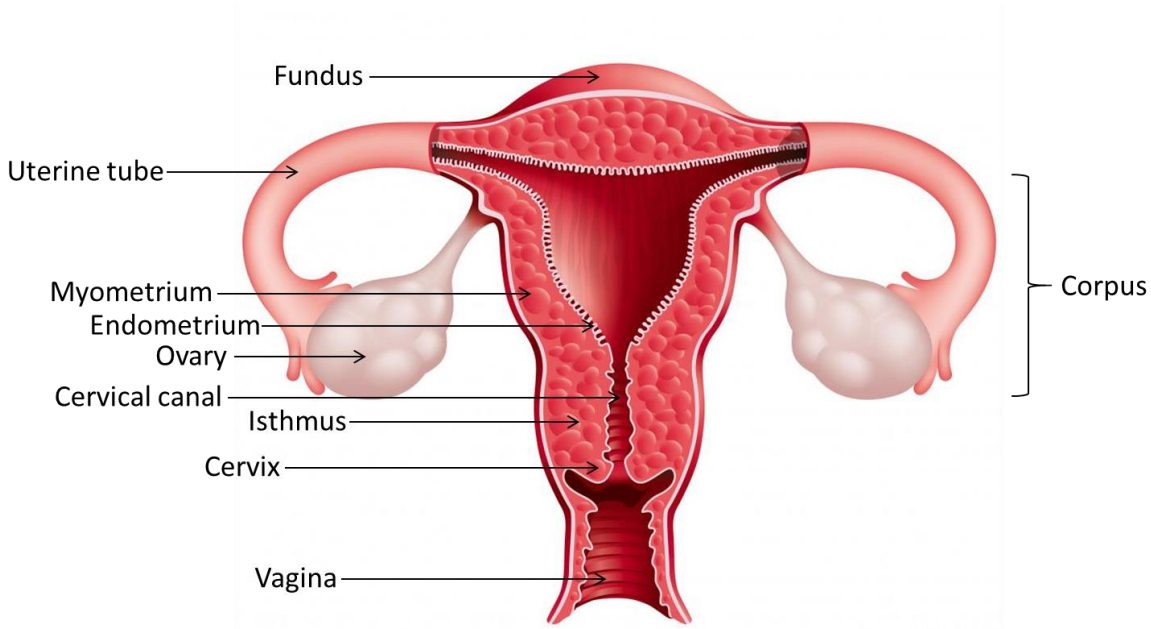


Figure 1-1. Diagram showing a cross-section of the human uterus (*Adapted from http://www.uterus.com/*).

In the uterus, the myometrium forms the middle muscular layer of the uterine wall and consists mainly of uterine smooth muscle cells and fibres. The endometrium forms the innermost layer of the uterus lining, consisting mainly of epithelial cells and connective tissue (Krantz and Phillips, 1962).

During pregnancy, the uterus expands in size increasing from around 50 grams (g) at the start of gestation to 1100g at term (Reynolds, 1946; Reynolds, 1947). This is mainly due to an increase in the myometrial cell proliferation and size, resulting in the formation of dense smooth muscle cell

bundles in the innermost layer of the myometrium surface. These bundles are made up of actin and myosin protein myofilaments, and are responsible for the generation and transmission of force during uterine contractility (Wynn, 2013 p406 – 408). The reminder of these bundles consists of interconnecting proteins made up of microtubules and proteinaceous dense bodies (Uldbjerg et al., 1983a; Uldbjerg et al., 1983b).

During the first and second trimesters, the myometrium is in a state of relative quiescence, exhibiting short and infrequent contractions every twenty to thirty minutes (Kumar et al., 1961; Speert, 1956). During the third trimester, contractions slowly increase in duration and frequency (Braxton-Hicks contractions) until the onset of labour, whereby contractions become extremely forceful and occur every two to three minutes. Contractions continue to increase until the onset of parturition where the myometrium develops sufficient force to expel the fetus through the birth canal. Following parturition, involution of the myometrium causes a reduction in uterus size. This is due to proteolysis of the basal lamina resulting in significant epithelial regression and stromal fibrosis (Casey and MacDonald, 1997; MacKinnon and McIntyre, 2006) The main stages of pregnancy are summarised in Figure 1-2.

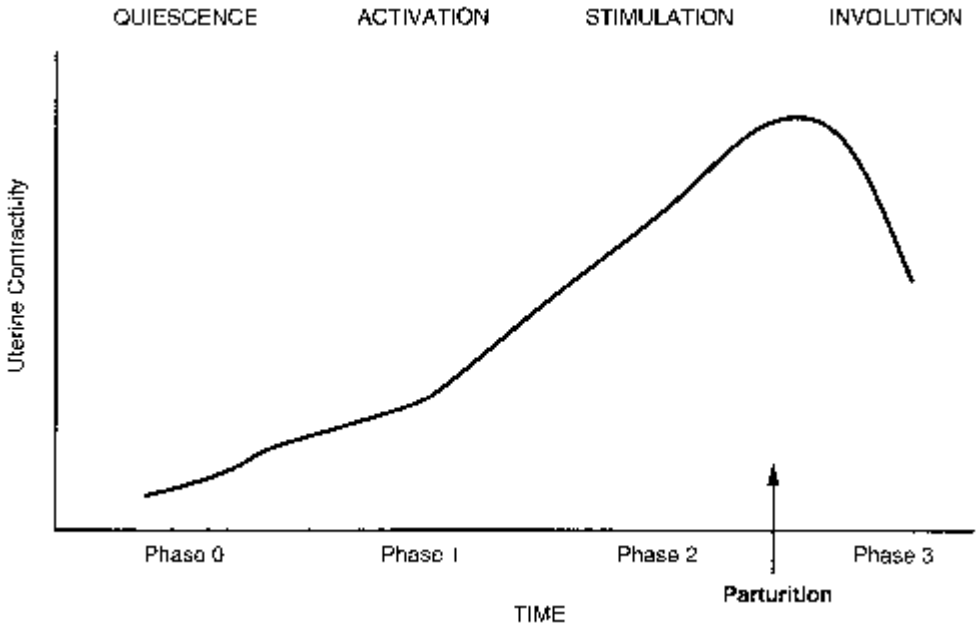


Figure 1-2. Diagram showing the correlation between the magnitude and frequency of uterine contractility, and the stages of pregnancy (Arrow indicating initiation of parturition) *(Adapted from Casey and MacDonald, 1997; Steer, 1990*).

1.2 Myometrial contractility

Myometrial contractility involves several signalling events that conclude with the activation of actin and myosin bundles to generate force. All myometrial contractions are triggered by an increase in the concentration of intracellular calcium ($[Ca^{2+}]i$). The basal $[Ca^{2+}]i$ in a myometrial cell is significantly lower (<158nM) than the threshold concentration required to initiate a contraction (158 – 177nM) (Amedee et al., 1987; Andersson, 1982; Kao and McCullough, 1975; Kyozuka et al., 1987). An increase in $[Ca^{2+}]i$ above this threshold causes Ca^{2+} to bind to the Ca^{2+} binding protein calmodulin (CaM), resulting in the formation of the Ca^{2+}-calmodulin complex (Ca^{2+}-CaM). This complex then binds to the CaM-binding domain located on the myosin light chain kinase (MLCK) enzyme, causing in the reversal of its auto-inhibited state. This in turn results in the phosphorylation of serine/threonine amino acid residues located

on the regulatory myosin light chains (MLC) of myosin (Krueger et al., 1995). Phosphorylation of the MLC allows the myosin head to rotate towards actin to create a cross-link, resulting in the formation of the actin-myosin cross-bridge. Force in the form of a contraction is generated by the active displacement of this cross-link to create a pulling force between the actin and myosin myofilaments (Tansey et al., 1994; Word et al., 1994) (**See Figure 1-3A**).

Myometrial relaxation occurs when a decrease in $[Ca^{2+}]i$ is detected resulting in a decrease in Ca^{2+}-CaM complex formation, and the inactivation of the MLCK enzyme as it reverts to its auto-inhibited state. The absence of MLCK-induced phosphorylation allows myosin light chain phosphatase (MLCP) to dephosphorylate MLCK. This occurs by activation of magnesium adenosine triphosphatase (Mg-ATPase) in the myosin-head region, resulting in further dephosphorylation of the MLC (Aguilar & Mitchell, 2010). This disrupts the actin-myosin cross-link and removes the tension between the actin and myosin myofilaments resulting in myometrial relaxation (Luckas et al., 1999; Wray and Shmygol, 2007) (**See Figure 1-3B**).

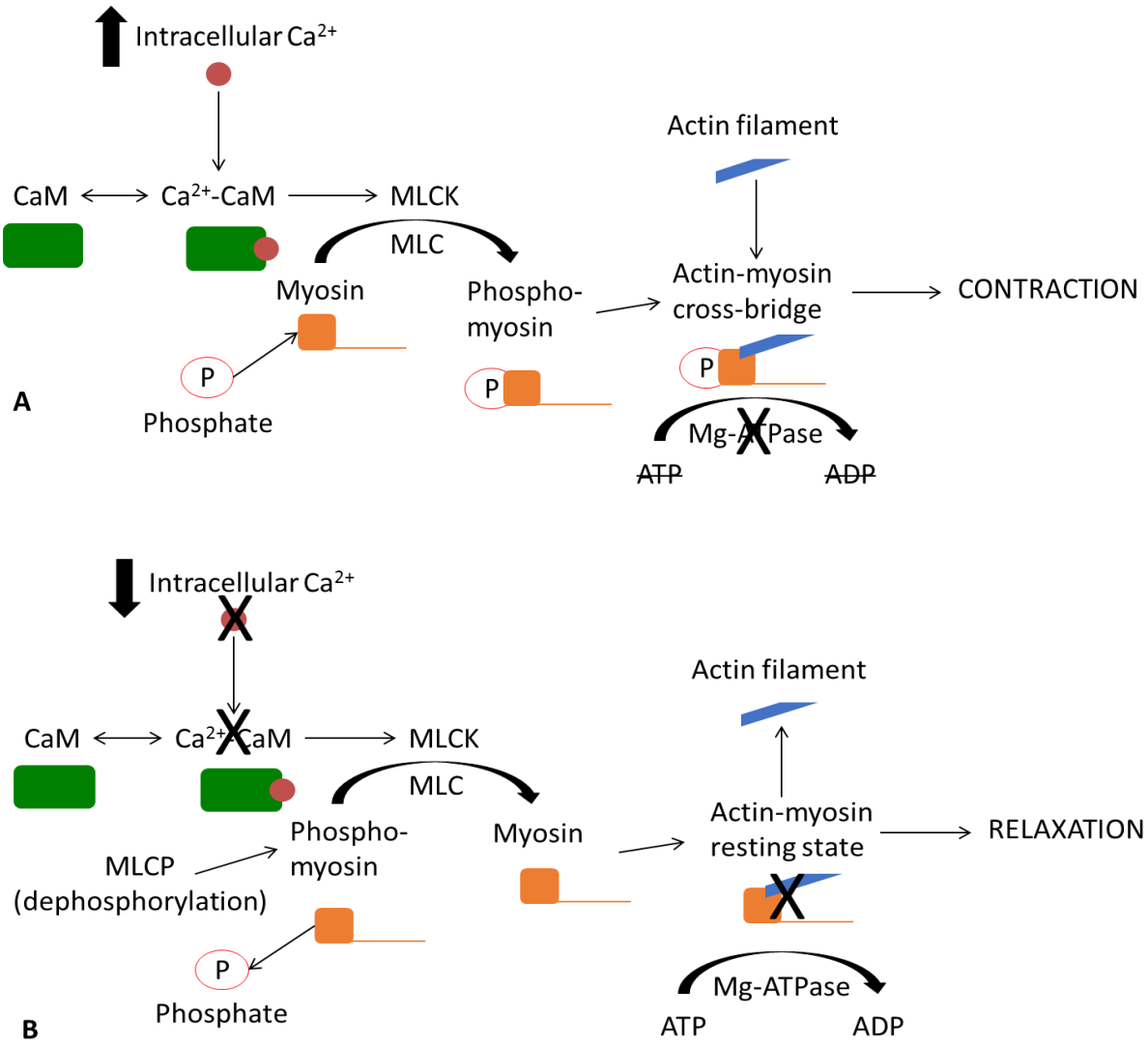


Figure 1-3. Diagrams showing the regulatory pathways involved in myometrial smooth muscle (**A**) contraction and (**B**) relaxation (*Adapted from Aguilar and Mitchell, 2010)*.

1.3 Control of intracellular Ca^{2+}

The control of $[Ca^{2+}]i$ entry across the cell plasmalemma is regulated by several different channels and receptors. In the myometrium, this occurs primarily via voltage-operated Ca^{2+} channels (VOCC) (Coleman et al., 2001), supported by receptor-operated (ROCC) and store-operated Ca^{2+} channel activation (Sanborn et al., 2005; Wray et al., 2003). Voltage-operated and receptor-operated ion channels are also referred to as voltage-gated and ligand-gated channels respectively (Alexander et al., 2011).

1.4 Voltage-operated Ca^{2+} channels

The activation of VOCCs and other voltage-dependent ion channels are dependent on changes in membrane potential, which is defined as the overall electrical voltage in the intracellular environment relative to its extracellular environment (Perney and Kaczmarek, 1991). The membrane potential of a cell is dictated by the ionic equilibrium created between Ca^{2+}, sodium (Na^{+}), potassium (K^{+}) and chloride (Cl^{-}) ions (Hodgkin et al., 1952). The resting membrane potential of a human myometrial cell fluctuates around -35 millivolts (mV) (Anderson, 1969). During pregnancy, the membrane potential is typically around -60mV, before becoming more positive to around -40mV and above as term approaches (Anderson, 1969; Kao and McCullough, 1975).

The VOCCs consist of two main types: long-lasting (L-type), and transient (T-type) Ca^{2+} channels (Lee et al., 2009; Ohkubo et al., 2005). Evidence of both channel types have been found in pregnant rat and human myometrial tissues

(Honore et al., 1989; Inoue et al., 1990; Ohya and Sperelakis, 1989; Sperelakis et al., 1992a; Sperelakis et al., 1992d). Furthermore, it has been shown that the level of expression for both channel types are altered during pregnancy (Mershon et al., 1994). Ca^{2+} transport in myometrial cells occur mainly via L-type channels. These channels, normally closed under basal conditions, have a higher permeability to Ca^{2+} compared to the T-type channels. During depolarisation, changes in corresponding membrane potential cause these channels to open and promotes the influx of Ca^{2+} ions into the cell resulting in the initiation of a contraction.

T-type channels are associated with action potential transmission rather than contraction initiation (Sanborn et al., 2005; Wray et al., 2003). Like L-type channels, their activation promotes the influx of Ca^{2+} ions into the cell but at a relatively lower voltage. These channels also exhibit rapid activation and inactivation cycles, resulting in smaller and shorter changes in $[Ca^{2+}]i$ (Amedee et al., 1987; Jmari et al., 1987).

1.5 Receptor-operated and store-operated Ca^{2+} channels

In the myometrium, ROCC opening is generally dependent on the activation of G-protein coupled receptors (GPCRs), resulting in the release of Ca^{2+} into the intracellular environment from internal sarcoplasmic reticulum (SR) stores (Taggart and Wray, 1998). GPCRs are made up of three main subunits: α, β, and γ. When the GPCR is inactive, the α-subunit is constantly bound to guanosine diphosphate (GDP). When a suitable ligand binds to the GPCR, a conformational change converts the receptor into a guanine nucleotide

exchanger, which substitutes GDP for guanosine triphosphate (GTP). This exchange causes the α-subunit to dissociate from the other two subunits, which binds to GTP to form a complex. This complex forms the basis for the activation of several GPCR-based signalling pathways, including the phospholipase C enzyme (PLC), mitogen-activated protein kinase (MAPK), and adenylyl cyclase pathways (DeVivo and Iyengar, 1994).

In the myometrium, ligands such as the neurohypophysial peptide oxytocin can induce contractility through ROCCs. The oxytocin receptor is a rhodopsin-type (class I) member of the GPCR family consisting of seven transmembrane protein domains (Fanelli et al., 1999). Oxytocin binding to its receptor results in the dissociation of the α-subunit and allows it to form a complex with GTP. This complex then binds and activates the phospholipase C (PLC) enzyme, which in turn catalyses the hydrolysis of phosphatidylinositol 4,5-biphosphate (PIP_2), resulting in the formation of inositol 1,4,5-triphosphate (IP_3) and diacylglycerol (DAG). IP_3 then binds to IP_3-receptors located on the surface of the SR membrane, which in turn triggers the release of Ca^{2+} into the cytosol from the internal SR Ca^{2+} stores (Hedin et al., 1993; Lustig et al., 1993; Shmygol and Wray, 2005; Young and Zhang, 2001) (**See Figure 1-4**).

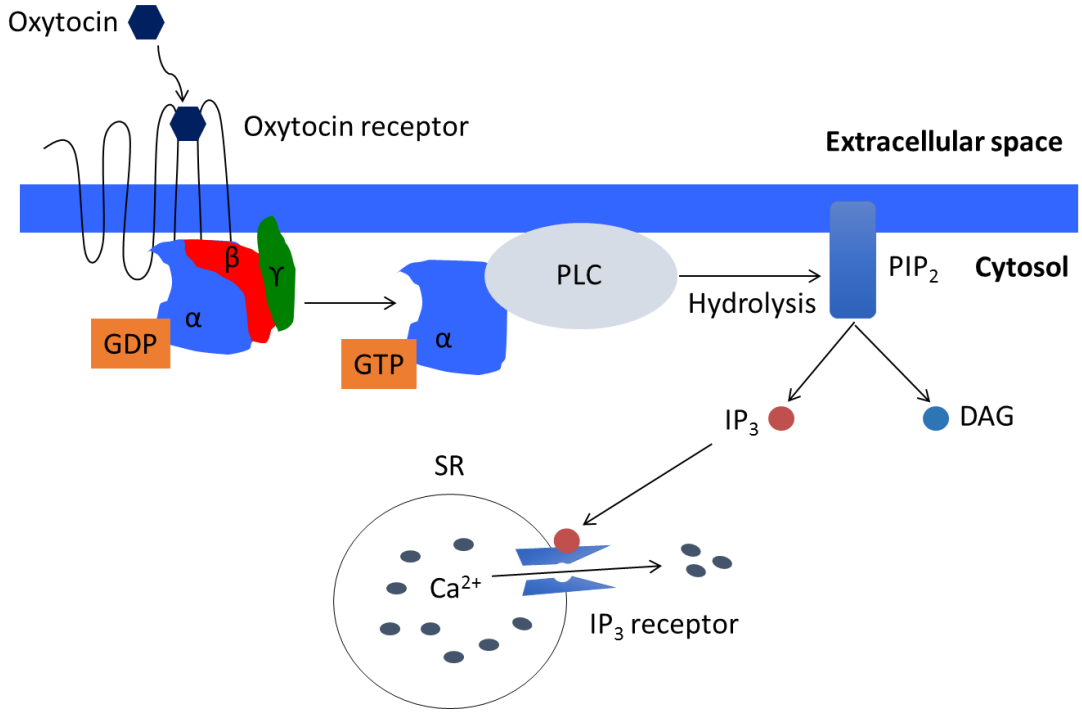


Figure 1-4. Diagram showing oxytocin-induced release of intracellular Ca^{2+} from internal SR stores via IP_3-receptors (*Adapted from Shmygol and Wray, 2005)*.

Ca^{2+} release from the SR can also be induced by the activation of store-operated Ca^{2+} channels through Ca^{2+}-induced Ca^{2+} release (Phillippe and Basa, 1996). An increase in cytosolic Ca^{2+} binds to and activates ryanodine receptor-coupled Ca^{2+} channels on the SR membrane. This in turn releases Ca^{2+} from IP_3-insensitive internal SR stores to increase $[Ca^{2+}]I$ (Berridge, 1993a; Berridge, 1993b; Harootunian et al., 1991). Depleted internal SR Ca^{2+} stores are replenished then by an SR Ca^{2+}-ATPase (SERCA) enzyme, which actively transports Ca^{2+} back into the SR against its concentration gradient (Dubuis et al., 2006) (**See Figure 1-5**).

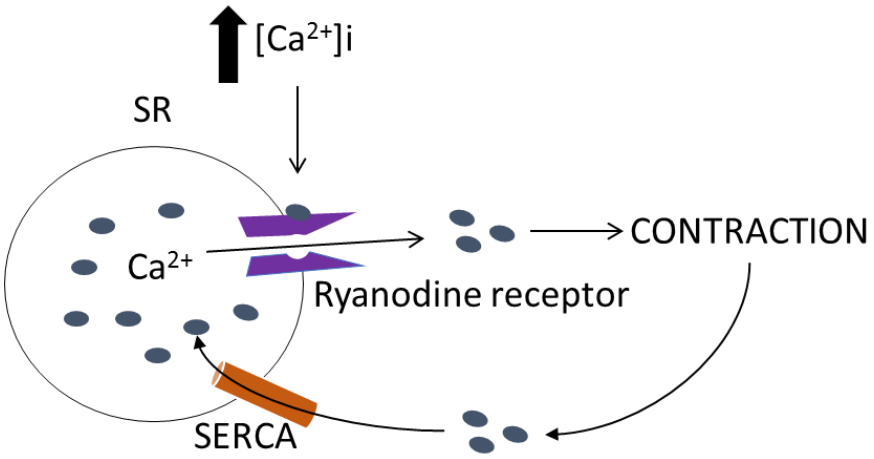


Figure 1-5. Diagram showing Ca^{2+}-induced Ca^{2+} release via ryanodine receptor binding, and internal SR Ca^{2+} recycling via SERCA (*Adapted from Phillippe and Basa, 1996).*

At term, mRNA expression of the oxytocin GPCR has been shown to increase in the rat myometrium, suggesting a role for oxytocin-induced myometrial contractions during labour (Fuchs et al., 1995; Ivell et al., 1995; Kimura et al., 1996b). An increase in PLC activation was also observed at term, specifically in the PLC-β3 subtype (Lajat et al., 1996). In the human myometrium, PLC-β1 to 4 are the main PLC subtypes currently known to be activated by the oxytocin GPCR (Ku et al., 1995; Lajat et al., 1996). Furthermore, inhibition of the oxytocin GPCR by blocking antibodies, results in the inhibition of oxytocin-induced increase in $[Ca^{2+}]i$, further suggesting a role in increasing contractility at term (Lajat et al., 1996).

1.6 K^+ channels

The resting membrane potential of a cell is regulated by several K^+ channels that are responsible for both fast and slow outward currents, which regulate the movement of K^+ out of the cell (Amedee et al., 1986; Mollard et al., 1986). In the myometrium, Ca^{2+}- and voltage-operated, and ATP-sensitive K^+ channels are responsible for maintaining the resting membrane potential during uterine quiescence, after the initiation of an action potential, and during the repolarisation and hyperpolarisation phase (Cheuk et al., 1993; Benkusky et al., 2002; Brainard et al., 2007; Downing and Hollingsworth, 1991; Hollingsworth et al., 1987; Khan et al., 1993; McCallum et al., 2011; Morrison et al., 1993; Piper et al., 1990).

1.7 Ca^{2+}-operated K^+ channels

Ca^{2+}-operated K^+ channels are expressed in the myometrium as three different sub-types: large conductance (BK), small conductance (SK), and intermediate conductance (IK) channels. Both the BK and SK channel subtypes have been shown to play a role in promoting uterine quiescence by maintaining a negative myometrial cell resting membrane potential (Benkusky et al., 2002; Brainard et al., 2007; Khan et al., 1993). This is evident from the increase in membrane potential (caused by Ca^{2+} influx via voltage-sensitive L-type Ca^{2+} channels), when these channels are inhibited by agents such as barium, iberiotoxin, and tetraethylammonium (TEA) (Khan et al., 1998; Khan et al., 1993; Khan et al., 1997; Morrison et al., 1993).

During pregnancy, the expression of BK channels in the myometrium reduces towards term and during labour, decreasing from 30.6% of total channels expressed in pregnant non-labouring women, to 15.7% in labouring women at term (Chanrachakul et al., 2003; Eghbali et al., 2003; Haug et al., 2004; Orio et al., 2006; Savalli et al., 2007; Young, 2007; Young and Hession, 1997). Electrophysiological studies on individual myometrial cells taken from pregnant non-labouring women, observed relatively greater conductance to K^+ compared to cells from labouring women at term (Chanrachakul et al., 2003), indicating an increase in K^+ efflux out of the cell to promote uterine quiescence.

Three variations of the SK channel have been cloned from rat brain cDNA: SK1, SK2, and SK3 (Kohler et al., 1996). These channels are traditionally associated with the central nervous system (Bowden et al., 2001; Kohler et al., 1996; Sailer et al., 2002; Stocker et al., 1999; Stocker and Pedarzani, 2000) where they are responsible for mediating neuronal hyperpolarisation, regulation of neuronal firing patterns, dendritic excitability, and synaptic transmission (Bond et al., 2005; Faber and Sah, 2003; Sah and Faber, 2002). All three SK channel subtypes are expressed in the myometrium (Rosenbaum et al., 2012), in particular the SK3 subtype, which was also found to be overexpressed in tissues of women experiencing delayed parturition (Pierce et al., 2008). In pregnant mice, activation of SK channels by Cyclohexyl-(2-(3,5-dimethyl-Pyrazol-1-yl)-6-methyl-Pyrimidin-4-yl)-Amine (CyPPA) resulted in the inhibition of spontaneous uterine contractility (Noble et al., 2010; Skarra et al., 2011). This effect was reversed by addition of the bee-venom toxin

apamin (Noble et al., 2010), which acts as a blocker of all three variants of the SK channel family (Blatz and Magleby, 1986; Burgess et al., 1981; Romey et al., 1984). Furthermore, apamin-induced inhibition of SK channels in rat myometrial cells caused a reduction in K^+ outward currents, resulting in a decrease of K^+ efflux out of the cell, which in turn promotes Ca^{2+} influx into the cell causing membrane depolarisation (Noble et al., 2010).

1.8 Voltage-operated K^+ channels

Voltage-operated K^+ channels in the myometrium function as K^+ inward-rectifiers that favour K^+ influx over efflux, which results in a smaller outward K^+ current that returns the cell membrane back to resting potential voltages (Boyle et al., 1987). These channels are activated by membrane potentials of around -40mV and inactivate relatively slowly, suggesting a possible role in membrane repolarisation (Folander et al., 1990; Pragnell et al., 1990). Recent studies have shown that the mRNA expression of these channels are reduced towards term, and that their activation results in the inhibition of myometrial contractility (McCallum et al., 2011).

1.9 ATP-sensitive K^+ channels

ATP-sensitive K^+ channels in the myometrium also function as K^+ inward-rectifiers, but are regulated by the concentrations of ADP and ATP in the cell rather than changes in membrane voltage (Kakei et al., 1985; Noma, 1983). In cardiac tissues, channel activation by a reduction in intracellular ATP has been shown to inhibit cardiomyocyte activity (Ashcroft, 1988; Noma, 1983). In the myometrium, activation of these channels by aprikalim and levcromakalim

resulted in the inhibition of oxytocin-induced contractility in tissues from both pregnant and non-pregnant women (Cheuk et al., 1993; Downing and Hollingsworth, 1991; Hollingsworth et al., 1987; Morrison et al., 1993; Piper et al., 1990).

1.10 Other ion channels

There are several other ion channels in the myometrium that have been shown to regulate uterine contractility. Studies investigating these additional channels have observed potential roles in pace-making (Jones et al., 2004), excitation propagation (Arnaudeau et al., 1994a; Jones et al., 2004) and increasing Ca^{2+} sensitivity (Arnaudeau et al., 1994c).

Na^{+} channels have been found in both pregnant rat and human myometrial tissues, and their mRNA expression has been observed to increase towards term (Inoue and Sperelakis, 1991). Electrophysiological experiments have observed fast Na^{+} inward currents resulting in the influx of Na^{+} ions into the cell, which is regulated by a Na^{+}-K^{+}-ATPase pump. This influx is thought to promote excitation propagation by contributing to the membrane potential increase during an action potential (Inoue and Sperelakis, 1991; Kosterin et al., 1994; Ohya and Sperelakis, 1989; Parkington and Coleman, 2001; Sperelakis et al., 1992a; Young and Herndon-Smith, 1991).

Evidence of Cl^{-} channels that are part Ca^{2+}-, and part voltage-operated, have been found in both pregnant rats and guinea pigs (Coleman and Parkington, 1987; Jones et al., 2004). When activated, these channels produce Cl^{-} inward

currents that promote a negative membrane potential, which suggests a possible role in promoting repolarisation or hyperpolarisation. However, the inhibition of these channels with niflumic acid or anthracene-9-carboxylate resulted in the reduction of both spontaneous and oxytocin-induced myometrial tissue contraction frequency, and the inhibition VOCC and ROCC activity, indicating that the exact nature and function of these channels are no entirely clear (Jones et al., 2004).

Recently, studies have discovered several other channels expressed in the myometrium that may play a role in contraction regulation. Many of these channels have characteristics of voltage-operated, ATP-sensitive and stretch-activated channels. They have also been shown to be permeable to Ca^{2+}, which suggests a role in $[Ca^{2+}]i$ regulation. Examples of these channels include the KCNQ voltage-operated K^+ channel, the two-pore-domain K^+ channels, and the Human Ether-a-go-go-related Gene (hERG) K^+ channels (Brueggemann et al., 2012; Buxton et al., 2010; Greenwood and Tribe, 2014; Patel and Honore, 2002; Zhong et al., 2010).

1.11 Contractility dysfunctions in the uterus

Dysfunctions in uterine contractility during pregnancy is commonly associated with premature delivery of the fetus. Preterm birth is defined as delivery before 37 weeks of gestation, and is regarded as the main cause of neonatal mortality and morbidity (WHO, 1992). Approximately 28% of all early neonatal deaths, unrelated to congenital malformations, are due to preterm birth (Liu et al., 2015). Rates of preterm birth occur in 5 – 7% of all live births and are

increasing in both developed and developing countries (Lawn et al., 2006; Liu et al., 2012; Liu et al., 2015). For those that survive, risks of mortality from encephalopathy, cerebral palsy, and respiratory distress syndromes are significantly increased (Gleason and Back, 2005; Hulsey et al., 1993; Madan & Good, 2005; Simmons et al., 2010).

The principle causes of preterm birth are spontaneous preterm labour with intact membranes, preterm premature rupture of the membranes (PPROM), delivery by induction, and caesarean section. Among these conditions, preterm labour is responsible for 40 – 45% of all preterm births (Goldenberg et al., 2008). Preterm labour can be caused by several conditions including infection, inflammation, ischaemia of the uterus, and uterine overdistension. Risk factors for preterm labour include previous preterm labour, maternal stress during pregnancy, multiple gestations, maternal under and overweight, and previous pregnancy complications such as pre-eclampsia. (Copper et al., 1996; Goepfert and Goldenberg, 1996; Goldenberg and Culhane, 2005; Goldenberg et al., 2005; Goldenberg et al., 1996; Hendler et al., 2005; McDonald et al., 2010; Han et al., 2010).

The management of preterm births in developed countries is generally good. The consistent observation of high-risk patients, comprehensive post-natal care plans, rapid response times in the event of patient deterioration, and advances in medical technology, have all contributed to improving mortality rates in premature infants. Despite this, developmental issues such as respiratory difficulties and behavioural problems are still higher in premature

babies compared to those delivered at term (Chatterjee et al., 2007). Furthermore, pharmacological interventions only treat the symptomatic effects of premature birth. There is currently no established method for preventing preterm labour or preterm birth.

Tocolytic-based medicines are prescribed to delay premature delivery long enough to administer antenatal steroids, such as betamethasone and dexamethasone to promote fetal respiratory maturation (Chatterjee et al., 2007; Gyetvai et al., 1999). The most commonly prescribed tocolytics are nifedipine and atosiban, which function as Ca^{2+} channel blockers and oxytocin receptor antagonists respectively. However, their therapeutic effects are relatively short-lived, making them ineffective for treatment of extremely premature infants (<26 weeks of gestation) (Chatterjee et al., 2007; Gyetvai et al., 1999). Several tocolytic drugs are also contraindicated in conditions such as cardiac disease, and their use is avoided completely in women suffering from other pregnancy-related issues such as pre-eclampsia and placental abruption (D'Ercole et al., 2002; Groome et al., 1992; Gyetvai et al., 1999; Hosono et al., 2001; Jirapinyo et al., 1990).

1.12 The role of cholesterol in myometrial contractility

During the initial stages of pregnancy, an increase in appetite and accelerated lipogenesis can cause a 25 – 50% increase in maternal plasma cholesterol, and a greater accumulation of maternal body fat (Alvarez et al., 1996; Piechota and Staszewski, 1992). This increase in fat is rapidly broken down (Herrera, 2002; Ramon y Cajal et al., 1988) to promote fetoplacental growth

and embryonic development (Elias et al., 2003; Ruan et al., 2000). Maternal-derived cholesterol is no longer essential once the fetus matures and becomes capable of undergoing lipogenesis (Baardman et al., 2013; Ramon y Cajal et al., 1988). However, there is evidence to suggest that cholesterol may play a much larger role during pregnancy beyond fetoplacental development and maturation. Recent studies have shown that mothers with hypercholesterolaemia were more likely to deliver prematurely, while mothers with hypocholesterolaemia were linked with low birth weight deliveries (Maymunah et al., 2014; Oluwole et al., 2014). The association between elevated maternal cholesterol and incidence of preterm birth, suggests a possible role for cholesterol in uterine contractility.

1.13 The myometrial cell membrane

The myometrial cell membrane is made up of a 7 – 5nm thick asymmetrical lipid bilayer, consisting of phospholipid and glycolipid species heterogeneously distributed throughout the membrane (Sampaio et al., 2011; Simons and Sampaio, 2011). Most membrane lipids are either biosynthesised in the cytoplasmic region of the endoplasmic reticulum (ER) or derived from dietary intake (Ahyayauch et al., 2010; Urbina et al., 2011). The biophysical properties and functions of the membrane are dependent on the concentration and organisation of these lipids. This results in distinct parts of the membrane to have different roles, including barrier functions and the modulation of membrane-expressed signalling proteins (Janmey and Kinnunen, 2006).

The mammalian cell membrane lipid bilayer comprises of an outer leaflet that faces the extracellular space and an inner leaflet that faces the cytosol. Both layers are made up of five major phospholipids: phosphatidylcholine, phosphatidylethanolamine, phosphatidylserine, phosphatidylinositol, and sphingomyelin. These phospholipids are asymmetrically distributed between the two leaflets, with the outer leaflet made up of phosphatidylcholine and sphingomyelin, and the inner leaflet is made up of phosphatidylethanolamine, phosphatidylserine, and phosphatidylinositol (Williams et al., 2000). In addition to these phospholipids, the lipid bilayer also contains a mixture of glycolipids and cholesterol. Glycolipids constitute around 2% of the outer leaflet, while cholesterol makes up around 20% of both leaflets (Futerman & Hannun, 2004). Cholesterol is amphipathic, consisting of both hydrophobic and hydrophilic domains. The hydrophobic domains of cholesterol and that of other lipid species are responsible for the conformation of the cell membrane lipid bilayer in an aqueous environment (Balasubramanian and Schroit, 2003; Smith et al., 2002) (**See figure 1-6**).

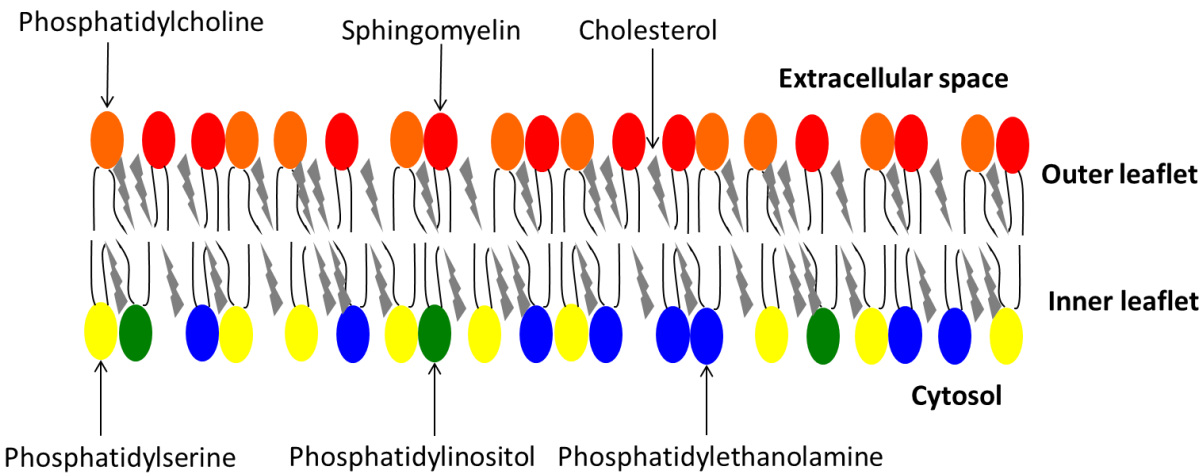


Figure 1-6. Diagram showing the main constituents of the myometrial membrane lipid bilayer (*Adapted from Williams et al., 2000*).

Traditionally, the cell membrane lipid bilayer was only thought to maintain the structural stability of the cell and to regulate cell permeability (Sampaio et al., 2011; Simons and Sampaio, 2011). However, the lipid bilayer is now known to be involved in the direct and indirect regulation of receptor/ion channel-coupling and signalling pathways. Specific regions within the membrane are enriched with cholesterol and sphingomyelin, forming discrete membrane domain structures known as lipid-rafts (Simons & Ikonen, 1997). These lipid-rafts have been shown to recruit membrane-bound proteins and affect their signalling pathways (Brown and London, 1998; Harder, 2003; Pralle et al., 2000; Samsonov et al., 2001; Sotgia et al., 2002).

Caveolae are 50 – 100nm long, predominately cholesterol-containing lipid-raft structures found within the cell membrane. These rafts are structurally stabilised and attached to the membrane by several cholesterol-binding proteins called caveolin, specifically caveolin-1 and -2. Due to their small size, visual identification of caveolae can only be detected using scanning and transmission electron microscopy (Taggart et al, 2000; Samsonov et al., 2001; Sotgia et al., 2002) (**See Figure 1-7**). The presence of caveolae structures have been visually identified in myometrial cells via microscopy, and by the detection of their caveolin cholesterol-binding proteins (Engelman et al., 1998; Ikezu et al., 1998; Okamoto et al., 1998). However, the expression of both caveolae and caveolin in the myometrium during pregnancy and at term appear unchanged. This suggests that the mechanisms integrating myometrial signalling with the onset of labour may not involve alterations in the cellular expression of caveolae or caveolin (Taggart et al., 2006).

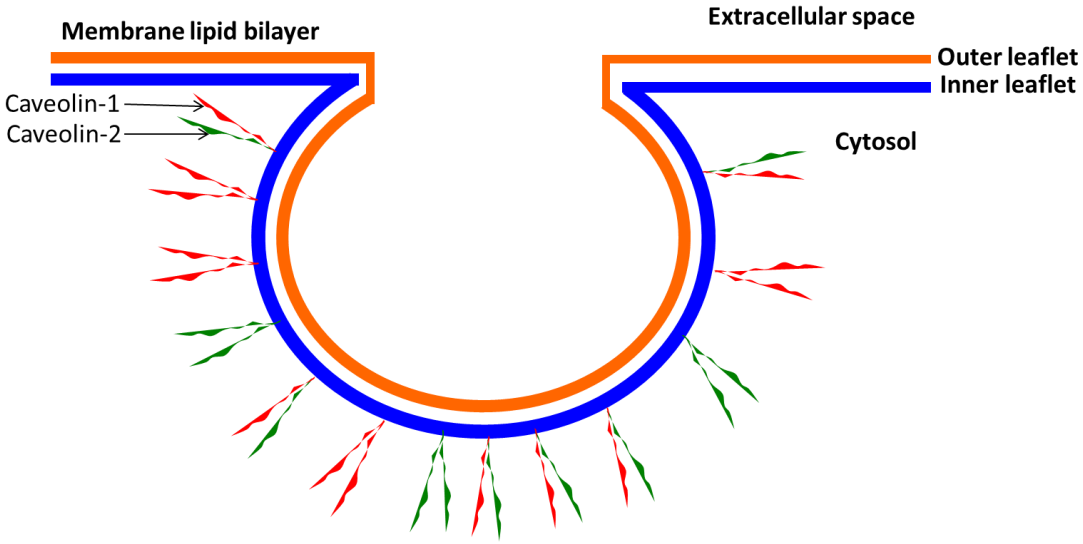


Figure 1-7. Diagram showing the basic structure of the caveolae lipid-raft structure and associated cholesterol-binding caveolin proteins in the membrane lipid bilayer (*Adapted from Simons & Ikonen, 1997*).

Although the expression of caveolae structures and caveolins remain unchanged during pregnancy (Taggart et al., 2006), their presence in the uterus suggests a potential role for these species in myometrial function. In other smooth muscle tissues, caveolae and their disruption by cholesterol-manipulating agents have been shown to result in the impairment of smooth muscle contractility. For example, the disruption of caveolae by cholesterol extraction using methyl-β-cyclodextrin (MCD), resulted in the impairment of vasopressin and endothelin-induced contractions in vascular smooth muscle tissues (Dreja et al., 2002). It was thought that cholesterol-induced disruption of caveolae structures can affect Ras homolog gene A protein (RhoA) kinase and store activated Ca^{2+} release mediated contractility pathways, as both have been shown to be co-localised in caveolae (Bergdahl et al., 2003a; Urban et al., 2003).

In the myometrium, studies from our group have observed the co-localisation of several ion channels to caveolae structures, including BK and L-type Ca^{2+} channels (Chanrachakul et al., 2004**;** Brainard et al., 2005). Subsequent functional studies have observed the inhibition of protein kinase C (PKC) and RhoA activation, following the introduction of additional caveolin proteins into the myometrial cell (Taggart et al., 2000). The disruption of caveolae by MCD-induced cholesterol depletion, resulted in an increase in myometrial contractions and Ca^{2+} channel activity (Smith et al., 2005). Caveolin disruption has also been shown to inhibit BK channel activity (Brainard et al., 2009), by internalising the channel away from the membrane surface (Shmygol et al., 2007).

1.14 Cholesterol-lowering drugs

Cholesterol-lowering drugs are commonly used to treat conditions involving hypercholesterolaemia, such as atherosclerosis and coronary heart disease, by returning plasma cholesterol back to physiological concentrations (<5.2 mmol/L). The statin family of drugs is the most commonly prescribed treatment for lowering elevated plasma cholesterol (Di Angelantonio et al., 2009; Preiss and Sattar, 2009).

Statins are classified as 3-hydroxy-3-methyl-glutaryl-CoA (HMG-CoA) reductase inhibitors (Ewang-Emukowhate and Wierzbicki, 2013; Packard, 2000; Stroes, 2005). Each statin family member contains a substrate domain that shares a structural similarity to the HMG-CoA molecule, consisting of an inactive lactone ring structure and a hydrophobic ring structure that interacts

with the HMG-CoA reductase enzyme (Ewang-Emukowhate and Wierzbicki, 2013; Packard, 2000; Stroes, 2005) (**See Figure 1-8**). Statins can be separated into two types based on whether the inactive lactone ring is found in a closed or open state. Open lactone ring statins do not require any activation, while closed lactone ring statins require activation by hydrolysis (Istvan and Deisenhofer, 2001).

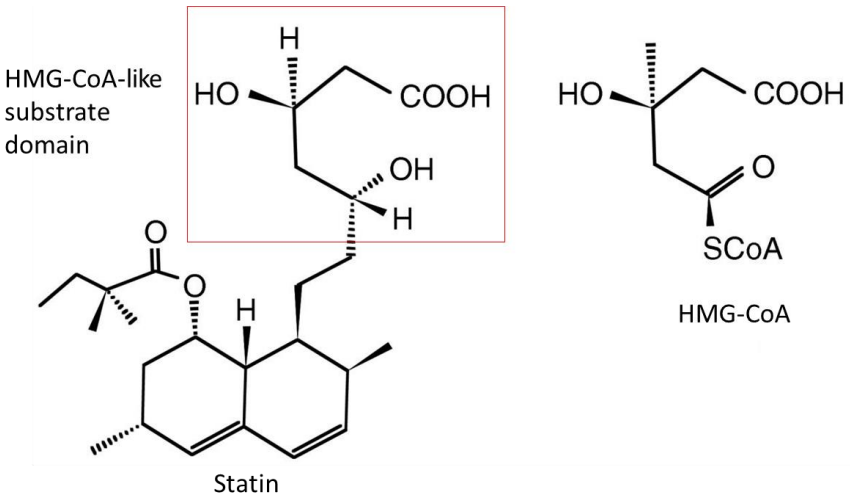


Figure 1-8. Diagram showing the basic structure of a statin molecule and the HMG-CoA-like substrate domain structure compared to a HMG-CoA molecule. (*Adapted from Friesen & Rodwell, 2004*).

Cholesterol synthesis is initiated when three molecules of acetyl-CoA bind together to form acetoacetyl-CoA, in the presence of a thiolase enzyme. Acetoacetyl-CoA is then converted into HMG-CoA by HMG-CoA synthase, which is reduced to form mevalonate by HMG-CoA reductase. Phosphorylation of mevalonate in the presence of mevalonate kinase results in the formation of 5-pyrophosphomevalonate (5-PP mevalonate). 5-PP mevalonate is then decarboxylated by mevalonate-5-pyrphosphate decarboxylase to form isopentenyl pyrophosphate (IPP). IPP can become isomerised to form 3,3-dimethylallyl pyrophosphate (DPP), and both IPP and

DPP undergo condensation to form geranyl-geranyl pyrophosphate (GGPP). GGPP itself can undergo further condensation with a second IPP molecule to produce farnesyl pyrophosphate (FPP). The combination of two FPP molecules and the release of a pyrophosphate group, results in the formation of squalene, which is then converted into lanosterol by ER-associated enzymes. Finally, the removal of two methyl groups converts the lanosterol into cholesterol (Istvan and Deisenhofer, 2000; Istvan et al., 2000) (**See Figure 1-9**).

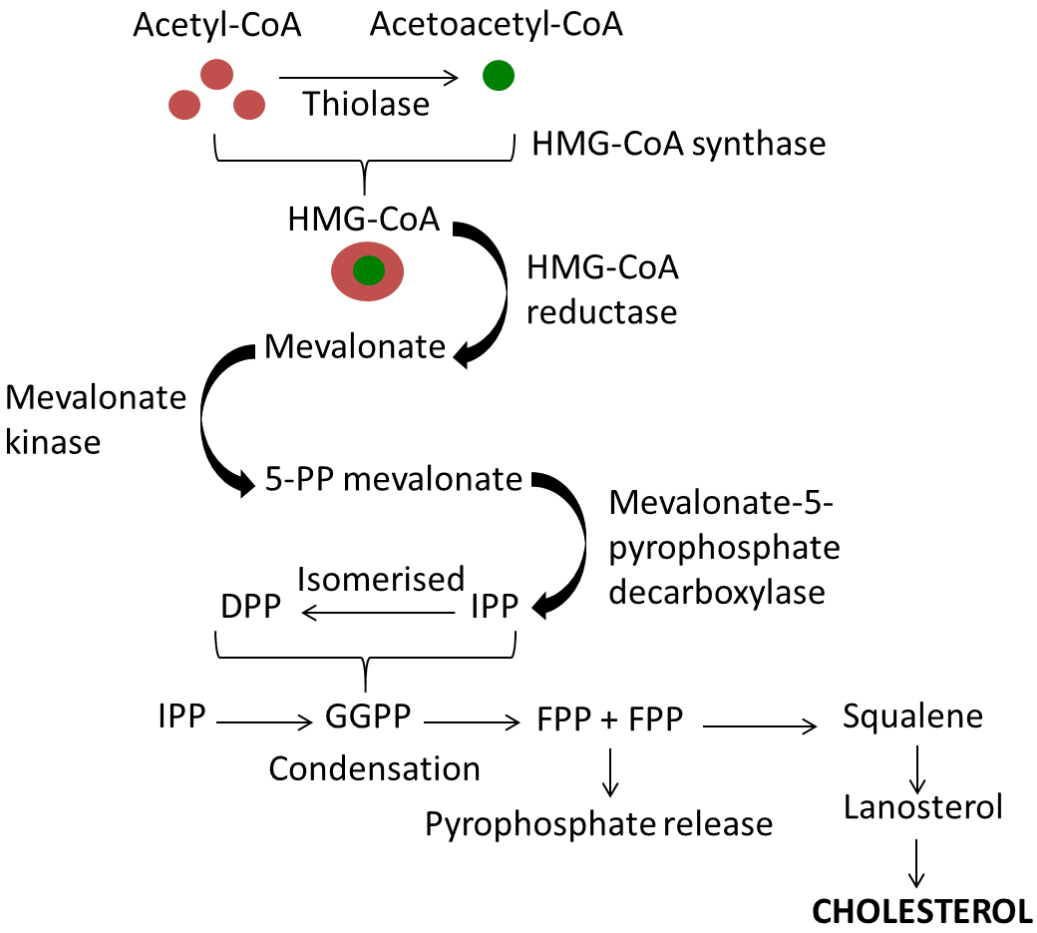


Figure 1-9. Diagram showing the HMG-CoA reductase cholesterol synthesis pathway (*Adapted from Hajar, 2012)*.

Statin-induced inhibition of cholesterol occurs by the activation of the statin lactone ring structure, which exposes the HM-CoA-like substrate domain and results in the competitive inhibition of the HMG-CoA substrate for the HMG-CoA reductase enzyme. Once bound, statins prevent the phosphorylation of mevalonate and inhibits all downstream signalling pathways involved in the synthesis of cholesterol (Istvan and Deisenhofer, 2000; Istvan et al., 2000) (**See Figure 1-10**).

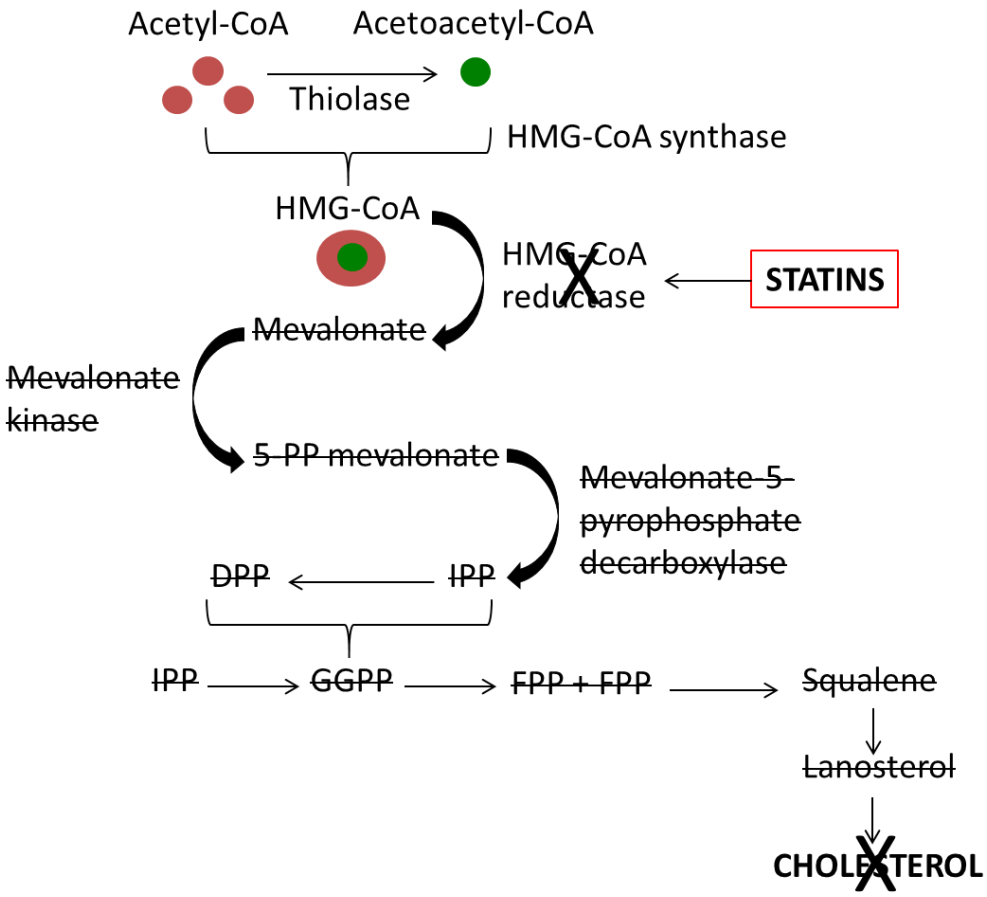


Figure 1-10. Diagram showing statin-induced inhibition of the HMG-CoA reductase pathway and the inhibition of cholesterol biosynthesis (*Adapted from Hajar, 2012)*.

1.15 Statins and smooth muscle physiology

It is not known whether the HMG-CoA reductase pathway is present in the human myometrium. To date, there has been no formal requirement to investigate the mechanisms of statins during pregnancy, as statins are not generally recommended for pregnant women. Therefore, most statin-based research has been carried out in the cardiovascular system, specifically to determine the potential toxicity and side effects of statin administration on cardiac smooth muscle function (Alvarez de Sotomayor et al., 1999; Alvarez de Sotomayor et al., 2001; Perez-Guerrero et al., 2000; Yada et al., 1999).

In pre-contracted rat aortic and superior mesenteric arteries, exposure to simvastatin results in blood vessel vasodilation. This effect was determined to be endothelium-dependent, and thought to involve nitric oxide (NO) release and inhibition of the HMG-CoA reductase pathway (de Sotomayor et al., 2005). Further investigations from the same group found that simvastatin inhibits VOCC activity, resulting in a decrease in $[Ca^{2+}]i$ (de Sotomayor et al., 2005). These effects were also observed in rat basilar artery preparations when exposed to lovastatin. Interestingly, the lack of recovery of lovastatin's effects after replenishment with mevalonate suggests an absence of the HMG-CoA reductase pathway in this system (Bergdahl et al., 2003b). Similarly, in pancreatic β-cells exposed to simvastatin, inhibition of type Ca^{2+} channels with no recovery after mevalonate or mevalonic acid replenishment was observed (Yada et al., 1999). These results suggest that statins can affect pathways associated with smooth muscle contractility, and that these

effects may occur in the absence of cholesterol modulation or the HMG-CoA reductase pathway.

1.16 Statin pleiotropic properties

The pleiotropic properties of statins are defined as characteristics that are independent of cholesterol inhibition. Several of these properties have been shown to involve proteins downstream of mevalonate, but before inhibition cholesterol biosynthesis in the HMG-CoA reductase pathway.

In the HMG-CoA reductase pathway, IPP, FPP, and GGPP are collectively known as isoprenoid proteins (Goldstein and Brown, 1990). These proteins are involved in the activation of GPCRs, small guanosine diphosphate (GTP)-binding proteins such as Ras, and other Ras-like proteins such as RhoA, via a process called prenylation. Activation by prenylation involves the addition of hydrophobic molecules, such cholesterol, to a protein, which facilitates its translocation and attachment to the plasma membrane surface where signalling can occur (Fujisawa et al., 1998; Van Aelst and D'Souza-Schorey, 1997). It is thought that statins can inhibit the production of isoprenoid proteins, which in turn inhibits the activation of proteins like GPCRs by prenylation and prevents their attachment to the plasma membrane surface for signalling (Laufs and Liao, 1998).

There is evidence to suggest that statins can directly affect NO activity, independent of cholesterol inhibition. During a study that investigated statins effects on blood vessels in patients suffering from atherosclerosis, both statin

treatment and acute plasma low-density lipoprotein (LDL) cholesterol apheresis improved NO-dependent vessel vasodilation. A review of the data found that the statin-induced effect occurred before a significant reduction in cholesterol was observed, indicating a possible cholesterol-independent mechanism (Anderson et al., 1995; O'Driscoll et al., 1997; Treasure et al., 1995). Subsequent investigations have shown that statins can upregulate endothelial NO synthase (eNOS) protein expression and activity by increasing eNOS mRNA half-life. However, these effects are reversed with the addition of GGPP, suggesting that a partial involvement of the HMG-CoA reductase pathway may still be involved (Laufs et al., 1998).

1.17 Maternal weight, age, and statins during pregnancy

There is evidence to suggest that maternal cholesterol may have additional roles beyond fetal development and maturation. The correlation between hypercholesterolaemia and incidence of preterm birth indicates a possible relationship between changes in cholesterol and uterine contractility (Maymunah et al., 2014; Oluwole et al., 2014). This relationship is supported by several studies showing the expression of cholesterol-containing caveolae lipid-rafts in the human myometrium (Taggart et al, 2000; Samsonov et al., 2001; Sotgia et al., 2002), ion channel co-localisation to caveolae and caveolin (Chanrachakul et al., 2004**;** Bergdahl et al., 2003a; Brainard et al., 2005 Urban et al., 2003), and the disruption of uterine contractions following cholesterol manipulation (Dreja et al., 2002; Shmygol et al., 2007; Smith et al., 2005; Taggart et al., 2000).

Based on the potential relationship between cholesterol and uterine contractility, the rising global rates of obesity presents a possible significant risk factor to pregnancy-related conditions dysfunctions in uterine contractility. Current statistics indicate that approximately 2.1 billion adults worldwide are considered overweight (BMI 25 – 30kg/m^2), and around 700 million are considered obese (BMI>30kg/m^2) (Smith & Smith, 2016). In the UK, around 56% of women of childbearing age are believed to be either overweight or obese (Vahratian, 2009). A high maternal BMI is generally associated with poor fetal and pregnancy outcomes, including gestational diabetes, pre-eclampsia, and preterm birth (Palinski et al., 2009; Chiang et al., 1995; Catov et al., 2007; Khoury et al., 2005). Furthermore, some of the maternal conditions experienced during pregnancy can be carried over to the offspring, including the development of type-2 diabetes and gestational diabetes in females (Harper et al., 2007; Dabelea et al., 2000; Pettitt et al., 1983; Plagemann et al., 1997).

In addition to increasing maternal obesity rates, the average age of women choosing to bear children has also increased (Lampinen et al., 2009). Advanced maternal age has been associated with poor pregnancy outcomes, including preterm birth (Astolfi & Zonta, 1999; Newburn-Cook & Onyskiw, 2005; Waldenstrom et al., 2016). This is partly due to higher incidences of chronic conditions with increasing maternal age, including cardiac diseases such as coronary artery disease, stroke, and atherosclerosis (Braveman, 2006). The increase in the prevalence of maternal obesity and advanced maternal age during pregnancy, and associated cardiovascular disease, has

been shown to increase the likelihood of pregnant women requiring statin treatment to regulate cholesterol levels. Furthermore, evidence demonstrating statin-induced modulation of uterine contractility indicates the possibility that statins can be used as both a tocolytic for preterm birth, and as a cholesterol-lowering drug for the treatment of cardiovascular diseases involving hypercholesterolaemia during pregnancy.

The current NHS guidelines do not recommend the administration of statins to women undergoing pregnancy or who are breastfeeding. This is mainly due to queries over the potential teratogenic effects of statin exposure during pregnancy. However, there is emerging data to suggest that statins do not affect fetal development.

A recent systematic review of both animal and human clinical studies found that in most cases, statin exposure during pregnancy is unlikely to cause teratogenic effects (Kusters et al., 2014). For example, a study investigating the risk of statin-induced toxicity in normal pregnant women, found no increased risk of adverse pregnancy outcome or congenital defects after statin exposure (Taguchi et al., 2008). Several large pharmaceutical pharmacovigilance investigations also found no increased risk of congenital defects after exposure to lovastatin and simvastatin during pregnancy (Manson et al., 1996; Pollack et al., 2005). Recently, a large multicentre study investigating the effects of statin exposure during the first trimester, found either relatively small or no statistically significant differences in the rate of major congenital defects in statin-exposed women compared to the national

figures (Winterfeld et al., 2012). The few studies which did observe statin-induced congenital effects were either exposing animal models to maternally toxic statin concentrations (>40mg/kg/day) (Minsker et al., 1983), or isolated patient cases with no obvious pattern or consistency to suggest a common mechanism (Ghidini et al., 1992; Edison et al., 2004a; 2004b).

1.18 Statins as a therapeutic agent in pregnancy complications

Recently, a small number of studies have started to investigate the effects of statins on pregnancy complications. These include animal and human experimental models of pre-eclampsia, antiphospholipid syndrome, and preterm labour (Gonzalez et al., 2011; Gonzalez et al., 2014; Kumasawa et al., 2011), with one group conducting preliminary clinical trials investigating the therapeutic effects of pravastatin administration in women with pre-eclampsia (Brownfoot et al., 2015).

To date, only one group has investigated the effects of statins on myometrial contractility (Gonzalez et al., 2014). In a preliminary study using a lipopolysaccharide (LPS) preterm labour mouse model, myometrial tissue strips pre-incubated with statins overnight were found to inhibit contractions induced by the complement component C5a protein fragment (C5a), an anaphylatoxin used to generate an inflammation-induced increase in smooth muscle contractility (Gonzalez et al., 2011). The follow-up study using human myometrial tissue strips also observed the inhibition of C5a-induced contractility after overnight statin pre-incubation (Gonzalez et al., 2014). However, there are currently no published reports describing the effects of

independent, short-term statin exposure on spontaneous human myometrial contractions, or the complete mechanism of statin-induced activity in the human myometrium. Furthermore, the effects of statins on cholesterol and the presence of the HMG-CoA reductase pathway in the myometrium are also currently unknown.

1.19 Aims and hypothesis

Spontaneous preterm labour is the primary cause of preterm birth (Goldenberg et al., 2008), which remains the leading cause of neonatal mortality and morbidity (WHO, 1992). Current treatment strategies only provide symptomatic relief without disease prevention. Furthermore, the exact mechanisms involved during preterm labour remain unclear.

Cholesterol has been shown to have a functional role in the myometrium beyond fetal development. This has been evident in several studies observing modulations in uterine contractility following cholesterol manipulation, specifically through disruption of the cholesterol-containing lipid-raft caveolae structures (Brainard et al., 2009; Dreja et al., 2002; Smith et al., 2005; Shmygol et al., 2007; Taggart et al., 2000). However, the cholesterol and caveolae dependent pathways involved in uterine contraction regulation are still poorly understood.

Several studies investigating the effects of statins in smooth muscle tissues, have found evidence to suggest that statins can affect several pathways associated with smooth muscle contractility regulation (Bergdahl et al., 2003b;

de Sotomayor et al., 2005; Yada et al., 1999). These include mechanisms independent of cholesterol-inhibition such as VOCC inhibition (de Sotomayor et al., 2005), and upregulation of eNOS expression and activity (Laufs et al., 1998). Furthermore, a small number of studies have recently started to determine the potential therapeutic effects of statins in pregnancy complications, including preterm labour (Gonzalez et al., 2011, 2014). However, changes in spontaneous myometrial contractility after statin exposure, the role of statin-induced cholesterol manipulation, evidence of HMG-CoA reductase inhibition, and the presence of cholesterol independent pathways in the human myometrium are still unknown.

In this study, we hypothesised that the acute exposure of simvastatin would reduce spontaneous human myometrial contractions. This occurs by a combination of cholesterol reduction, inhibition of the HMG-CoA reductase pathway, upregulation of the NO-dependent pathway, modulation of $[Ca^{2+}]i$, modulation of Ca^{2+} and K^{+} ion channel activity, and the disruption of caveolae structures. The objectives of the study are as follows:

a) Determine the cumulative effects of simvastatin on spontaneous myometrial contractions.
b) Determine the effects of simvastatin on cholesterol concentration in the myometrial cell, and the role of cholesterol modulation on spontaneous myometrial contractions.
c) Determine the effects of NO inhibition on simvastatin-induced effects on spontaneous myometrial contractions.

d) Determine the presence or absence of the HMG-CoA reductase pathway in the myometrium.

e) Determine the effects of simvastatin on Ca^{2+} and K^{+} ion channel activity during spontaneous myometrial contractility.

f) Determine the effects of simvastatin on basal and oxytocin-induced $[Ca^{2+}]i$ release in myometrial cells.

g) Determine the effects of simvastatin on Hoechst 33342 dye tracer permeability in myometrial cells.

h) Determine the effects of simvastatin on the expression of caveolae cholesterol-binding protein caveolin-1 in the myometrial cell.

2 Materials and methods

This project was submitted to and approved by the Derbyshire Research Ethics Committee (09/H0401/90). The research study trial master file was kept in a secured cabinet located at the Clinical Sciences Laboratory research office, Academic Division of Obstetrics & Gynaecology, University of Nottingham, Royal Derby Hospital. Formal written and informed consent was obtained from all patients included in this study. All laboratory work was carried out at research facilities located in the School of Graduate Entry Medicine in Derby, the School of Veterinary Medicine and Science in Sutton Bonington, and the Queen's Medical Centre in Nottingham.

2.1 Materials

All reagents, drugs, stock solutions, and assay kits for in-vitro and ex-vivo experiments were purchased from either Sigma-Aldrich Co. Ltd (The Old Brickyard, New Road, Gillingham, Dorset, SP8 4XT, UK), or Invitrogen Life Technologies Ltd. (3 Fountain Drive, Inchinnan Business Park, Paisley, PA4 9RF, UK), unless stated otherwise. Stock solutions and buffers were prepared using filtered, double distilled water (ddH_2O) (Purite Limited, Bandel Way, Thame, Oxon, OX9 3SJ, UK). Details of stock solution and buffer compositions can be found in the appendices.

2.2 Informed patient consent

One intact myometrial biopsy sample per patient was obtained from term ($\geq$37 weeks), non-labouring women undergoing scheduled caesarean section delivery, or elective hysterectomy for benign conditions in the Department of Obstetrics and Gynaecology, Royal Derby Hospital. Caesarean section indication included maternal request, breech presentation, and previous caesarean section. Women with pre-existing conditions such as diabetes, gestational diabetes, hypertension (>140/90mmHg), renal and cardiac disease, and other conditions that compromised overall health were excluded.

All pregnant women attending the antenatal clinical at the Royal Derby Hospital were given patient information sheets in their antenatal packs at their booking appointment. Caesarean section patients were approached by a researcher or a research midwife, holding a current research passport and

certified in Good Clinical Practice (GCP). Elective hysterectomy patients were approached by a part-time research midwife only. Each patient was provided with a brief verbal overview of the project, followed by an explanation of their voluntary role in the study. The patient was then given time to consider and discuss the details of the study with the researcher if required. If the patient wished to proceed, a consent form was signed and dated in triplicate by both parties to validate inclusion into the study. Each research participant was given a copy of the signed consent form to keep, and issued with a unique experimental code to maintain patient anonymity. This consisted of a letter representing the origin of the sample, followed by a number representing the number of total samples obtained at the time of consent. All myometrial samples from this point onward were identified by their unique experimental code. Copies of the study consent forms for women undergoing caesarean section deliveries and hysterectomy procedures, and pregnancy research study information sheet can be found in the appendices.

One myometrial biopsy per patient measuring approximately 2 x 2 x 2 cm^3 was obtained from the upper margin of the lower uterine segment incision madeduring the caesarean section, or from the anterior wall of the lower uterine body following hysterectomy (**See Figure 2-1**). Once taken, biopsies were placed immediately in chilled physiological salt solution (PSS) (**See Appendix**) for transportation to the laboratory. Once received, biopsies were placed in freshly aerated (5% CO_2/95% O_2) PSS, and either used immediately or stored at 4^oC for use within 12-hours.

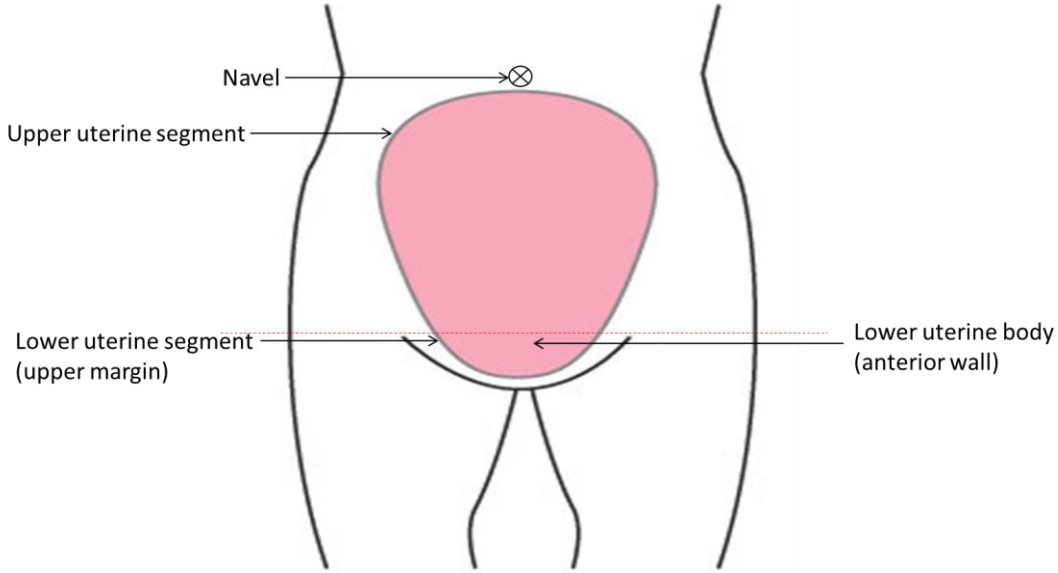


Figure 2-1. Diagram showing the location of biopsy sampling for both elective caesarean and hysterectomy patients. Myometrial biopsies measuring ~2 x 2 x 2 cm^3 were obtained from the upper margin of lower uterine margin during caesarean section, or at from the anterior wall of the lower uterine body after hysterectomy procedures *(Adapted from* http://medical-dictionary.thefreedictionary.com/cesarean+section*).*

2.3 Patient demographics

A total of 155 myometrial biopsies were used over the three-year period of this study, of which 92 biopsies were used for validation purposes or discarded and not used for analysis. Biopsies were discarded due to poor or inadequate spontaneous contractile activity based on an assessment of viability (**See Chapter 2.5.3**). In total, 63 patients were included in the study analysis consisting of 59 biopsies obtained from caesarean section patients, and 4 biopsies obtained from hysterectomy patients. The demographic characteristics of the study participants included in the analysis are displayed below (**See Table 2-1**).

Table 2-1. Table showing the characteristics of patients undergoing caesarean deliveries and hysterectomy procedures who participated in this study.

Caesarean delivery patients	
Age (years)	31.4 ± 6.2
Gravidity	3 [2 – 4]
Parity	1.5 [1 – 3]
Number of prior CD	1 [0 – 1]
Gestational age (weeks)	39.4 ± 2.4
Race/Ethnicity	
Caucasian	51 (68.4%)
African	1 (1.7%)
Asian	3 (5.1%)
Mixed-race	3 (5.1%)
Other	1 (1.7%)

Hysterectomy procedure patients	
Age (years)	44.2 ± 7.6
Parity	2 [1 – 3]
Race/Ethnicity	39.4 ± 2.4
Caucasian	3 (75%)
Mixed-race	1 (25%)

(CD=caesarean delivery; data reported as mean ± the standard deviation (SD), median [Interquartile range (IQR)], or number of participants (%).

2.4 Myometrial cell culture

Myometrial cells were prepared and cultured in Class II microbiological safety cabinets using aseptic cell culture techniques. Cultured myometrial cells were grown and maintained in complete cell medium containing Dulbecco's Modified Eagle Medium (DMEM) supplemented with 7% fetal calf serum (FCS) and penicillin/streptomycin (100U/100µg/mL), incubated at 37^{o}C under humidified conditions in a 5% CO_2 air mixture. Myometrial cells were cultured and used at up to passage 4 in all experiments. All materials used for cell culture protocols were purchased in sterile packaging or first sterilised in an Astell autoclave at 121^{o}C (Astell Scientific Ltd. Kent). Antiseptic solutions used consisted of a 70% industrial methylated spirit (IMS) solution made up in distilled water, and applied to all instruments introduced into sterile

environments. A 5% Trigene solution (Scientific Laboratory Supplies, UK) was used to clean surfaces before and after experimentation.

Myometrial biopsies were finely minced using a large (22mm) round-headed scalpel in collagenase (from *Clostridium histolyticum* (2mg/mL)), diluted in fresh Ca^{2+} and Mg^{2+}-free Hanks Balanced Salt solution (HBSS), and passed through a 0.22μM diameter filter (Millipore) to remove any residual tissue debris. The sample was then mechanically broken down via gentle trituration using a 10mL syringe, then incubated at 37^{o}C to promote enzyme activity for 30-mins. The resultant sample suspension was then centrifuged at 2000 revolutions per minute (rpm) for 5-mins in an Eppendorf 5804 lab centrifuge (Eddendorf UK Ltd., Stevenage). The supernatant was then aspirated and the cell pellet re-suspended in 5mL of complete cell medium to neutralise collagenase activity. After an additional centrifugation at 2000 rpm for 5-mins, the cell pellet was re-suspended in complete cell medium, transferred to a T25 cell culture flask (Greiner Bio One) and incubated in a Sanyo CO^2 incubator (Sanyo, Loughborough). Spent cell medium was aspirated and refreshed on alternate days. Evidence of cell infection and overall cell health was monitored daily under light microscopy.

2.4.1 Myometrial cell passage

Myometrial cells were grown to between 75 – 80% confluence in a T25 cell culture flask before passage. Spent cell medium was aspirated and cells washed twice in 5mL of HBSS to remove any residual traces of the cell medium. Cells were then enzymatically detached using a 0.025%

trypsin/EDTA solution (Thermo Fisher, UK) for 5-mins in 37^{o}C, followed by a further 2-mins of careful shaking to ensure complete cell detachment from the flask plastics. The cell suspension was then collected into 14mL Falcon tubes and an equal volume of fresh complete cell medium was added to the suspension to neutralise trypsin activity. Cells were centrifuged for 5-mins at 2000 rpm and the resultant cell pellet was washed twice in fresh HBSS. The cell pellet was then re-suspended in 10mL of complete cell medium and transferred into a T50 cell culture flask (Greiner Bio One) for incubation.

2.5 Myometrial tissue contractility

For tissue contractility experiments, myometrial biopsies were placed into a 60mm petri dish containing 10mL of freshly aerated PSS for dissection. The tissue was then cut along the longitudinal plane of the muscle fibres into individual 3 x 3 x 10mm^3 myometrial tissue strips. Care was taken to remove any adjacent serosal, decidual, and necrotic tissues that may affect the generation of spontaneous contractions. Each strip was then carefully attached to a mounting hook using a piece of cotton thread and suspended inside an organ bath (Panlab, ADInstruments, Oxford). Each organ bath was filled with pre-warmed PSS maintained at 37^{o}C, and continuously aerated with 5% CO_2/95% O_2 throughout the duration of the experiments (**See Figure 2-2**). After each experiment, used organ baths were cleaned immediately with repeated ddH_2O washes. Once a month, the whole contractility apparatus was disassembled and subjected to a complete clean and transducer re-calibration (**See Chapter 2.5.1**).

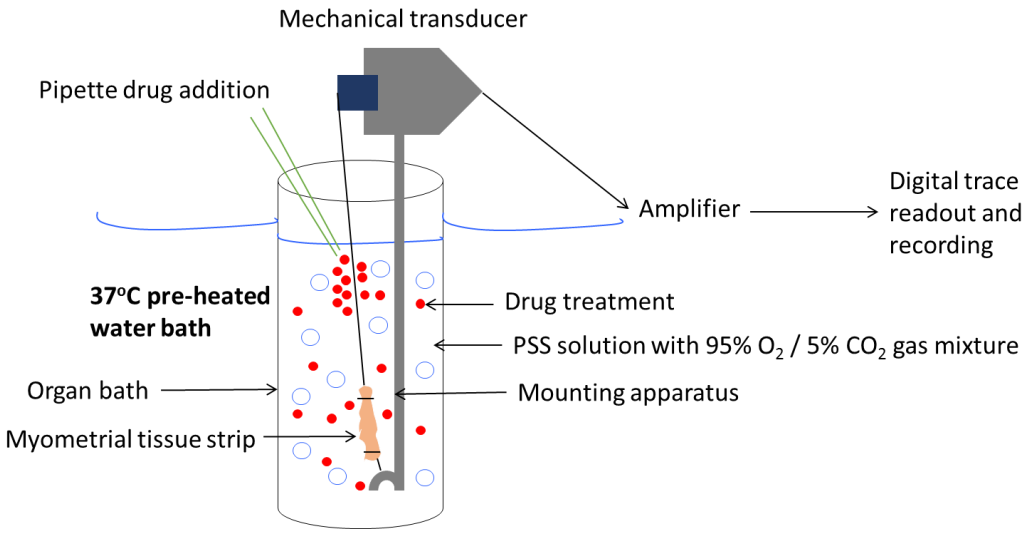


Figure 2-2. Diagram showing a dissected and mounted myometrial tissue strip suspended in an organ bath for contractile force experimentation.

2.5.1 Contractility transducer calibration

Before experimentation, each organ bath transducer was calibrated to ensure accurate force measurements and unit conversion. This was conducted using a dedicated calibration program within the Powerlab LabChart ver. 6.0 software at monthly intervals. At the start of a transducer calibration, a raw trace measuring detected force over a period of 10-seconds was recorded, showing the reflection created from zero applied tension, and the tension created when a 10g weight was suspended on the transducer. This trace was then visualised in the Powerlab LabChart ver. 6.0 software Unit Converter program and a 2-point calibration sequence was conducted. The reflection observed with zero tension and with the addition of 10g, was converted into 0 and 98.1 millinewtons of force (mN) respectively. This process was repeated for each transducer on the contractility apparatus and the calibration settings saved for subsequent contractility experiment.

2.5.2 Myometrial tissue length tension optimisation

At the start of this study, dissected myometrial tissue strips were subjected to preliminary length tension experiments. This was conducted to calculate the minimum tissue tension required to produce measurable and consistent contractions during experimentation.

Dissected myometrial tissue strips were mounted in an organ bath containing aerated PSS and held at slack length for 30-mins, whereby no downward deflection was observed but any additional increase in tension produced a visual reflection on the recorded raw trace. After 30-mins, tissue strips were suspended in a high (60mM) K^+ salt solution (KPSS) for 5-mins (**See Appendix**) to induce a contraction. Tissue strips were then re-suspended in PSS for 10-mins, and additional tension was placed on the tissue for a further 10-mins. This additional tension was generated by increasing the length of the tissue by 1mm increments (**See Figure 2-3**). This process was repeated until the addition of 60mM KPSS produced a strong and consistent contraction, with no observed reduction in baseline tension after 5-mins.

For myometrial tissues, our preliminary length tension studies observed that a tension of 20mN was sufficient to elicit measurable and consistent contractions, without loss of force through lack of tissue tension. In all subsequent contractility experiments, myometrial tissue strips were subjected to a starting tension of 20mN before the generation of spontaneous contractions. Protocols for myometrial tissue strip dimension, dissection,

length tension optimisation experiments, and apparatus choice were selected based on previous work by Khan et al. (2004a; 2004b; 2005a; 2005b; 2010).

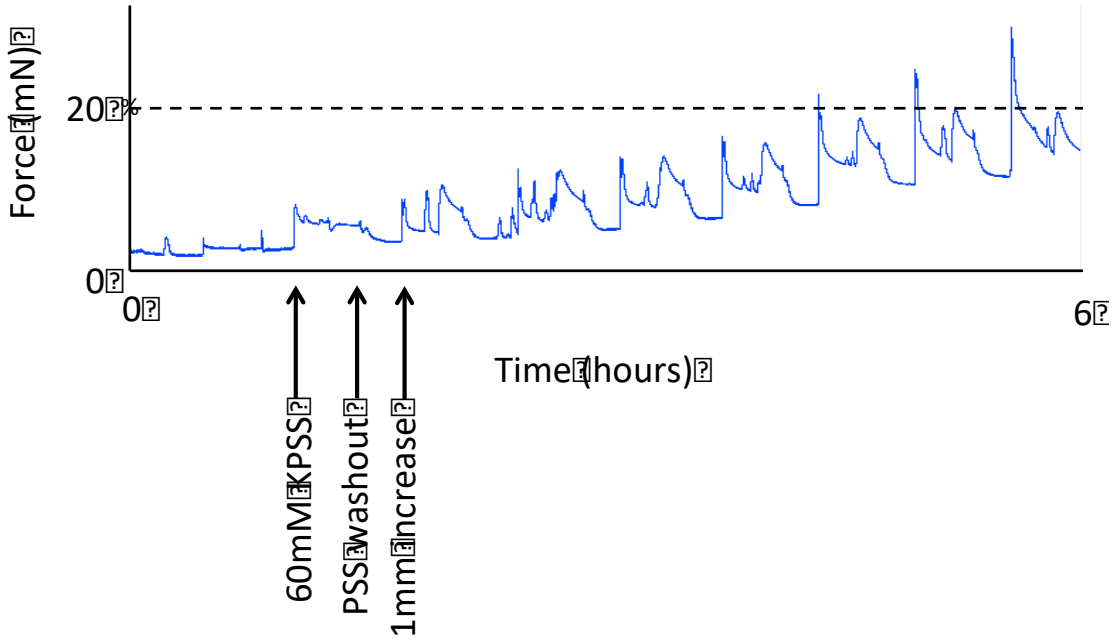


Figure 2-3. Representative raw contractility trace showing changes in force (mN) after exposure to high KPSS, followed by 1mm incremental increases in tissue length, achieving consistent contraction magnitude and baseline after application of 20mN of force.

2.5.3 Assessment of myometrial tissue viability

Viable myometrial tissue samples were selected based on observed consistent spontaneous contractions, with a minimum peak contractile force of 10mN. This value was based on previously published data from our group by Khan et al. (2004a; 2004b; 2005a; 2005b; 2010), and from those investigating similar parameters using tissue contractility protocols relevant to this study (Smith et al., 2005). Any tissue samples that did not meet the minimum peak contractile force were excluded from the study. Contraction stimulation by a high KPSS was used to assess tissue viability at the end of each experiment

to avoid any potential interference with contractions by KPSS exposure (**See Figure 2-4**). Tissues that failed to respond to high KPSS stimulation were also excluded from the study.

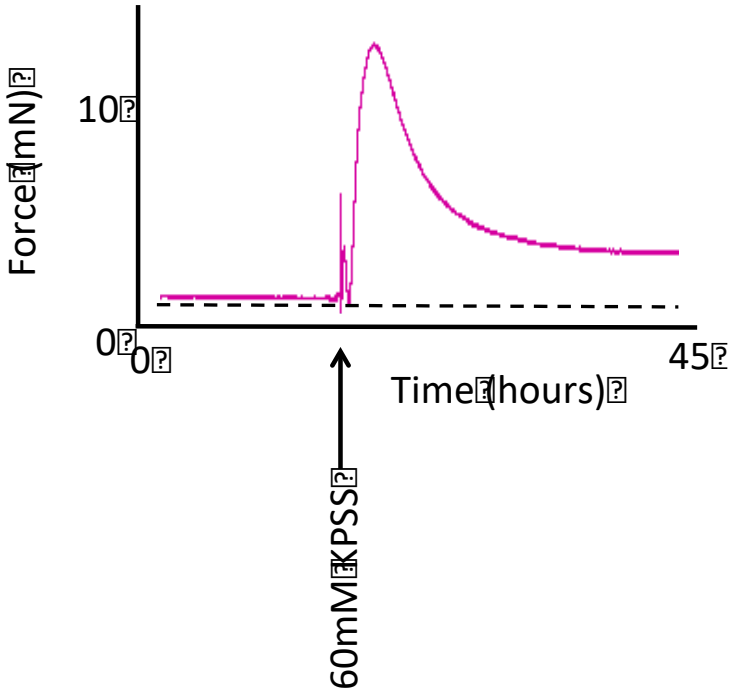


Figure 2-4. Representative raw contractility trace showing myometrial tissue response to exposure with a high KPSS at the end of experimentation.

2.5.4 Myometrial tissue contractility experimental conditions

2.5.4.1 Simvastatin

Simvastatin was reconstituted in a 0.1% dimethyl sulfoxide (DMSO) solution (**See Appendix**) and a concentration-response curve performed. For tissue contractility experiments, cumulative additions relative to each concentration of simvastatin (3.3nM – 330μM) was added directly to the organ bath every 45-mins, and changes in spontaneous contractions recorded. For cell culture in-vitro experiments, simvastatin (3.3μM – 33μM) was added directly to myometrial cells.

2.5.4.2 Methyl- β-cyclodextrin

MCD is a member of the cyclodextrin family of glucose monomer compounds, with a high binding affinity for several aromatic and aliphatic molecules (Formoso, 1973). MCD forms soluble complexes with cholesterol and increases cholesterol solubility in aqueous solutions. In cells, MCD exposure results in the perturbation of the membrane (Rodal et al., 1999).

MCD was reconstituted in PSS and used as a comparative cholesterol-depleting agent to simvastatin. For tissue contractility experiments, MCD was added independently at a single concentration of 330μM, in cumulative doses (330μM – 33mM), and in the presence of simvastatin (33nM - 330μM) at a single concentration of 15mM. All experimental concentrations of MCD were taken from published data in rat myometrial tissue, using concentrations of 330μM – 33mM (Smith et al., 2005).

2.5.4.2 Water-soluble cholesterol

Water-soluble cholesterol was reconstituted in PSS and used as a cholesterol-replenishing agent, added at a concentration of 0.5mM immediately after the exposure to a single concentration of simvastatin (330μM) in tissue contractility experiments. Experimental concentrations of water-soluble cholesterol were taken from published data in both human and guinea pig myometrial tissue (Wray et al., 2004; Vittori & Buxton, 2005).

2.5.4.3 NG-nitro L-arginine methyl ester

NG-nitro L-arginine methyl ester (L-NAME) is a member of the L-arginine substrate family and is known to be a specific inhibitor of NO via eNOS inhibition (Knowles et al., 1989; Moore et al., 1990). L-NAME was reconstituted in PSS and added at a concentration of 300μM in the presence of simvastatin (33nM - 330μM) in tissue contractility experiments. Experimental concentrations of L-NAME were taken from published data using human myometrial small arteries (Kenny et al., 2002). Although L-NAME was used at 100μM in this study, it was decided that a higher concentration of 300μM would be used to ensure sufficient inhibition of eNOS in the much larger myometrial tissue strips. Spontaneously contracting myometrial tissues were pre-incubated with L-NAME for 45-mins before simvastatin co-incubation

2.5.4.4 Mevalonate

Mevalonate is a cholesterol pre-cursor molecule and a product of HMG-CoA reduction by the HMG-CoA reductase enzyme (Ferguson et al., 1959). In tissue contractility experiments, mevalonate was reconstituted in PSS and added at a concentration of 200μM immediately after the addition of a single concentration of simvastatin (330μM). Experimental concentrations of mevalonate were taken from published data investigating the effects of mevalonate replenishment on arterial smooth muscle function (Ali et al., 2011; Copaja et al., 2011).

2.5.4.5 Geranyl-geranyl-pyrophosphate

GGPP is an isoprenoid protein formed from the condensation of IPP and DPP in the HMG-CoA reductase pathway (Casey, 1992; Moomaw and Casey, 1992), and is inhibited by simvastatin independent of cholesterol inhibition (Ali et al.; Kinsella and Maltese, 1992; Lachance et al.).

In tissue contractility experiments, GGPP was reconstituted in PSS and added at a concentration of 20μM immediately after the addition of a single concentration of simvastatin (330μM). Experimental concentrations of GGPP were taken from published data investigating the effects of simvastatin on arterial and internal anal sphincter smooth muscle tone (Rattan, 2010; Seto et al., 2007).

2.5.4.6 Tetraethylammonium chloride

TEA is a quaternary ammonium cation originally used as an autonomic ganglia blocker (Freyburger et al., 1950; Honda, 1971). In skeletal muscle and pituitary cells, TEA acts as a blocker of voltage-operated K^+ and Ca^{2+}-operated K^+ channels (Khan et al., 1993; Khan et al., 1997; White et al., 1993).

In tissue contractility studies, TEA (5mM) was reconstituted in PSS and added in the presence of simvastatin (33nM - 330μM). Experimental concentrations were derived from previously published work by our group in human myometrial tissues (Khan et al., 1993). Spontaneously contracting myometrial tissues were pre-incubated with TEA for 45-mins before simvastatin co-incubation.

2.5.4.7 BayK 8644

BayK 8644 is a member of the 1,4-dihydropyridine family of chemical compounds, known to be both Ca^{2+} agonists and antagonists. BayK 8644 is a derivative of nifedipine, which acts as a positive inotropic agent (Schramm et al., 1983a; Schramm et al., 1983c). However, unlike nifedipine, which is a specific Ca^{2+} channel blocker (Vater et al., 1972), BayK 8644 acts as both a competitive antagonist of nifedipine and a Ca^{2+} agonist, resulting in an increase in Ca^{2+} influx by activating VOCCs (Schramm et al., 1983a; Schramm et al., 1983c).

BayK 8644 was reconstituted in PSS and added at a concentration of 1μM in the presence of simvastatin (33nM - 330μM). Experimental concentrations of BayK 8644 were derived from published data investigating the effects of $[Ca^{2+}]i$ inhibition on human myometrial contractility (Heaton et al., 1993). Spontaneously contracting myometrial tissues were pre-incubated with BayK 8644 for 45-mins before simvastatin co-incubation.

2.5.4.8 Apamin

Apamin is a peptide neurotoxin found in bee venom and has been shown to specifically inhibit SK channels (Hugues et al., 1982a; Hugues et al., 1982b). In tissue contractility experiments, apamin was reconstituted in PSS and added at a concentration of 500nM in the presence of simvastatin (33nM - 330μM). Experimental concentrations were taken from published data investigating the function of SK channels in the rat myometrium (Noble et al., 2010). Spontaneously contracting myometrial tissues were pre-incubated with apamin for 45-mins before simvastatin co-incubation.

2.5.4.9 Paxilline

Paxilline is a tremorgenic alkaloid mycotoxin, which stimulates the binding of charybdotoxin to BK channels resulting in their inhibition (Knaus et al., 1994). Paxilline was reconstituted in PSS and added at a concentration of 1μM in the presence of simvastatin (33nM - 330μM) in tissue contractility experiments. Experimental concentrations of 1μM were taken from published work by our group, investigating the effects of BK channel inhibition in human myometrial tissue (Chanrachakul et al., 2004). Spontaneously contracting myometrial

tissues were pre-incubated with paxilline for 45-mins before simvastatin co-incubation.

2.6 Total cholesterol and protein assay

For total cholesterol and protein assay experiments, myometrial cells were seeded onto 6-well cell culture plates at a concentration of 100,000 cells per well, and cultured overnight in a 5% CO_2 air mixture incubator at 37^oC to between 75% - 80% confluence before experimentation. Spent cell medium was aspirated and washed twice in PSS to remove any residual traces of cell medium, before being resuspended in 5mL of fresh PSS. Myometrial cells were exposed to 3.3μM, 10μM, and 33μM concentrations of simvastatin over 45-mins, 4-hours, and 24-hours. 15mM MCD was used as a positive control for cholesterol assay experiments, and a negative control for protein assay experiments. Simvastatin concentrations were derived from myometrial tissue contractility experiments to reflect the effective concentration range that elicited a statistically significant change in spontaneous contractions.

Cell treatment solutions were pipetted directly into each well and placed into an 5% CO_2 air mixture incubator at 37^oC. After each time point, cells were removed from the incubator and washed twice in PSS to remove any residual traces of treatment solution, before being lysed in 200L of myometrial cell lysis buffer (**See Appendix**) per well on ice for 10-mins. Cells that were still attached to the plastic were dislodged using a cell scraper, and the resultant cell suspension was triturated using a pipette before being transferred into individual Eppendorf tubes (Eddendorf UK Ltd., Stevenage). The cell suspension was centrifuged at 2000 rpm and 4^oC for 15-mins using a Sanyo Falcon 6/300 refrigerated centrifuge (Sanyo, Loughborough), and the

resultant supernatant snap frozen in liquid nitrogen (N_2) for storage at -80^{o}C until required.

2.6.1 Amplex red® cholesterol assay protocol

Total myometrial cell cholesterol concentration was measured using the Amplex red® cholesterol assay kit (Life Technologies, UK) to investigate changes in cholesterol after simvastatin treatment over time. All cholesterol assay reagents were prepared in advance according to the Amplex red® cholesterol assay kit manufacturer's protocol (**See Appendix**). Changes in cholesterol were quantified via the detection of hydrogen peroxide (H_2O_2), a by-product of cholesterol oxidation. In the presence of horse-radish peroxidise (HRP), the Amplex red® reagent reacts with H_2O_2 to produce the fluorescent molecule resorufin, which can be detected using a fluorescence plate reader (Zhou et al., 1997; Zhou and Panchuk-Voloshina, 1997).

The collected sample supernatants were removed from -80^{o}C and thawed slowly on ice. A 1:10 dilution was made using 1M phosphate buffered saline (PBS) and transferred into a blacked-sided, clear-bottomed 96-well cell culture plate (NUNC, UK). 50µL of diluted sample was mixed with 50µL Amplex red® reagent per well, and incubated for 30-mins at 37^{o}C under constant agitation in the dark. After incubation, the plate was placed into a Thermo Fluoroskan Ascent F2 fluorescence plate reader (Thermo Fisher, UK), and read at an excitation wavelength between 530nm – 560nm and a detection wavelength of 590nm. An additional positive cholesterol control was created by adding a 10µM H_2O_2 solution diluted in 1M PBS.

For every experiment, a cholesterol standard curved was created to determine the percentage change in cholesterol compared to positive controls in each experimental sample, and to validate the viability and accuracy of the assay. Standard curves were constructed using the provided cholesterol standard (2mg/mL) found in the manufacturers kit. The standard was diluted in the manufacturers' sample buffer to produce a cholesterol concentration range of 0 - 10µg/mL. Standard curves that did not produce a final r^2 value of 0.50 were rejected and any associated data not subjected to further analysis.

2.6.2 BCA protein assay protocol

Total myometrial cell protein concentration was measured using a bicinchoninic acid (BCA) protein assay to investigate changes in protein concentration after simvastatin treatment over time. Changes in protein concentration were quantified by the reduction of Cu^{2+} to Cu^{1+} by amino acids such as cysteine, tryptophan, tyrosine. BCA forms a complex with Cu^{1+} in alkaline conditions, resulting in a purple-blue solution that can be detected using a fluorescence plate reader (Smith et al., 1987).

The collected sample supernatants were removed from -80^{o}C and thawed slowly on ice. Samples were diluted in 1M PBS at a ratio of 1:100 and transferred into a clear 96-well cell culture plate (Greiner Bio One). 10µL of diluted sample was mixed with 150µL of BCA working solution per well, and incubated for 30-mins at 37^{o}C under constant agitation in the dark. After incubation, the plate was placed into a Wallac Victor 1420 multi-label counter

plate reader (Perkin Elmer, US) and read at a maximum excitation wavelength of 570nm.

In all experiments, a protein standard curve was used to determine the percentage change in protein compared to positive controls in each experimental sample, and to validate the viability and accuracy of the assay. Standard curves were constructed using a 1mg/mL bovine serum albumin (BSA) solution made up in myometrial lysis buffer. The stock solution was further diluted in myometrial lysis buffer to produce a concentration range of 0 – 0.95 mg/mL. Standard curves that did not produce a final r^2 value of 0.50 were rejected and any associated data not subjected to further analysis.

2.7 Intracellular FLUO-4AM® Ca^{2+} assay

Changes in myometrial cell basal and oxytocin-induced increases in $[Ca^{2+}]i$ after immediate simvastatin exposure, were measured using the FLUO-4M® Ca^{2+} assay (Thermo Fisher, UK). This assay utilised the manufactured FLUO-4AM fluorophore, which is transported into cells upon exposure. The FLUO-4AM® fluorophore contains a Ca^{2+} selective 1,2-bis (aminophenoxy)-ethane-tetraacetic acid (BAPTA)-like chelator, which is linked to a fluorogenic, fluorescein-like component with an excitation wavelength of 488nm.

2.7.1 Intracellular FLUO-4AM® Ca^{2+} assay protocol

All FLUO-4AM® assay reagents were prepared in advance according to the manufacturer's instructions (**See Appendix**). Myometrial cells were seeded at a concentration of 50,000 cells per well onto a black walled, blacked-sided, clear-bottomed 96-well cell culture plate (NUNC, UK), and incubated in a 5% CO_2 air mixture incubator at 37^{o}C overnight until a cell confluence of between 75% - 80% was reached. Spent cell medium was aspirated, and cells were washed twice with PSS. 100µL of a pre-prepared FLUO-4AM® working solution was transferred to each well and incubated for a further 45-mins at 37^{o}C. Following incubation, cells were placed into a Thermo Fluoroskan Ascent F2 fluorescence plate reader (Thermo Fisher, UK) and set to record 1000 events at 3 ms intervals for a total duration of 24-seconds. Plates were read at an excitation wavelength of 485nm and an emission wavelength of 538nm.

All treatments were added during recording by pipetting directly into each well via a porthole in the lid of the plate reader, using a custom-made long-tipped pipette (**See Figure 2-5**).

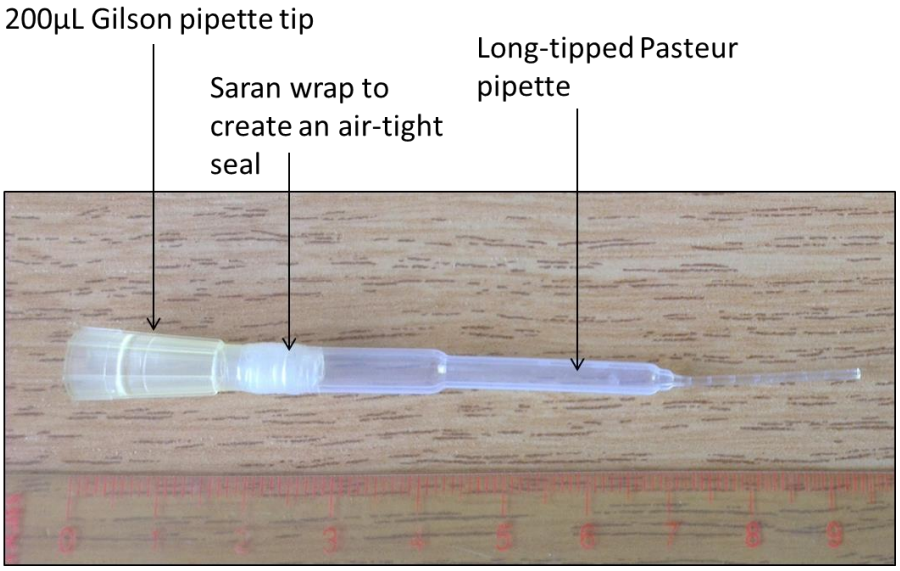


Figure 2-5. Photo showing the custom-made pipette tips used to transfer up to 200µL of solutions into the each well of a 96-well cell culture plate during recording, using a Thermo Fluoroskan Ascent F2 fluorescence plate reader.

To determine the effects of simvastatin exposure on basal $[Ca^{2+}]i$, myometrial cells were exposed to 3.3µM, 10µM, and 33µM concentrations of simvastatin, and resultant changes in fluorescence recorded for 24-seconds. To determine the effects of simvastatin on oxytocin-induced increase in $[Ca^{2+}]i$, cells were exposed to the same concentrations of simvastatin immediately after the addition of oxytocin (2µM), reconstituted in PSS.

2.8 FLIPR® Ca^{2+} 5 assay

Changes in oxytocin-induced increase in $[Ca^{2+}]i$ in the myometrial cell after overnight exposure to simvastatin, was measured using the FLIPR® Ca^{2+} 5 assay. The FLIPR® Ca^{2+} 5 fluorophore is an enhanced analogue of the FLUO-4AM® fluorophore, which produces a larger fluorescent signal in the presence of free Ca^{2+}. Furthermore, the fluorophore is suspended in a masking solution that decreases non-specific background fluorescence during measurement.

2.8.1 FLIPR® Ca^{2+} 5 assay protocol

All FLIPR® Ca^{2+} 5 assay reagents were prepared in advance according to the manufacturer's instructions (**See Appendix**). Myometrial cells were grown to between 75 – 80% confluence in T75 cell culture flasks at the laboratories in the School of Graduate Entry Medicine, Derby, and transported to the laboratories located at the School of Medicine at the Queens Medical Centre, Nottingham. Upon arrival, cells were enzymatically detached with 5mL of 0.25% trypsin/EDTA solution for 5-mins. The cell suspension was mixed with 10mL of complete cell medium and centrifuged for 5-mins at 2000 rpm. The resultant cell pellet was washed twice in cell medium and seeded at a concentration of 40,000 cells per well onto a black walled, blacked-sided, clear-bottomed 96-well cell culture plate (NUNC. UK), and incubated in a 5% CO_2 air mixture incubator at 37^{o}C overnight to allow the formation of a confluent monolayer.

To determine the effects of overnight simvastatin exposure on oxytocin-induced increase in $[Ca^{2+}]i$, myometrial cells were exposed to 3.3μM, 10μM, and 33μM concentrations of simvastatin overnight for 18-hours. After treatment, the cell medium was aspirated, and 100μL of FLIPR® Ca^{2+} 5 fluorophore loading solution was transferred to each well, and incubated in a 5% CO_2/95% air mixture incubator at 37ºC for 30-mins in the dark. After incubation, cells were left to acclimatise at room temperature for 15-mins, before being placed into incubator of a FlexStation 3 microplate reader, pre-heated to 25ºC. Oxytocin (10μM) was added directly to cells in each well by the FlexStation 3 microplate reader treatment pipetting system, and resultant changes in fluorescence recorded at 1.6-second intervals for 260-seconds, at an excitation wavelength of 485nm and an emission wavelength of 525nm.

2.9 Hoechst 33342 dye tracer permeability assay

The Hoechst 33342 dye tracer is a fluorescent molecule commonly used to identify nuclear material in cells by binding to the adenine and thymine sites located in the nucleus. Detection occurs through excitation by ultra-violet (UV) light, resulting in a detectable blue light at wavelengths of between 510 – 540nm. In several studies, Hoechst 33342 has also been used as a probe to measure changes in cell membrane permeability (Dehelean et al., 2012; Hubbard et al., 2012; Lalande et al., 1981; Zhao et al., 2012). In this experiment, Hoechst 33342 was used as a tracer to determine changes in myometrial cell permeability after exposure to simvastatin.

2.9.1 Hoechst 33342 dye tracer permeability assay protocol

Myometrial cells were grown to between 75 – 80% confluence in T25 cell culture flasks at the laboratories in the School of Graduate Entry Medicine, Derby, and transported to the clinical laboratories located at the School of Veterinary Medicine and Science in Sutton Bonington. Upon arrival, cells were enzymatically detached with 5mL of 0.25% trypsin/EDTA solution for 5-mins. The resultant cell suspension was mixed with 10mL of complete cell medium and centrifuged for 5-mins at 2000 rpm. The cell pellet was then washed twice in PSS and transferred into a white, blacked-sided, clear-bottomed 96-well cell culture plate (NUNC, UK), seeded at a concentration of 50,000 cells per well, and placed into the 37^{o}C pre-heated incubator of a FLUOstar OPTIMA plate reader (BMG Labtech, Germany).

To determine the effects of simvastatin on myometrial cell permeability to Hoechst 33342 dye tracer, cells were exposed to 3.3μM, 10μM, and 33μM concentrations of simvastatin in the presence of Hoechst 33342 (8μM). Changes in emitted blue light were recorded for 55-seconds at a wavelength of between 510 – 540nm.

2.10 Immunocytochemistry

Immunofluorescence imaging involves the specific binding of one or more primary antibodies to their antigens on the target tissue or cell sample. This involves using a primary antibody manufactured to recognise a specific component in the tissue or cell, which is then bound to a secondary antibody conjugated to a fluorescent probe. The excitation of the fluorescent probe allows any primary antibody-tagged structures to be observed under fluorescent microscopy (Cuello et al., 1983; Valnes and Brandtzaeg, 1982).

Most antibodies used in immunocytochemical experiments are G immunoglobulins (IgG). These are Y-shaped molecules consisting of two identical light, and heavy chains. The light chains contain a C-terminal half and a variable N-terminal half, which can bind to a specific antigen via non-covalent bonds (De Preval et al., 1970; Edelman et al., 1969; Milstein and Pink, 1970) (**See Figure 2-6**).

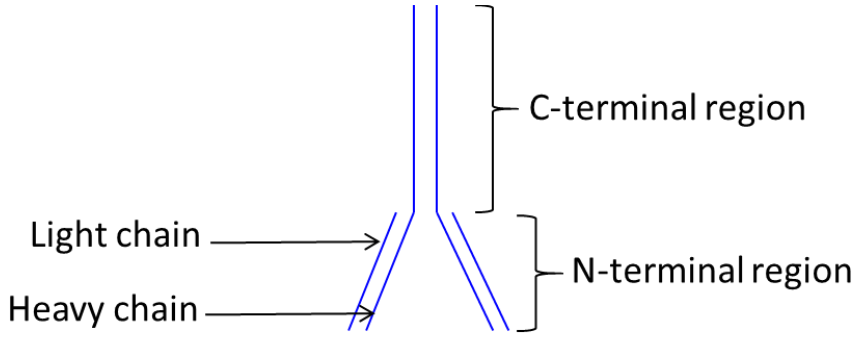


Figure 2-6. Diagram showing the basic structure of a primary IgG antibody (*Adapted from Milstein and Pink, 1970*).

Once bound to the antigen, a secondary antibody manufactured against the species, in which the primary antibody was raised, can bind to the C-terminal region of the primary antibody. This binding can be detected if the secondary antibody is conjugated to a fluorescent reporter molecule, resulting in the production of fluorescence after excitation by a light or a laser emitting a suitable range of wavelengths (**See Figure 2-7**).

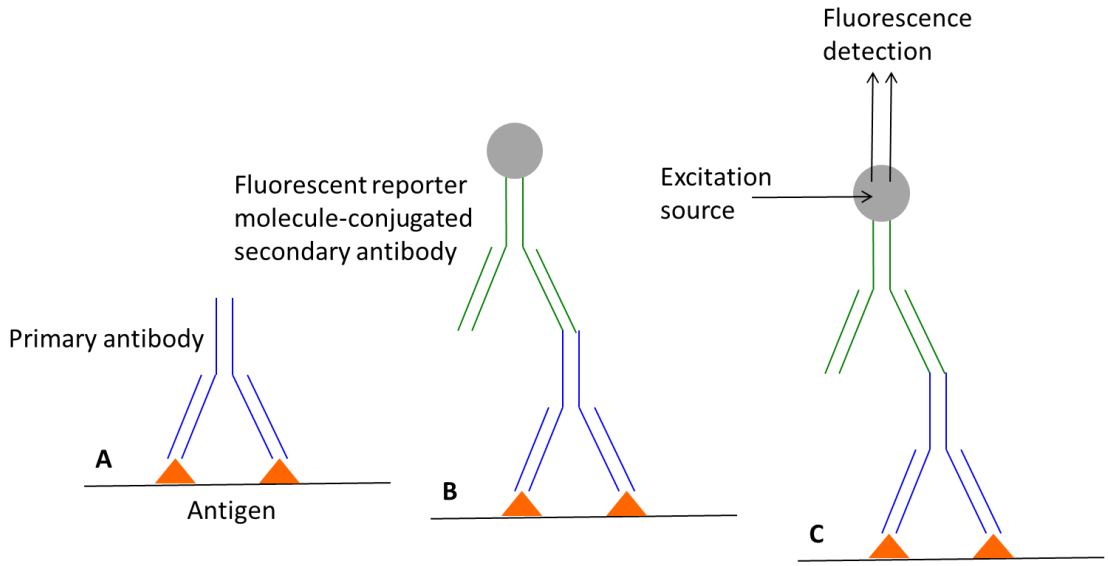


Figure 2-7. Diagram showing the interaction between (**A**) the primary antibody binding to exposed antigens on the cell or tissue sample surface, (**B**) a fluorescent reporter-conjugated secondary antibody binding to the primary antibody, and (**C**) excitation of the secondary antibody fluorescent reporter and detection of the emitted fluorescence (*Adapted from Milstein and Pink, 1970*).

2.10.1 α-actin and caveolin-1 protein expression by immunocytochemistry protocol

Changes in myometrial cell expressions of α-actin and caveolin-1 protein after exposure to simvastatin and MCD were investigated. Myometrial cells were seeded onto sterile 0.27mm glass coverslips at a concentration of 50,000 cells per coverslip, and incubated in a 5% CO_2 air mixture incubator at 37^{o}C overnight. Once a confluent monolayer was formed, cells were exposed to 3.3μM, 10μM, and 33μM concentrations of simvastatin, and 330μM of MCD over 45-mins, 4-hours, and 24-hours. After each time point, cells were removed from the incubator and the treatment solution aspirated before cell fixation for immunocytochemical probing.

2.10.2 Cell fixation and non-specific blocking

Cells were fixed to preserve any treatment-induced changes to cellular structures after experimentation. A 4% paraformaldehyde (PFA) solution (**See Appendix**) was used as the chosen fixative in this experiment. Cells were fixed with a 4% PFA solution for 20-mins at room temperature and washed three times with a with 0.1% BSA/PBS buffer solution (**See Appendix**). Cells were then permeabilised with a 0.5% Igepal detergent solution (**see Appendix**) for 15-mins at 4^{o}C to facilitate antibody penetration into the cell. This detergent was chosen over the commonly used Triton X-100 solution in immunofluorescence experiments using myometrial cells (Khan et al., 2009). This was because Triton X-100 has been shown to disrupt lipid structures, such as caveolae, which may interfere with our experiments (Hooper, 1999). After permeabilisation, cells were washed three times in a 0.1% BSA/PBS

buffer solution and blocked with a 5% normal goat serum blocking solution (**See Appendix**) for 1-hour at room temperature. Incubation in a blocking solution was used to prevent any non-specific binding of antibodies once the primary antibody is introduced.

2.10.3 Primary antibody incubation

Primary antibodies were prepared in a 5% normal goat serum blocking solution at a dilution ratio of 1:500. 200µL of the primary antibody working solution was transferred to relevant wells and incubated under constant agitation overnight at 4^{o}C. The properties of each primary antibody used in this experiment are displayed below (**See Table 2-2**).

Table 2-2. Table showing the properties of the caveolin-1 and α-actin primary antibodies used for immunocytochemical experiments in this study.

Antibody	Epitope	Species	Manufacturer	Dilution
Caveolin-1	N-terminal	Mouse	Sigma-Aldrich	1:500
α-actin	C-terminal	Rabbit	Sigma-Aldrich	1:500

2.10.4 Secondary antibody

Secondary antibodies conjugated with a fluorescein isothiosyanate (FITC) fluorescent reporter were used to visualise the expression, and location of bound caveolin-1 and α-actin primary antibodies. Successful binding of the secondary antibody produced a detectable fluorescent emission when excited by light of a specific wavelength range, observable via the correct filter on a fluorescence microscope.

After incubation, the primary antibody solution was aspirated, and cells washed three times in 0.1% BSA/PBS buffer solution. Secondary antibodies were prepared in 5% normal goat serum blocking solution at a dilution ratio of 1:50. The secondary antibody working solution was transferred to relevant wells and incubated under constant agitation for 2-hours at room temperature. After incubation, the secondary antibody was aspirated, and cells were washed a further three times in 0.1% BSA/PBS buffer solution before being prepared for visualisation. In all experiments, relevant antibody negative controls were conducted to determine evidence of auto-fluorescence and non-specific binding of antibodies. The properties of the secondary antibody used in this experiment are displayed below (**See Table 2-3**).

Table 2-3. Table showing the properties of the FITC-conjugated secondary antibody used for immunocytochemical experiments in this study.

Antibody	Epitope	Species	Manufacturer	Dilution
FITC-labelled	Heavy chain of rabbit/mouse IgG, IgA and IgM	Rabbit/Mouse	Sigma-Aldrich	1:50

2.10.5 Slide preparation for immunofluorescence imaging

Before visualisation, coverslips were carefully lifted from each well with a pair of fine watch-maker forceps (Fisher Scientific, UK), and placed onto an un-treated glass slide. Fixed cells were treated with 10µL of Vectashield mounting media containing 4',6-diamidino-2-phenylindole (DAPI) (Vectashield), to preserve fluorescence for repeated viewings over time and to identify the cell nucleus. Colourless nail varnish was applied to the edges of each coverslip and allowed to dry before viewing. All slides were stored in opaque slide boxes to avoid exposure to light and stored at 4^{o}C. Slides were visualised using a Zeiss Axiovert 25 CFL fluorescence microscope (Zeiss, UK). Bright field and fluorescent images were captured using an Olympus DP70 Cell-F digital camera (Olympus, UK) for visual assessment and analysis.

2.11 Study experimental data analysis

Before experimentation, an estimated required study sample size of four patients per experiment repeat was obtained from previously published studies in our group by Khan et al. (2004a; 2004b; 2005a; 2005b; 2010), using the Altman's nomogram method (Whitley and Ball, 2002). Replicates for each experiment were represented as n=#, where # represents the number of patients sampled.

In all experiments, recorded data was transferred to the Microsoft Office Excel and GraphPad Prism ver. 6.00 statistical software packages (GraphPad Software Inc, San Diego, CA, USA) for statistical analysis. The statistical significance between datasets were calculated using either one-way and two-way ANOVA, followed by the Dunnett's or Bonferroni post hoc tests for comparisons over time or of multiple datasets. Datasets yielding a p-value of <0.05 were regarded as statistically significant and represented as a single * on all graphs.

2.11.1 Analysis of tissue contractility data

Assessment of spontaneous myometrial tissue contractility utilised four measurements obtained from a 45-min period of recording using arbitrary units (a.u.): overall contractility (contraction curve integrals), contraction amplitude (maximum recorded force), contraction frequency (number of contractions), and contraction baseline (minimum recorded force). Measurement data was represented as a percentage change compared to the corresponding measurement obtained from vehicle-treated tissues, and

expressed as the mean percentage change ± the standard error of the mean (SEM). Resultant mean percentages were plotted against log-concentration as a concentration-response curve.

For concentration-response curves, each contractility measurement dataset was plotted and analysed using a three-parameter log (inhibitor) vs. response variable slope equation:

$$y = (y\ min) + (y\ max - y\ min)/1 + 10(\log IC_{50} - x)$$

Where ***y max*** is the maximum percentage contraction observed, ***y min*** is the minimum percentage contraction observed, and ***y*** is the overall contractile response. The IC_{50} represented the concentration of simvastatin required to inhibit an effect by 50%.

2.11.2 Analysis of cholesterol and protein assay data

For total cholesterol and protein assay experiments, changes in fluorescence intensity were recorded as an optical density (OD) value. The relative concentrations of myometrial cell cholesterol and protein were calculated using a two-parameter linear regression slope equation from the standard curve of each assay:

$$y = mx + b$$

Where ***y*** is detected fluorescence (OD), ***x*** is cholesterol/protein concentration, ***m*** represents the gradient slope, and ***b*** is the y-axis intercept. Calculated concentrations were converted and expressed as a mean percentage ± SEM, and represented on a histogram.

2.11.3 Analysis of FLOU-4AM® and FLIPR® Ca^{2+} assay data

For FLOU-4AM® and FLIPR® Ca^{2+} assay experiments, changes in fluorescence intensity OD were plotted against time. From this graph, the mean area under the curve (AUC) and the mean peak fluorescence were calculated. These two measurements were used determine the effects of simvastatin on total myometrial cell $[Ca^{2+}]i$, and the maximum increase in oxytocin-induced $[Ca^{2+}]i$ release. All datasets were normalised by subtracting all detected background fluorescence, and represented as the mean a.u.± SEM on a histogram.

2.11.4 Analysis of Hoechst 33342 tracer dye permeability data

The presence of Hoechst 33342 tracer dye was recorded as fluorescence intensity (OD), indicative of Hoechst 33342 binding to the nucleus and plotted against time. From this graph, the mean peak fluorescence was calculated to determine the effects of simvastatin exposure on Hoechst 33342 tracer dye movement into the myometrial cell. All datasets were normalised by subtracting all detected background fluorescence and represented as the mean a.u. ± SEM on a histogram.

2.11.5 Immunofluorescence image analysis

Changes in α-actin and caveolin-1 expression were determined by visual quantification of immunofluorescence intensity and location in the myometrial cell. Each coverslip was separated into 10 areas for imaging, which were chosen using a random number generator to determine the selection frequency. This method utilises a sequential pattern for area selection to provide an un-biased sample for analysis (**See Figure 2-10**).

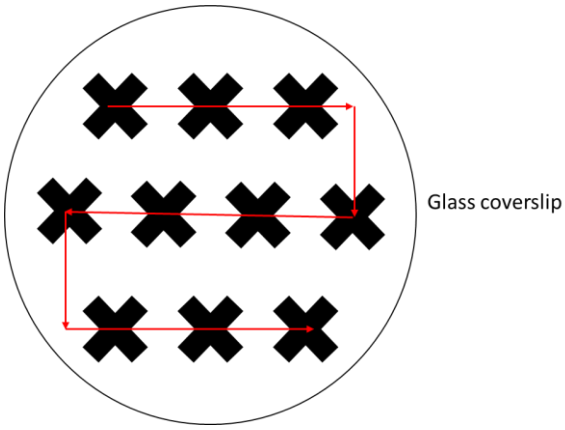


Figure 2-10. Diagram showing the sequential pattern used to select sample areas for immunofluorescence analysis.

Preliminary immunofluorescence images identified caveolin-1 staining to be expressed in three separate locations in the myometrial cell: co-localised in the nucleus (red arrow), in the extra-nuclear spaces (white arrow), and throughout areas of the cell body (orange arrow) (**See Figure 2-11**).

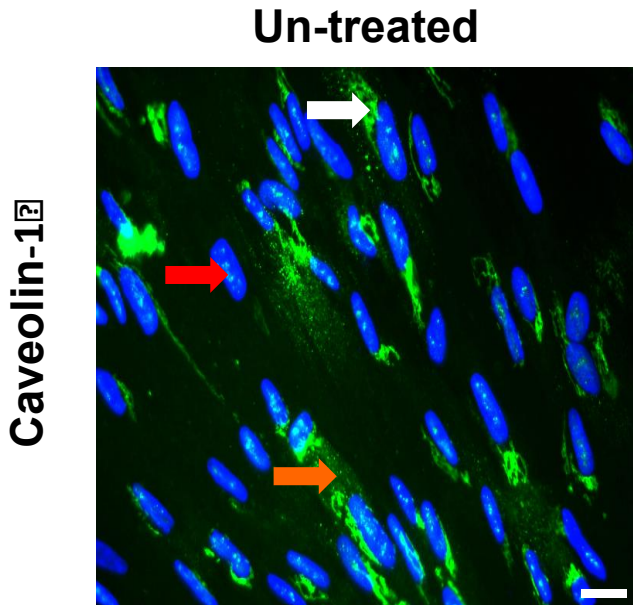


Figure 2-11. Representative immunofluorescent image showing caveolin-1 staining co-localised in the nucleus (red arrow), in the extra-nuclear spaces (white arrow), and throughout areas of the cell body (orange arrow) in un-treated myometrial cells. Staining: Caveolin-1/DAPI (Scale bar = 100μm).

For each patient sample, a total of 5 randomised fluorescent myometrial cell images were taken per treatment condition. The total number of cells per sample image were quantified by positive nuclear expression of 4',6-diamidino-2-phenylindole (DAPI). The number of nuclei showing nuclear co-localisation and extra-nuclear expression of caveolin-1 were counted and expressed as a mean percentage ± SEM of the total number of DAPI positive cells.

3 Results and analysis

3.1 Determine the cumulative effects of simvastatin on spontaneous myometrial contractions.

3.1.1 Aims

These experiments aim to investigate:

a) The effects of cumulative additions of simvastatin on spontaneous contractions in myometrial tissue samples obtained from women undergoing caesarean deliveries (pregnant), and hysterectomy procedures (non-pregnant).

3.1.2 Simvastatin reduced spontaneous contractions in myometrial tissues obtained from pregnant women

In myometrial tissue samples obtained from women undergoing caesarean deliveries, the cumulative exposure of simvastatin (3.3nM - 330μM) caused a concentration-dependent reduction in spontaneous contractions and an IC_{50} value of 0.84 ± 1.67μM (n=20, $p<0.05$). Tissues exposed to the highest concentration of simvastatin (330μM) resulted in a reduction of 81.83% in overall contractility (17.09 ± 11.91%) (n=20, $p<0.05$) and 71.20% in contraction amplitude (24.97 ± 4.04%) (n=4, $p<0.05$), compared to vehicle-treated tissues. No change in contraction frequency (n=11, $p>0.05$) or contraction baseline (n=4, $p>0.05$) was observed following simvastatin exposure (**See Figure 3-1**).

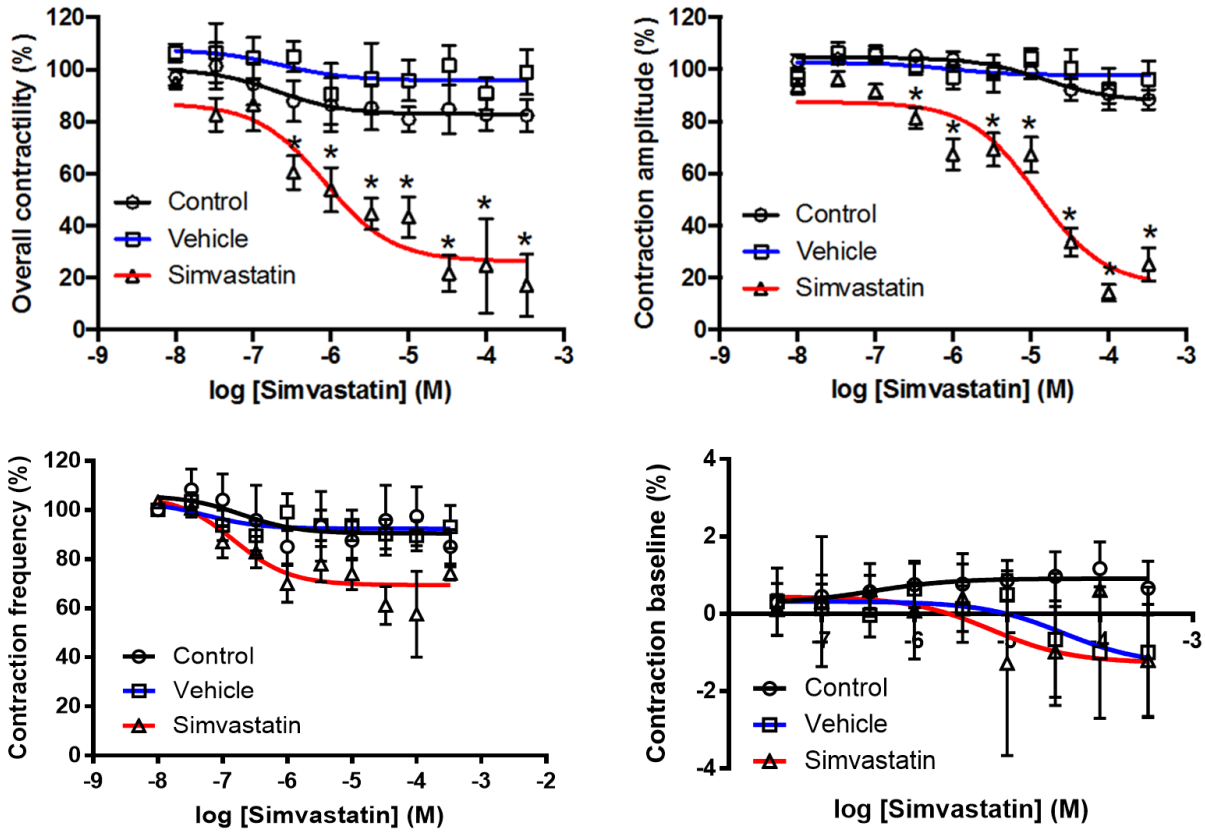


Figure 3-1. Effects of cumulative simvastatin (3.3nM - 330μM) exposure on overall spontaneous contractility (n=20), contraction amplitude (n=4), contraction frequency (n=11), and contraction baseline (n=4), in myometrial tissue samples obtained from women undergoing caesarean deliveries. Data is expressed as the mean contraction % of vehicle-treated samples ± SEM (ns $p>0.05$, *$p<0.05$).

3.1.3 Simvastatin reduced spontaneous contractions in myometrial tissues obtained from non-pregnant women

In myometrial tissue samples obtained from hysterectomy procedures, the cumulative exposure of simvastatin (33nM - 330μM) caused a similar concentration-dependent reduction of spontaneous contractions, generating an IC_{50} value of 1.66 ± 1.98μM. The addition of simvastatin (330μM) caused a significant 85.05% reduction in overall contractility (13.87 ± 3.11%) ($n=4$, $p<0.05$) and a 114.89% reduction in contraction amplitude (-36.64 ± 14.57%) ($n=4$, $p<0.05$), compared to vehicle-treated tissues. Contraction frequency (26.83 ± 9.67%) was also reduced by 54.42% after exposure to simvastatin ($n=4$, $p<0.05$) compared to vehicle. However, no change in contraction baseline ($n=4$, $p>0.05$) was observed (**See Figure 3-2**).

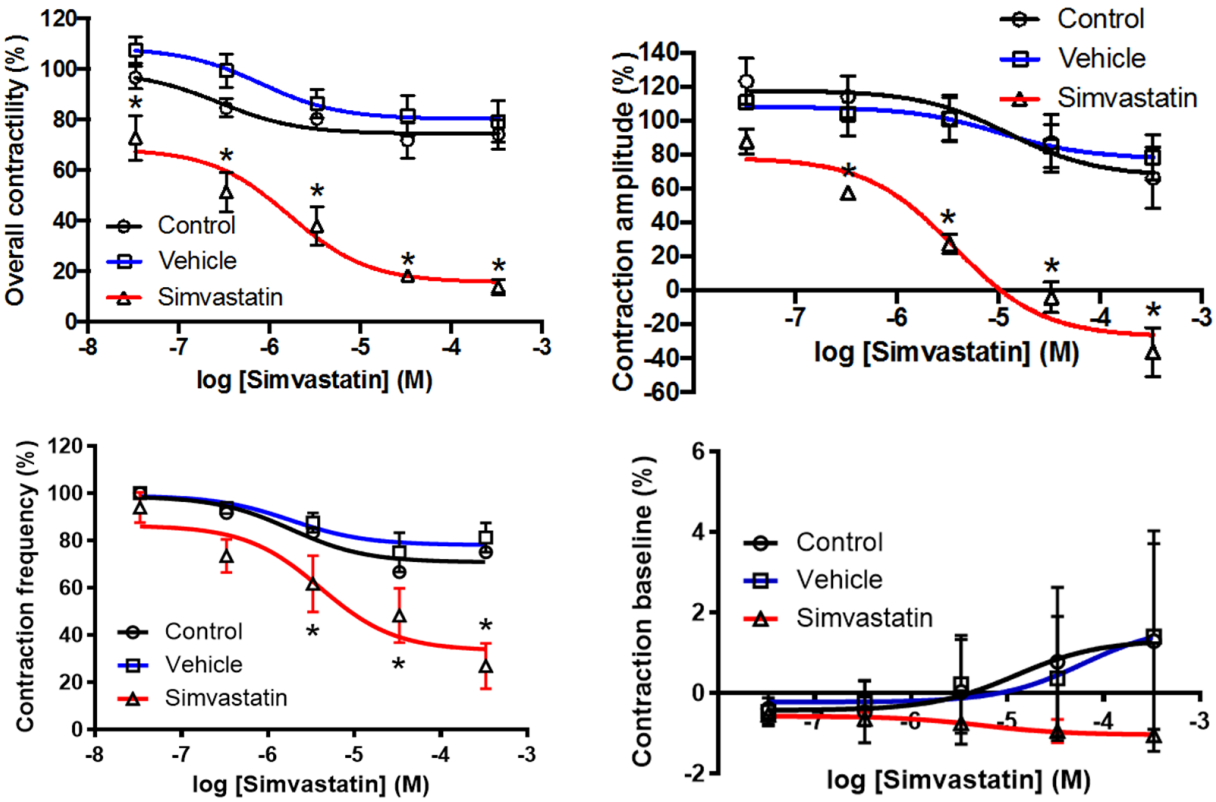


Figure 3-2. Effects of cumulative simvastatin (33nM - 330μM) exposure on overall spontaneous contractility (n=4), contraction amplitude (n=4), contraction frequency (n=4), and contraction baseline (n=4), in myometrial tissue samples obtained from women undergoing hysterectomy procedures. Data is expressed as the mean contraction % of vehicle-treated samples ± SEM (ns $p>0.05$, *$p<0.05$).

3.1.4 Simvastatin-induced reduction of spontaneous contractions is more potent in myometrial tissues obtained from non-pregnant women

The effects of simvastatin on spontaneous contractions in samples obtained from four women undergoing hysterectomy procedures, were compared with four randomly chosen samples from women undergoing caesarean deliveries. Tissues from non-pregnant women exposed to simvastatin (330μM) resulted in an additional 61.60% reduction in contraction amplitude (-36.64 ± 14.57% vs. 24.97 ± 4.04%) ($n=4$, $p<0.05$), and an additional 47.33% reduction in contraction frequency (26.83 ± 9.66% vs. 61.14 ± 3.83%) ($n=4$, $p<0.05$), compared to tissues from pregnant women. No significant difference in overall contractility or contraction baseline between the two groups were observed ($n=4$, $p>0.05$) (**See Figure 3-2**).

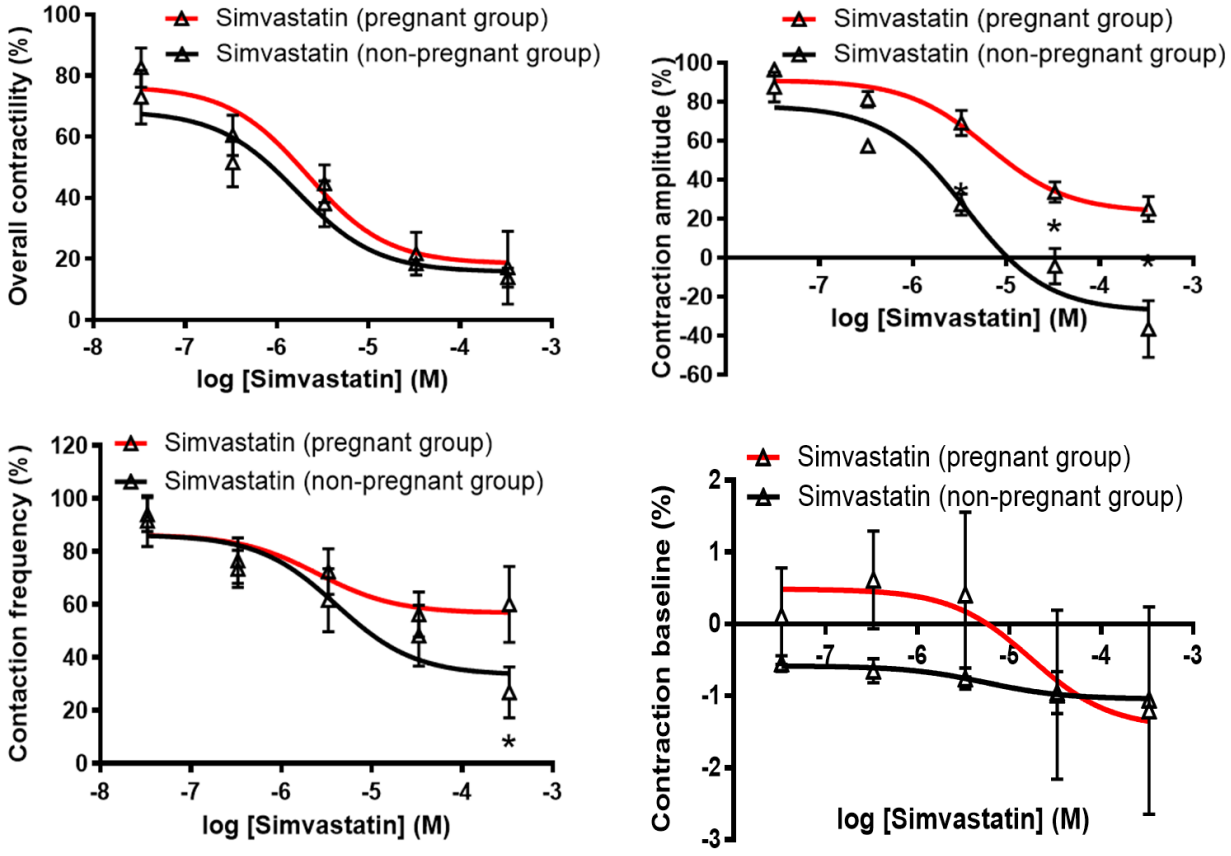


Figure 3-3. Comparative effects of cumulative simvastatin (33nM - 330μM) exposure on overall spontaneous contractility (n=4), contraction amplitude (n=4), contraction frequency (n=4), and contraction baseline (n=4), in myometrial tissue samples obtained from women undergoing caesarean deliveries (pregnant group), and hysterectomy procedures (non-pregnant group) (n=4). Data is expressed as the mean contraction % of vehicle-treated samples ± SEM (ns $p>0.05$, *$p<0.05$).

3.1.5 Discussion

Simvastatin exposure resulted in a concentration-dependent reduction in spontaneous myometrial contractility in both tissue samples taken from women undergoing caesarean deliveries, and hysterectomy procedures. This suggests that the mechanisms responsible for spontaneous myometrial contractility regulation in pregnant and non-pregnant women are responsive to simvastatin within 45-mins of exposure. This supports observations from other studies investigating the effects of statins on vascular smooth muscle tissue function (Alvarez de Sotomayor et al., 1999; Alvarez de Sotomayor et al., 2001; Perez-Guerrero et al., 2000; Yada et al., 1999), and from studies showing a reduction in C5a-induced human myometrial contractility, after overnight pre-incubation with simvastatin (Gonzalez et al., 2014).

Simvastatin-induced reduction of myometrial contractions appears enhanced in tissues from non-pregnant women, as shown by a greater decrease in contraction amplitude and contraction frequency compared to tissues from pregnant women. This difference in simvastatin potency may be due to pregnancy-related changes myometrium physiology and structure. During pregnancy, the uterus and myometrium undergoes structural remodelling to better accommodate the developing fetus (Harkness et al., 1956; Shynlova et al., 2006). This also includes an increase in the number of receptors and ion channels associated with promoting contractility, such as oxytocin receptors and VOCCs. In the absence of the fetus, these changes do not occur in non-pregnant women, which contributes to a lower basal contraction magnitude and frequency compared to pregnant women (Kimura et al., 1996; Inoue &

Sperelakis, 1991). It is possible that simvastatin reduces spontaneous contractions by inhibiting the activity of these receptors and ion channels. Therefore, a comparably weaker basal contractility and a reduction in ion channels and receptors associated with promoting contractility may result in the enhanced effect of simvastatin on myometrial tissues from non-pregnant women.

3.1.6 Critique and further work

In our experiments, we used simvastatin at concentrations ranging from 3.3nM to 330μM, with subsequent experiments starting at a concentration of 33nM or 3.3μM. These concentrations were within the levels used by other studies investigating the effects of simvastatin on smooth muscle function. However, these values are substantially higher than the mean concentration of statins found in human serum (1 – 15nM), after commonly prescribed therapeutic doses of between 0.1 – 1mg/kg of patient body weight (Bjorkhem-Bergman et al., 2001). Our experiments are therefore not directly applicable when considering simvastatin as a potential tocolytic agent for premature labour. Further experiments using therapeutic concentrations are required to determine whether simvastatin can be used in therapy.

Obtaining sufficient myometrial tissue samples from non-pregnant women suffered from logistical limitations related to patient consent. A single, part-time research midwife was tasked with obtaining consent from women undergoing hysterectomy procedures, and to organise tissue transport to the laboratory. This resulted in viable samples from only four patients for

simvastatin concentration-response contractility experiments only. These issues may be resolved by obtaining access permission for an additional researcher to approach these patients for consent, thereby increasing the number of patients approached for research and distributing tissue collection responsibilities among a team of staff. There is also the possibility of employing a dedicated bio-banking organisation tasked with procuring human samples for medical research on a full-time basis.

The difference in simvastatin potency between tissues obtained from pregnant and non-pregnant women, require further investigation to determine this discrepancy. It would be useful to repeat all subsequent mechanistic experiments in this study using non-pregnant myometrial tissues and cells. The data collected from these studies would determine whether the difference in the potency of simvastatin-induced effects between pregnant and non-pregnant women are consistent, and whether it is due to the lack of pregnancy-related changes in contraction promoting receptors and ion channels in the latter.

3.2 Determine the effects of simvastatin on cholesterol concentration in the myometrial cell, and the role of cholesterol modulation on spontaneous myometrial contractions

3.2.1 Aims

These experiments aim to investigate:

a) The effects of cholesterol modulation on simvastatin-induced reduction of spontaneous contractions in myometrial tissue samples obtained from pregnant women.
b) Whether simvastatin alters total cholesterol concentrations in myometrial cells obtained from pregnant women.

3.2.2 MCD increases spontaneous myometrial contraction amplitude

Myometrial tissue samples exposed to cumulative additions of MCD (330μM – 33mM) showed no statistically significant alterations in overall contractility (n=4, $p>0.05$), contraction amplitude (n=4, $p>0.05$), and contraction baseline (n=4, $p>0.05$), compared to vehicle-treated tissues. However, a significant increase of 194.45% in contraction frequency (280 ± 55.04%) (n=4, $p<0.05$) was observed following MCD (33mM) exposure, compared to vehicle-treated tissues (**See Figure 3-4**).

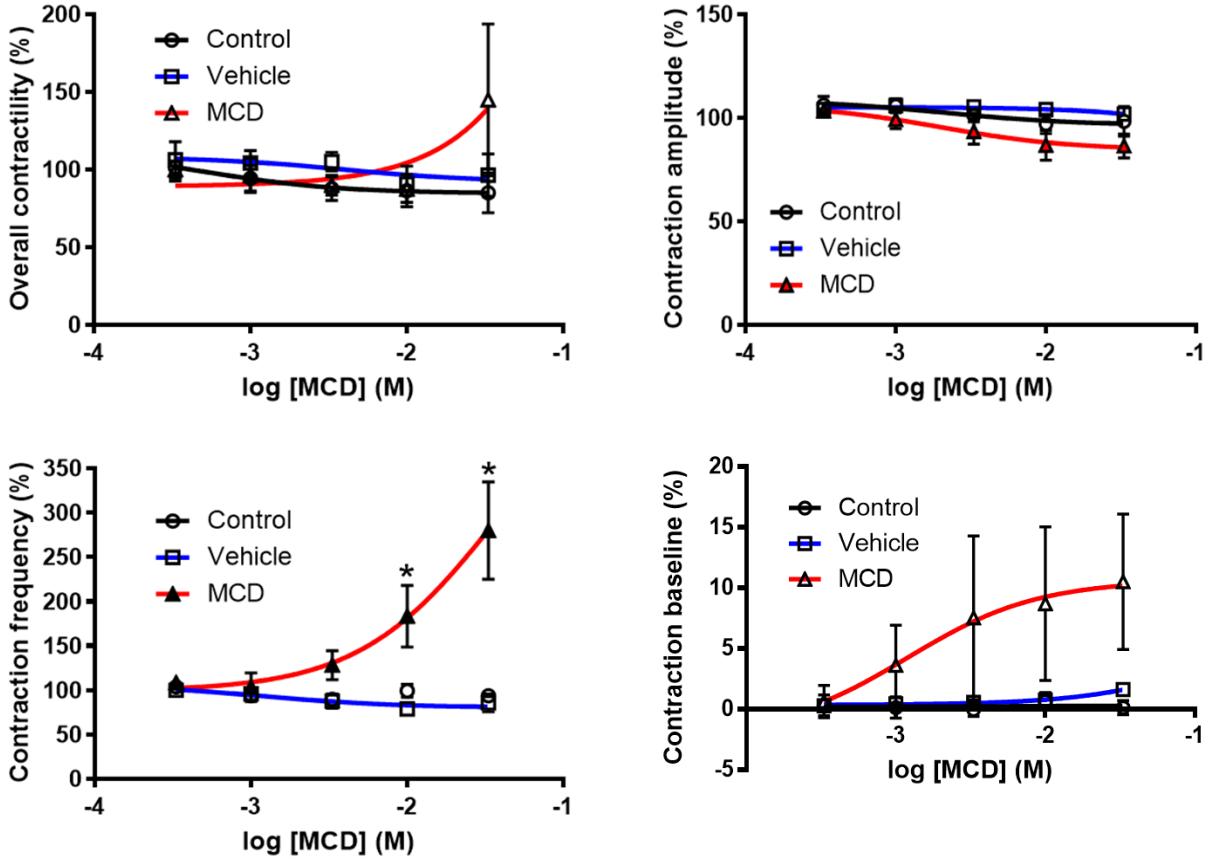


Figure 3-4. Effects of cumulative MCD (330μM – 33mM) exposure on overall spontaneous contractility (n=4), contraction amplitude (n=4), contraction frequency (n=4), and contraction baseline (n=4), in myometrial tissue samples obtained from women undergoing caesarean deliveries. Data is expressed as the mean contraction % of vehicle-treated samples ± SEM (ns $p>0.05$, *$p<0.05$).

3.2.3 Simvastatin-induced reduction of spontaneous myometrial contractions does not involve cholesterol depletion

Myometrial tissues exposed to a single concentration of simvastatin (330μM), resulted in reductions of 93.89% in overall contractility (6.09 ± 1.99% vs. 99.98 ± 5.67%) (n=4, $p<0.001$), 75.52% in contraction amplitude (30.79 ± 3.50% vs. 103.31 ± 1.50%) (n=4, $p<0.001$), and 34.16% in contraction frequency (74.17 ± 2.76% vs 108.33 ± 4.81%) (n=4, $p<0.05$) after 45-mins, compared to tissues exposed to the equivalent concentration of MCD. No change in contraction baseline was observed between the two treatment groups (n=4, $p>0.05$) (**See Figure 3-5**).

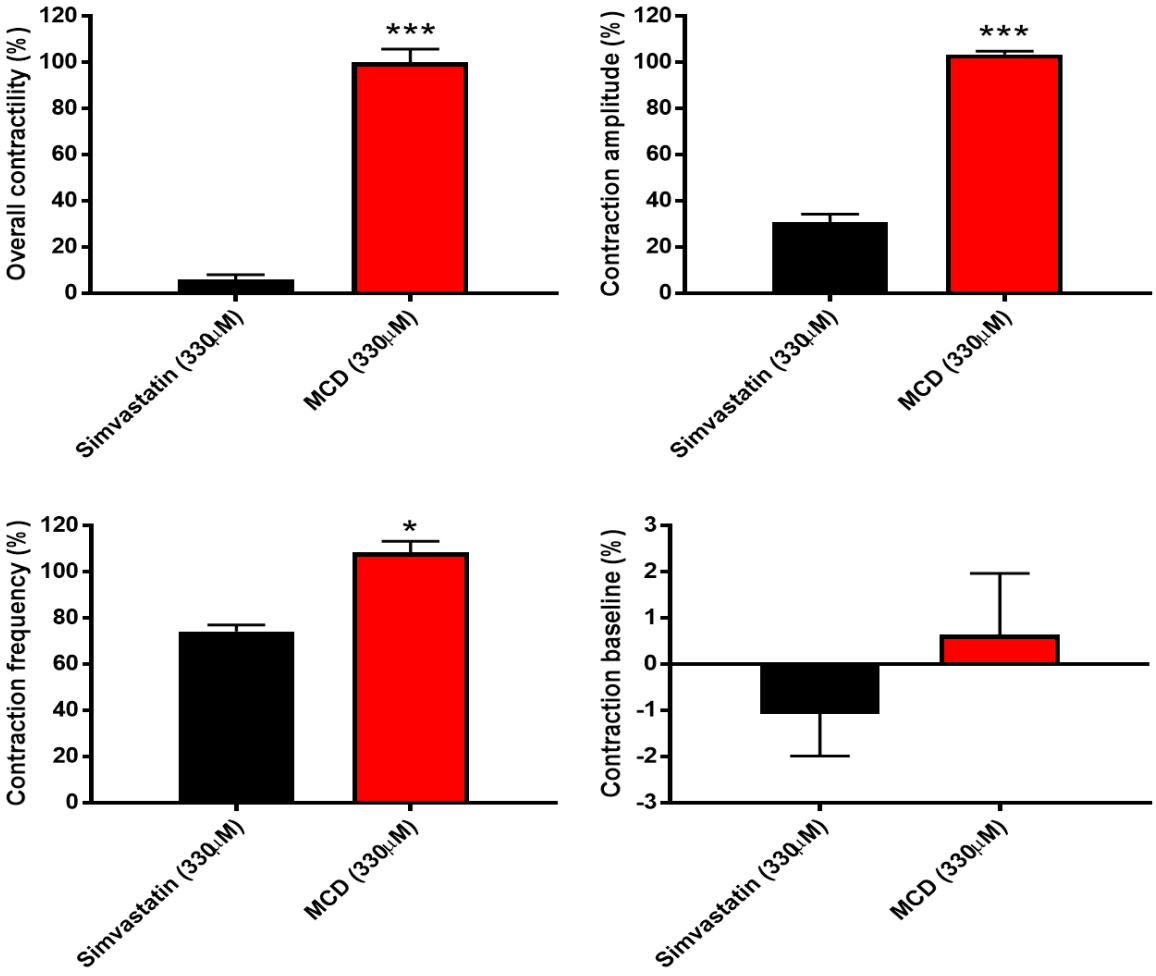


Figure 3-5. Effects of independent MCD (330μM) and simvastatin (330μM) exposure on overall spontaneous contractility (n=4), contraction amplitude (n=4), contraction frequency (n=4), and contraction baseline (n=4) after 45-mins, in myometrial tissue samples obtained from women undergoing caesarean deliveries. Data is expressed as the mean contraction % of vehicle-treated samples ± SEM (ns $p>0.05$, *$p<0.05$. ***$p<0.001$).

3.2.4 MCD co-incubation inhibits simvastatin-induced effects on spontaneous myometrial contractions

Myometrial tissues exposed to simvastatin (33nM - 330μM) in the presence of MCD (15mM) inhibited simvastatin-induced effects on spontaneous contractions, and increased the IC_{50} value for simvastatin from 0.88 ± 1.51μM to 6.0 ± 3.73μM (n=4, $p<0.05$). At a simvastatin concentration of 330μM, MCD co-incubation resulted in an increase in overall contractility by 47.44% (53.53 ± 13.11% vs. 6.09 ± 1.99%), (n=4, $p<0.05$), and in contraction frequency by 287.50% (361.66 ± 99.89% vs. 74.17 ± 2.76%) (n=4, $p<0.05$), compared to tissues exposed to the equivalent simvastatin concentration alone. Co-incubation with MCD did not alter simvastatin's effects on contraction amplitude or contraction baseline (n=4, $p>0.05$) (**See Figure 3-6**).

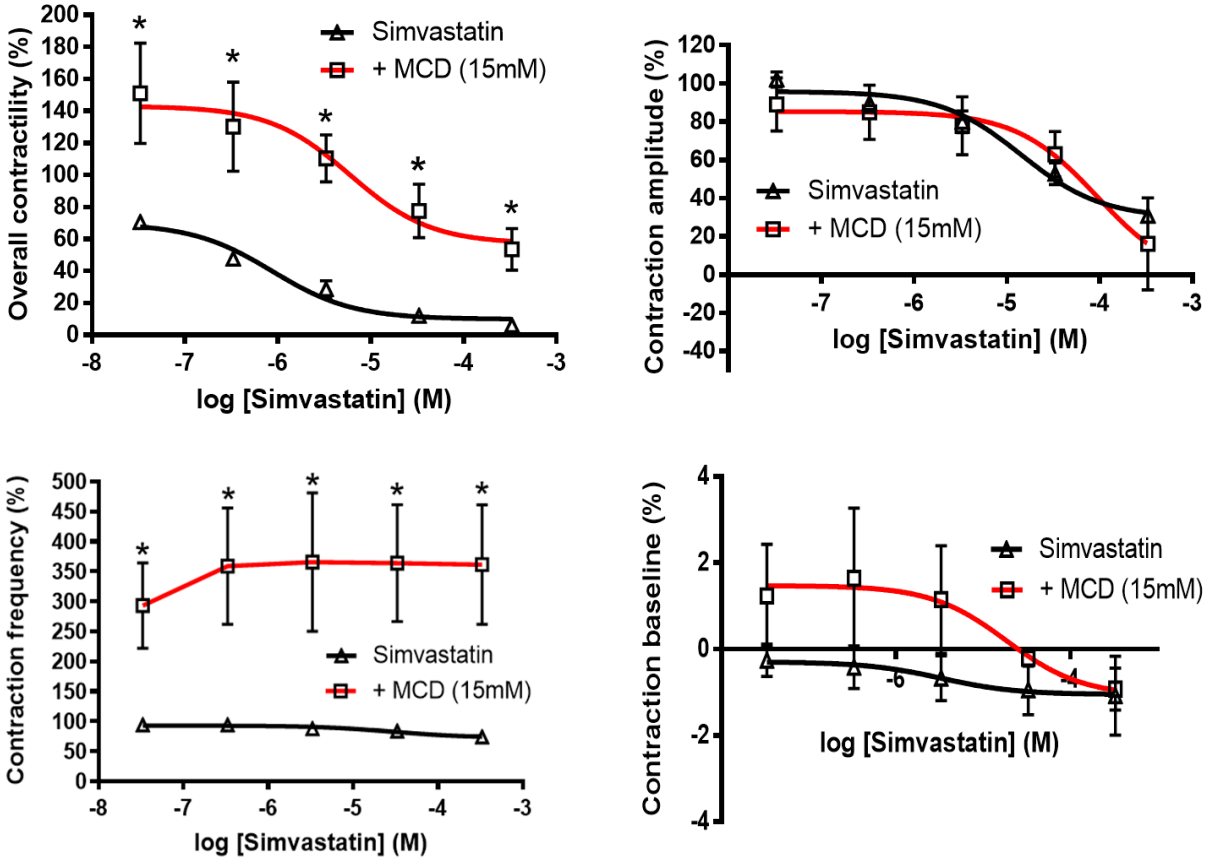


Figure 3-6. Effects of cumulative simvastatin (33nM - 330μM) exposure on overall spontaneous contractility (n=4), contraction amplitude (n=4), contraction frequency (n=4), and contraction baseline (n=4), in the presence of MCD (15mM) in myometrial tissue samples obtained from women undergoing caesarean deliveries. Data is expressed as the mean contraction % of vehicle-treated samples ± SEM (ns $p>0.05$, *$p<0.05$).

3.2.5 The addition of water-soluble cholesterol did not reverse simvastatin-induced reduction of spontaneous myometrial contractions

The addition of water-soluble cholesterol (0.5mM) immediately after a 45-mins single concentration of simvastatin (330μM), did not alter simvastatin-induced effects on overall spontaneous contractility, contraction amplitude, frequency, or baseline, compared to vehicle-treated tissues (n=4, $p>0.05$) (**See Figure 3-7**).

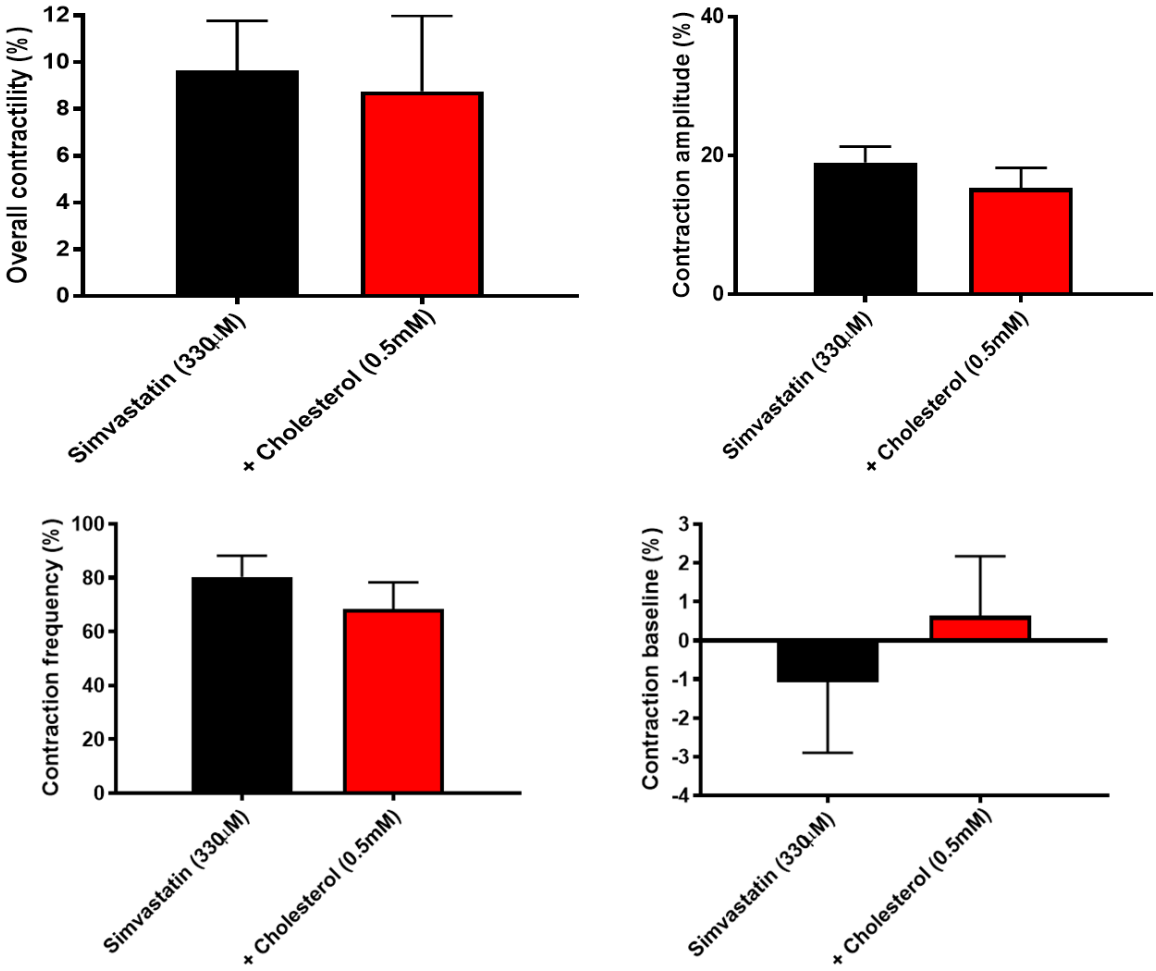


Figure 3-7. Effects of water-soluble cholesterol (0.5mM) addition immediately after a 45-mins single concentration of simvastatin (330µM) on overall spontaneous contractility (n=4), contraction amplitude (n=4), contraction frequency (n=4), and contraction baseline (n=4), in myometrial tissue samples obtained from women undergoing caesarean deliveries. Data is expressed as the mean contraction % of vehicle-treated samples ± SEM (ns $p>0.05$).

3.2.6 Simvastatin does not alter cholesterol in myometrial cells

Changes in total myometrial cell cholesterol after simvastatin (3.3μM, 10μM, and 33μM) and MCD (15mM) exposure over time were determined. Cells exposed to MCD resulted in a significant decrease in total cholesterol concentration after 45 mins (33.23 ± 2.07%), 4 hours (32.04 ± 5.87%), and 24 hours (35.43 ± 3.51%), compared to vehicle-treated cells ($n=5$, $p<0.001$). Cells exposed to simvastatin at all investigated concentrations did not alter total cholesterol concentrations compared to vehicle-treated cells over time ($n=5$, $p>0.05$) (**See Figure 3-8**). Control experiments measuring changes in total myometrial cell protein concentration, showed no change after both MCD and simvastatin compared to vehicle-treated cells over time ($n=5$, $p>0.05$) (**See Figure 3-9**).

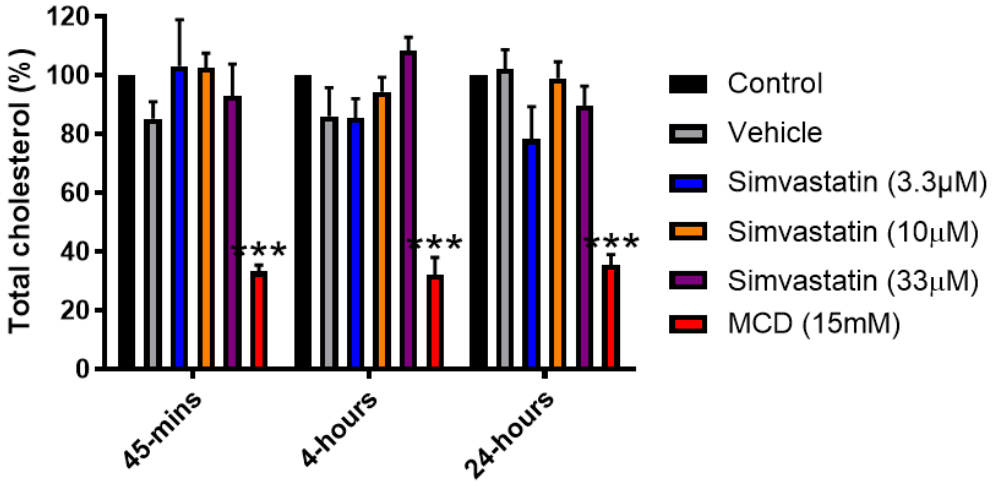


Figure 3-8. Effects of simvastatin (3.3μM, 10μM, and 33μM) and MCD (15mM) exposure on total cholesterol concentrations in myometrial cells after 45-mins, 4-hours, and 24-hours. Cells were obtained from women undergoing caesarean deliveries. Data expressed as the mean total cholesterol % of control untreated cells ± SEM (n=4, ns $p>0.05$, ***$p<0.001$).

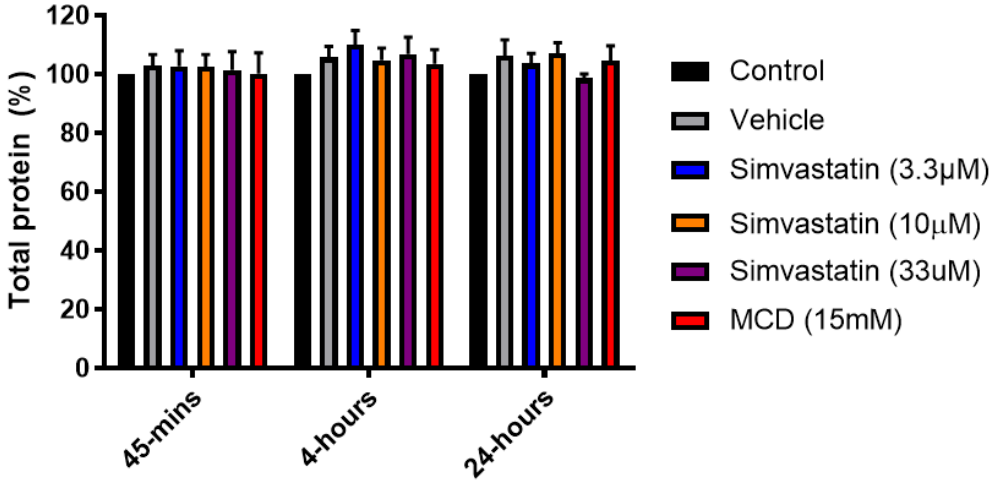


Figure 3-9. Effects of simvastatin (3.3μM, 10μM, and 33μM) and MCD (15mM) exposure on total protein concentrations in myometrial cells after 45-mins, 4-hours, and 24-hours. Cells were obtained from women undergoing caesarean deliveries. Data expressed as the mean total protein % of control untreated cells ± SEM (n=4, ns $p>0.05$).

3.2.7 Discussion

Myometrial contractility experiments observed contrasting effects between MCD and simvastatin exposure on spontaneous contractions. Tissues exposed to MCD independently resulted in an increase of spontaneous contraction frequency, rather than a reduction of contractility. In the presence of simvastatin, MCD resulted in the inhibition of simvastatin-induced effects on spontaneous contractions. Experiments on the role of cholesterol modulation observed no change in simvastatin's effects on contractions after replenishment with water-soluble cholesterol. Furthermore, total cholesterol concentration remained unchanged after simvastatin exposure to myometrial cells. These observations suggest that simvastatin-induced reduction of spontaneous contractions may occur in the absence of cholesterol modulation. The mechanisms resulting in simvastatin's effects are therefore likely to include pathways independent of cholesterol-inhibition, such as voltage-operated Ca^{2+} channel inhibition (de Sotomayor et al., 2005), and upregulation of eNOS expression and activity (Laufs et al., 1998), as observed in previous studies investigating the effects of statins on smooth muscle function.

Our data on the effects of MCD exposure on spontaneous contractions are consistent with previous studies investigating the effects of MCD-induced cholesterol depletion in the myometrium (Kendrick et al., 2004; Smith et al., 2005). Spontaneous contractions were also observed to increase after cholesterol reduction by other agents, such as cholesterol oxidase (Smith et al., 2005). Furthermore, increasing cholesterol concentration by adding LDLs

to myometrial tissues, resulted in a reduction of spontaneous and oxytocin-induced contractions (Smith et al., 2005). These observations further support the conclusion that simvastatin-induced reduction in spontaneous myometrial contractions occurs independently of cholesterol inhibition.

3.2.8 Critique and further work

In our experiments, we determined whether simvastatin-induced reduction of myometrial spontaneous contractions is cholesterol dependent by using MCD as a comparative cholesterol-depleting agent. MCD was chosen based on its use in similar myometrial contractility experiments in other studies, reporting consistent cholesterol depletion, and subsequent changes in contractile force (Kendrick et al., 2004; Smith et al., 2005). However, it was discovered after the completion of these experiments that the mechanisms by which MCD decreases cholesterol is different, when compared to simvastatin's inhibition of cholesterol biosynthesis through HMG-CoA reductase. It may be useful to include an alternative cholesterol depleting agent such as cholesterol oxidase, which catalyses the conversion of cholesterol into cholest-4-en-3-one (Smith et al., 2005), to better mimic the reduction in novel cholesterol as observed with simvastatin in our experiments. Furthermore, cholesterol replenishment after MCD exposure would also be useful to distinguish the difference in cholesterol modulation involved in simvastatin's effects on spontaneous contractions. Inhibition of MCD's effects after replenishment with cholesterol would further suggest a lack of cholesterol depletion involved in simvastatin's mechanisms in the myometrium.

Finally, our experiments determined the effects of simvastatin on cholesterol concentrations in myometrial cells. A more comparable method would be to measure cholesterol concentrations directly in tissues obtained from contractility experiments after simvastatin exposure. A similar result would further suggest that simvastatin's effects on spontaneous contractions occur independently of cholesterol modulation in the myometrium.

3.3 Determine the effects of NO inhibition on simvastatin-induced effects on spontaneous myometrial contractions

3.3.1 Aims

These experiments aim to investigate:

a) The effects of NO inhibition, via L-NAME induced inhibition of eNOS, on simvastatin-induced reduction of spontaneous contractions in myometrial tissue samples obtained from pregnant women.

3.3.2 L-NAME-induced inhibition of eNOS partially inhibited simvastatin-induced effects on spontaneous myometrial contractions

Myometrial tissues pre-incubated with L-NAME (300μM) followed by exposure to simvastatin (33nM - 330μM) resulted in the partial inhibition of simvastatin-induced effects on spontaneous contractions, and increased the IC_{50} value for simvastatin from 1.20 ± 0.41μM to 5.44 ± 0.20μM (n=6, $p<0.05$). At a simvastatin concentration of 300μM, inhibition of eNOS resulted in an increase in overall contractility by 33.82% (48.56 ± 2.45% vs. 13.74 ± 2.11%) (n=6, $p<0.05$), in contraction amplitude by 65.69% (82.71 ± 1.01% vs. 12.02 ± 1.56%) (n=7, $p<0.05$), and in contraction frequency by 36.34% (88 ± 4.89% vs. 51.66 ± 3.76%), compared to tissues exposed to the equivalent simvastatin concentration alone (n=6, $p<0.05$). L-NAME-induced eNOS inhibition did not alter simvastatin's effects on contraction baseline (n=4, $p>0.05$) (**See Figure 3-10**).

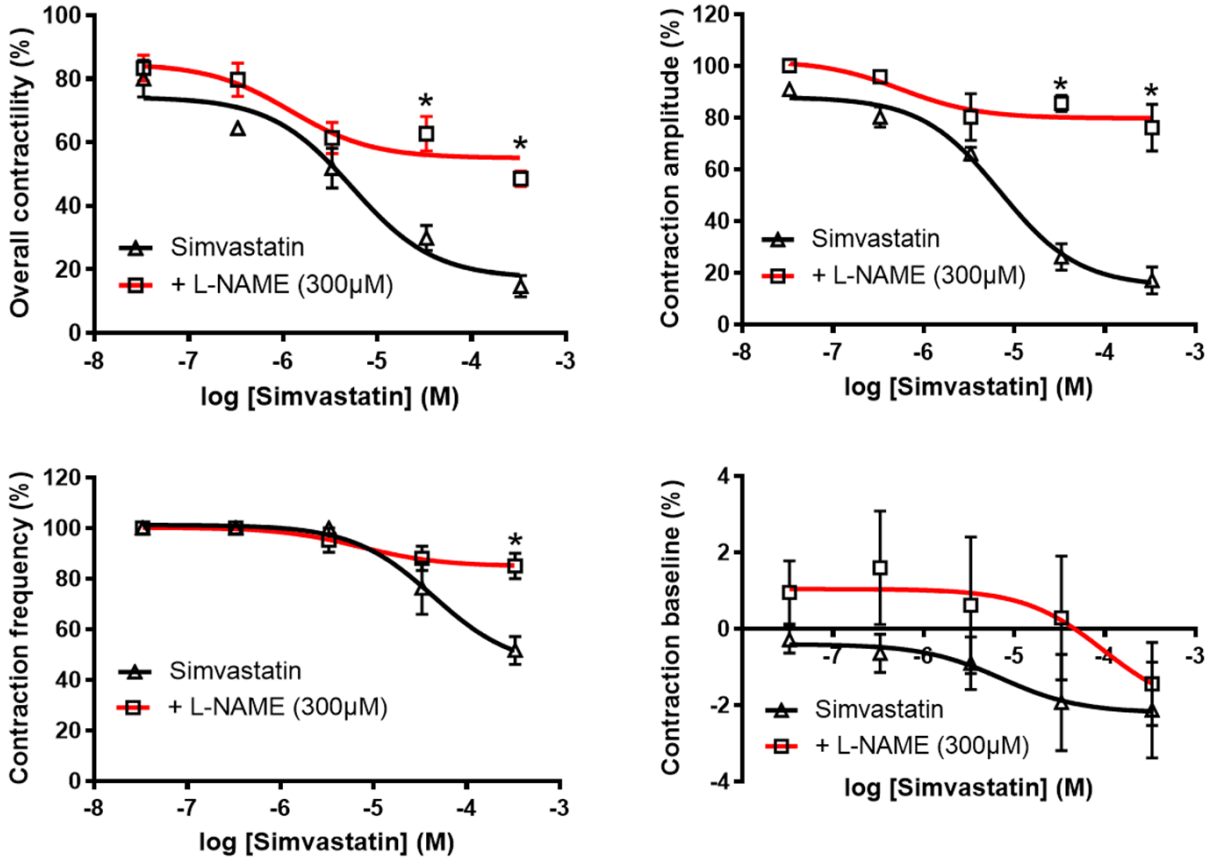


Figure 3-10. Effects of eNOS inhibition by L-NAME on cumulative simvastatin (33nM - 330μM) exposure on overall spontaneous contractility (n=6), contraction amplitude (n=7), contraction frequency (n=6), and contraction baseline (n=4), in myometrial tissue samples obtained from women undergoing caesarean deliveries. Data is expressed as the mean contraction % of vehicle-treated samples ± SEM (ns $p>0.05$, *$p<0.05$).

3.4 Determine the presence or absence of the HMG-CoA reductase pathway in the myometrium

3.4.1 Aims

These experiments aim to investigate:

a) Whether the addition of mevalonate or GGPP can reverse the simvastatin-induced reduction of spontaneous contractions in myometrial tissue samples obtained from pregnant women.

3.4.2 The addition of mevalonate or GGPP did not reverse simvastatin-induced reduction of spontaneous myometrial contractions

The addition of either mevalonate (200μM) (**See Figure 3-11**) or GGPP (20μM) (**See Figure 3-12**) immediately after a 45-mins single concentration of simvastatin (330μM), did not alter simvastatin-induced reduction of spontaneous contractility, contraction amplitude, frequency, or baseline, compared to vehicle-treated tissues (n=4, $p>0.05$).

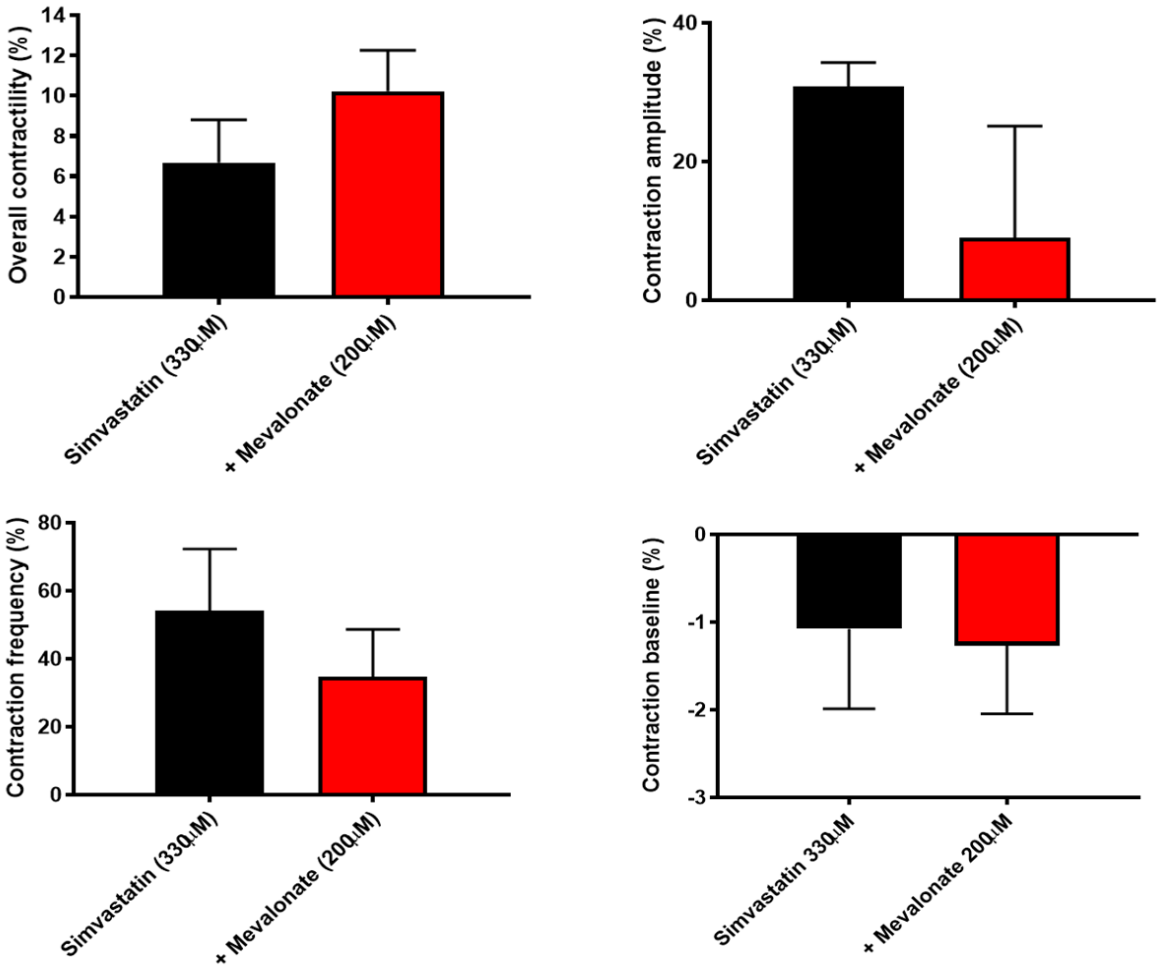


Figure 3-11. Effects of mevalonate (200µM) addition immediately after a 45-mins single concentration of simvastatin (330µM), on overall spontaneous contractility (n=4), contraction amplitude (n=4), contraction frequency (n=4), and contraction baseline (n=4), in myometrial tissue samples obtained from women undergoing caesarean deliveries. Data is expressed as the mean contraction % of vehicle-treated samples ± SEM (ns $p>0.05$).

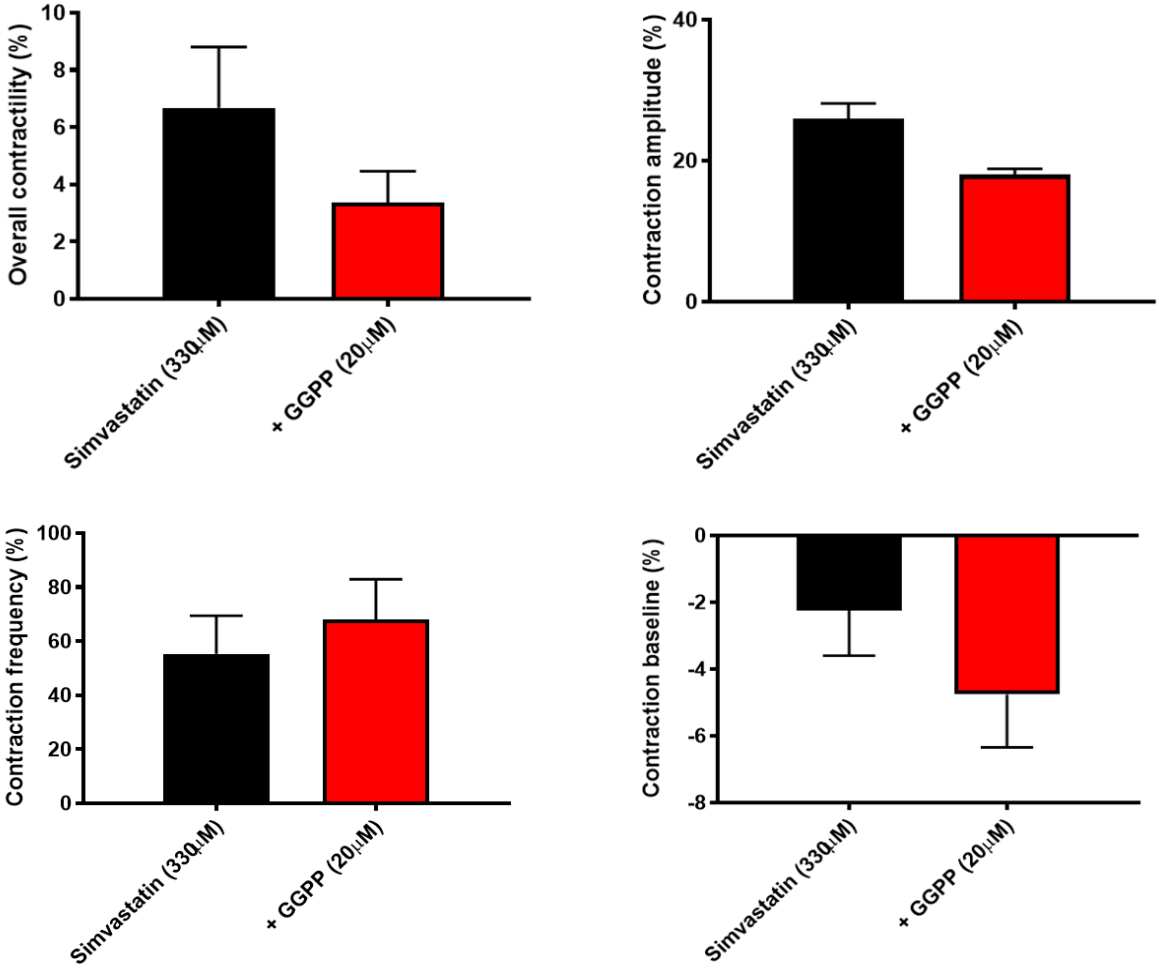


Figure 3-12. Effects of GGPP (20μM) addition immediately after a 45-mins single concentration of simvastatin (330μM), on overall spontaneous contractility (n=4), contraction amplitude (n=4), contraction frequency (n=4), and contraction baseline (n=4), in myometrial tissue samples obtained from women undergoing caesarean deliveries. Data is expressed as the mean contraction % of vehicle-treated samples ± SEM (ns $p>0.05$).

3.4.3 Discussion

The inhibition of eNOS-derived NO by L-NAME exposure resulted in the partial inhibition of simvastatin-induced reduction of spontaneous myometrial contractions. This suggests that simvastatin's effects may pathways involved in NO signalling and promoting NO-induced smooth muscle relaxation. These observations were consistent with several studies investigating the role of NO-induced relaxation after statin exposure in smooth muscle tissues and blood vessels. For example, simvastatin-induced relaxation of rat aortic and superior mesenteric arteries was inhibited after co-incubation with the NOS inhibitor L-N^G-nitroarginine (L-NOARG) (de Sotomayor et al., 2005). In patients with hypercholesterolaemia, statin treatment resulted in an increase in endothelium-dependent arterial vasodilation, which was subsequently inhibited by L-N^G-monomethyl arginine citrate (L-NMMA), another known NOS inhibitor (John et al., 1998). In patients with coronary artery disease, pravastatin-induced forearm vasodilation was similarly inhibited by L-NMMA (Masumoto et al., 2001).

Studies investigating the interactions between statins and NO have determined that statins can affect NO bioavailability, by modifying eNOS mRNA transcription. In the presence of statins, both eNOS mRNA and eNOS protein expression increases. This occurs by statin-induced polyadenylation of the nuclear 3' site on the eNOS mRNA, resulting in an increase in its rate of transcription (Kosmidou et al., 2007). It is possible that simvastatin can also increase NO bioavailability by modifying eNOS transcription in the myometrium. An increase in NO-activated guanylyl cyclase results in the

production of cyclic GMP (cGMP), which in turn activates protein kinase G (PKG) to promote smooth muscle relaxation (Norman, 1996; Ramsay et al., 1996). PKG activation can affect several different contraction regulatory pathways to promote smooth muscle relaxation. These include the activation of BK channels by phosphorylation (Alioua et al., 1995; Archer et al., 1994; Fukao et al., 1999), inhibition of VOCC activity, and promoting the recycling uptake of Ca^{2+} into the SR by SERCA activation (Hofmann et al, 2000; Lincoln & Komalavilas, 2000) (**See Figure 3-13**).

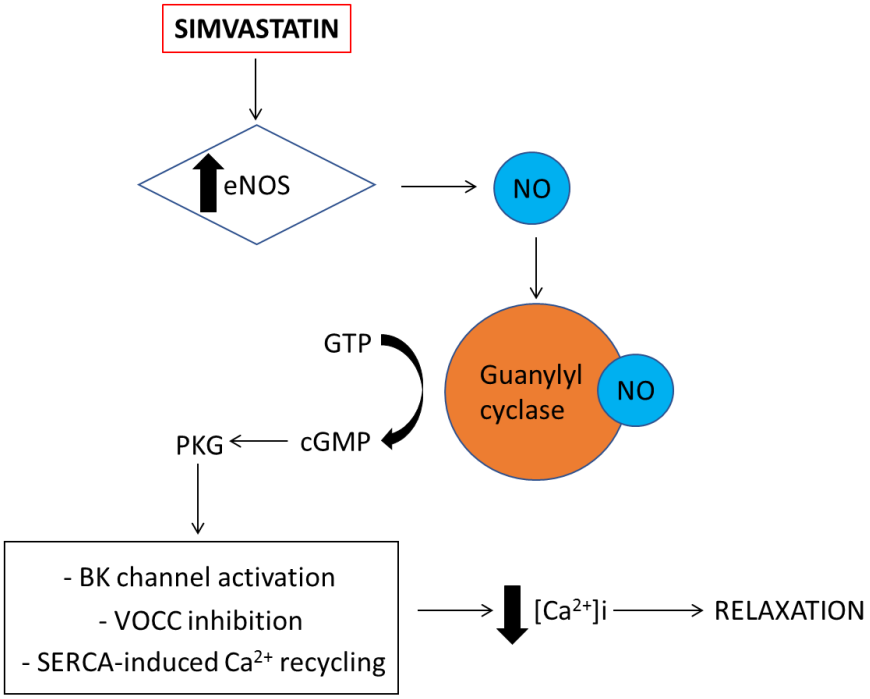


Figure 3-13. Diagram showing simvastatin upregulation of eNOS activity, and the possible promotion of eNOS-induced smooth muscle relaxation by BK channel activation, VOCC inhibition, and SERCA-induced Ca^{2+} recycling.

Mevalonate and GGPP are integral proteins involved in the HMG-CoA reductase pathway and are known to be inhibited by statins (Istvan and Deisenhofer, 2000; Istvan et al., 2000). In the absence of statins, phosphorylation of mevalonate in the presence of mevalonate kinase results in the formation of several isoprenoid proteins including GGPP (Goldstein and Brown, 1990). GGPP-induced activation of RhoA through the process of prenylation, facilitates the translocation and attachment of small GTP-binding proteins, such as RhoA, to the plasma membrane (Fujisawa et al., 1998; Van Aelst and D'Souza-Schorey, 1997). Once in the plasma membrane, RhoA can activate the Rho-kinase enzyme, which then inhibits MLCP by phosphorylating its myosin-binding subunit. Once inhibited, Mg-ATPase-induced dephosphorylation of MLC can no longer occur, causing the actin-myosin cross-bridge to remain intact and resulting in the generation of a contraction (Kimura et al., 1996; Kureishi et al., 1997) (**See Figure 3-14**).

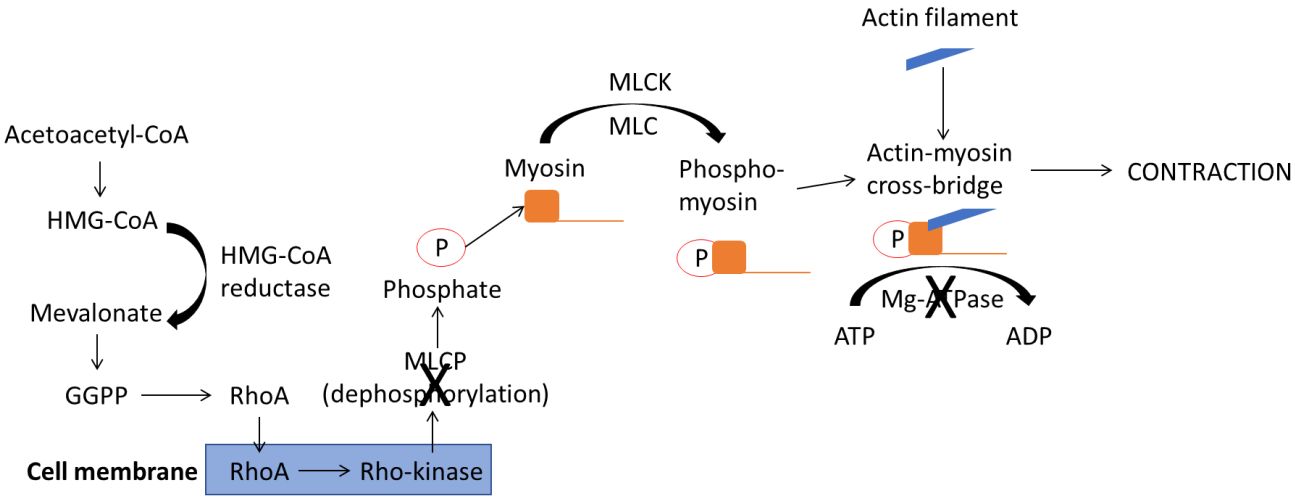


Figure 3-14. Diagram showing the role of HMG-CoA-activated Rho-kinase in promoting smooth muscle contractility by MLCP inhibition.

In addition to RhoA-induced contractions via inhibition of MLCP, several studies have found that RhoA can also directly reduce eNOS production by decreasing eNOS mRNA stability, resulting in an increase in smooth muscle contractility. (Hall, 1998; Van Aelst L., 1997). This effect was shown to be reversed in the presence of statins, and by RhoA inhibition (Laufs et al., 1998, 1997; Yoshizumi et al., 1993).

Our experiments showed no change in simvastatin-induced reduction in spontaneous myometrial contractions, after replenishment with mevalonate and GGPP. However, these observations contradict previous studies linking statin inhibition of small GTP-binding proteins, to smooth muscle relaxation. This suggests that simvastatin's effects may be independent of the HMG-CoA reductase pathway, or that the pathway is not present in the myometrium.

3.4.4 Critique and further work

Our experiments observed a partial inhibition of simvastatin-induced effects in the presence of L-NAME, suggesting the possible promotion of NO-induced smooth muscle relaxation in our system. However, to determine whether NO concentrations are altered in the presence of simvastatin, further experiments are required to collect and measure the NO produced from our treated tissues. It is possible to collect any NO gas produced by the tissue during experimentation, by creating a closed-circuit chamber on top of each tissue contractility organ bath chamber. Changes in NO can be quantified by measuring the concentration of NO metabolites using high-performance liquid chromatography and chemiluminescence detection analyses (Jiang et al.,

2012), whereby changes in NO concentration can be determined by quantification of the NO precursor, nitrosothiols (Singh et al., 1996). Changes in NO levels in the tissues themselves can also be quantified in the same way. Furthermore, changes in eNOS can be quantified using immunoblotting techniques in myometrial tissues before, and after experimentation.

In our experiments, replenishment with mevalonate and GGPP did not alter simvastatin-induced reduction of spontaneous contractions. It is possible that the concentrations of mevalonate and GGPP used in our studies were too low to cause an effect. One study investigating the effects of statins on porcine coronary artery function conducted replenishment studies using 500μM, and 20μM concentrations of mevalonate, and GGPP respectively. However, these concentrations were only able to prevent the effects of simvastatin at concentrations of under 3μM (Seto et al., 2007). It would be useful to repeat our replenishment experiments using a combination of high mevalonate/GGPP, and low simvastatin concentrations to determine whether simvastatin's effects can be reversed.

To determine whether the HMG-CoA reductase pathway is present in the myometrium, the concentration of HMG-CoA reductase before and after simvastatin exposure can be quantified. Detection of the protein using immunoblotting techniques on myometrial tissue samples after contractility experiments can determine whether simvastatin-induced reduction of spontaneous contractions involves inhibition of the HMG-CoA reductase pathway. Furthermore, proteins known to promote smooth muscle

contractility, such as RhoA and Rho-kinase, can also be quantified in the same way. A decrease in the concentration of these proteins after simvastatin exposure would indicate their inhibition during simvastatin-induced reduction of spontaneous contractions.

3.5 Determine the effects of simvastatin on Ca^{2+} and K^{+} ion channel activity during spontaneous myometrial contractility

3.5.1 Aims

These experiments aim to investigate:

a) Whether voltage-operated K^{+}, Ca^{2+}-operated K^{+}, and voltage-operated Ca^{2+} channels are involved in simvastatin-induced reduction of spontaneous contractions in myometrial tissue samples obtained from pregnant women.

3.5.2 TEA-induced broad inhibition of voltage-operated K^+ and Ca^{2+}-operated K^+ channels partially inhibited simvastatin-induced reduction of spontaneous myometrial contractions

Broad blockade of voltage-operated K^+ and Ca^{2+}-operated K^+ channels using TEA (5mM), partially inhibited simvastatin-induced effects on spontaneous contractions and increased the IC_{50} value for simvastatin from 2.91 ± 1.36μM to 12.70 ± 3.12μM (n=4, $p<0.05$). The inhibition of these channels after simvastatin exposure (300μM) resulted in an increase in overall contractility by 40.39% (47.67 ± 4.99% vs. 7.28 ± 3.49%) (n=4, $p<0.05$), contraction amplitude by 31.94% (56.91 ± 16.70% vs. 24.97 ± 4.01%) (n=4, $p<0.05$), contraction frequency by 113.05% (172.38 ± 54.84% vs. 59.33 ± 10.32%) (n=4, $p<0.05$), and contraction baseline by 4.71% (4.58 ± 3.03% vs. -0.13 ± 0.65%) (n=4, $p<0.05$), compared to tissues exposed with the equivalent simvastatin concentration alone (**See Figure 3-15**).

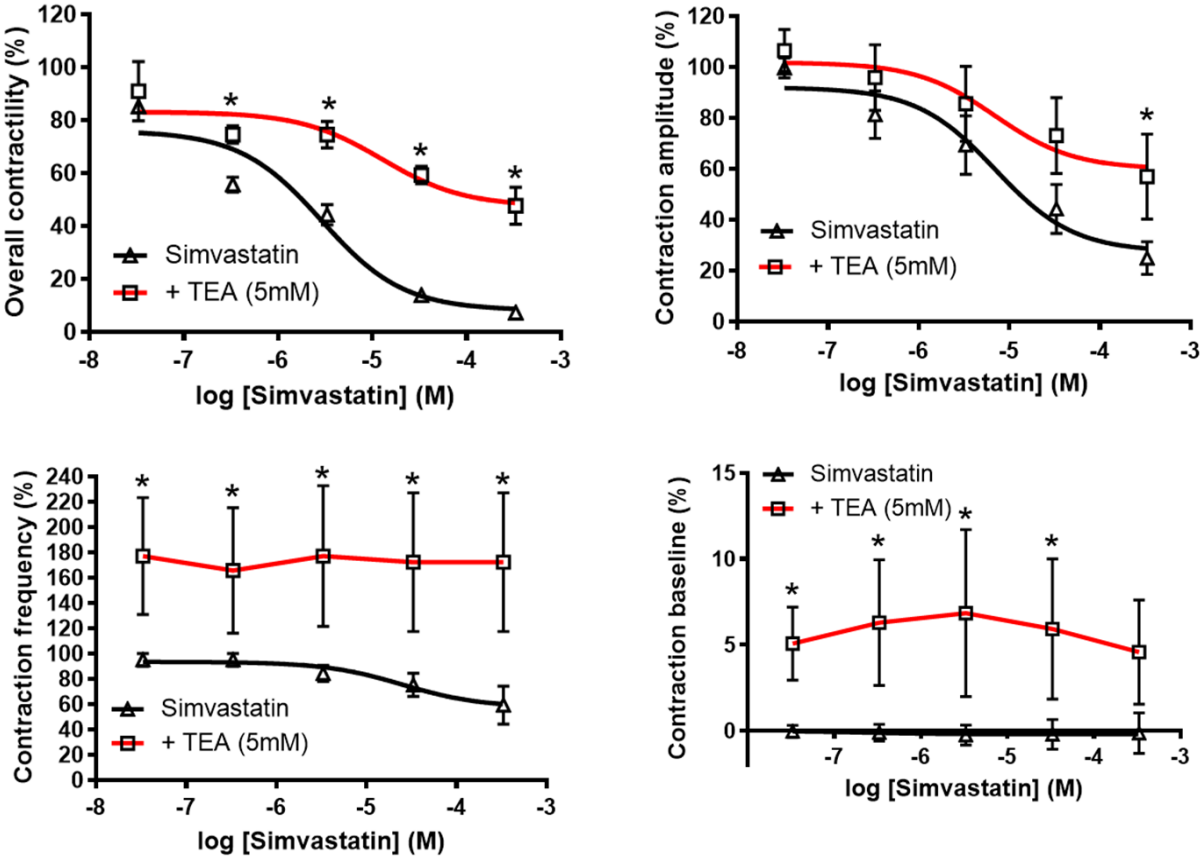


Figure 3-15. Effects of TEA-induced broad inhibition of voltage-operated K^+ and Ca^{2+}-operated K^+ channels alongside cumulative simvastatin (33nM - 330μM) exposure, on overall spontaneous contractility (n=4), contraction amplitude (n=4), contraction frequency (n=4), and contraction baseline (n=4), in myometrial tissue samples obtained from women undergoing caesarean deliveries. Data is expressed as the mean contraction % of vehicle-treated samples ± SEM (ns $p>0.05$, *$p<0.05$).

3.5.3 Apamin-induced inhibition of SK channels partially inhibited simvastatin-induced reduction of spontaneous myometrial contractions

Apamin-induced (500nM) inhibition of SK channels resulted in the partial inhibition of simvastatin-induced effects on spontaneous contractions, and increased the IC_{50} value for simvastatin from 2.91 ± 1.36μM to 4.31 ± 3.64μM (n=6, $p<0.05$). Simvastatin (330μM) exposure after SK channel inhibition resulted in an increase in overall contractility by 30.60% (37.88 ± 7.81% vs. 7.28 ± 3.49%) (n=6, $p<0.05$), compared to tissues exposed to the equivalent simvastatin concentration alone. However, no change was observed in contraction amplitude, frequency, or baseline (n=6, $p>0.05$) (**See Figure 3-16**).

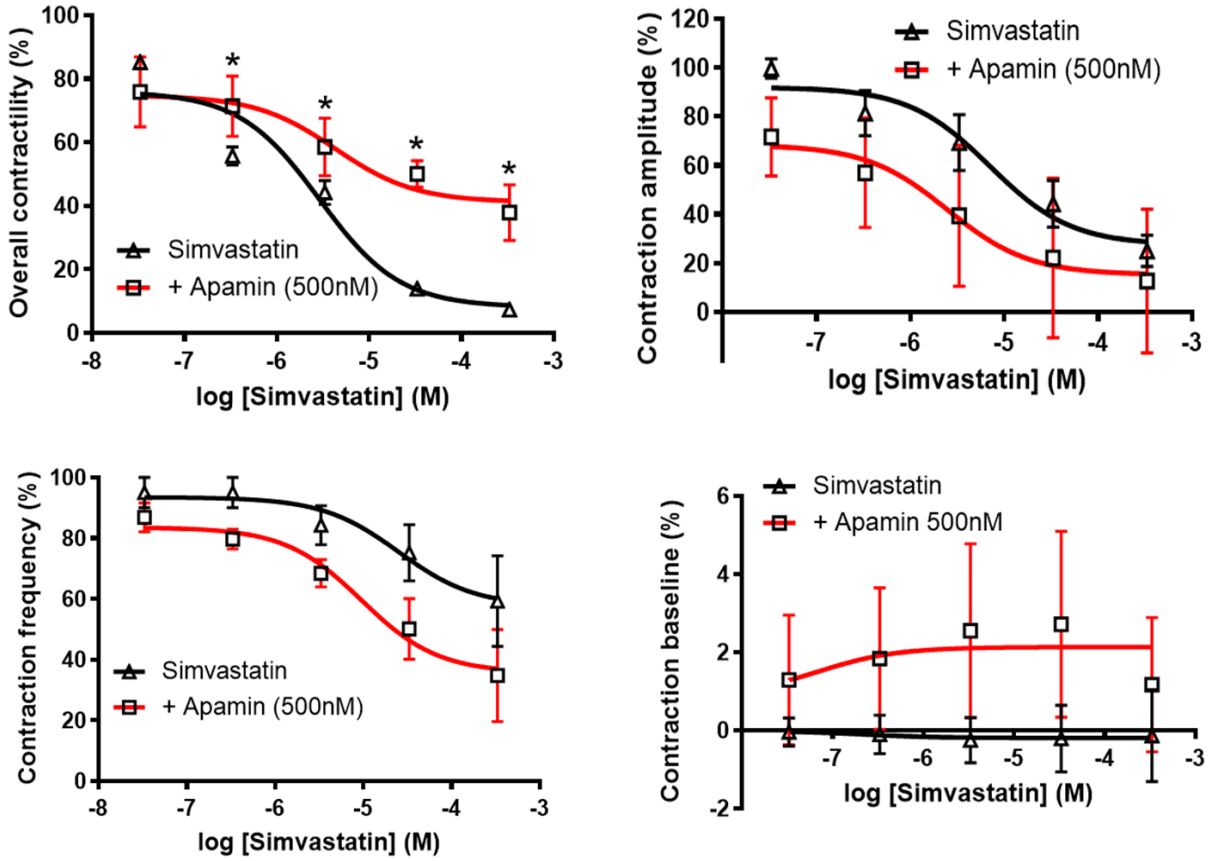


Figure 3-16. Effects of apamin-induced SK channel inhibition alongside cumulative simvastatin (33nM - 330μM) exposure, on overall spontaneous contractility (n=6), contraction amplitude (n=6), contraction frequency (n=6), and contraction baseline (n=6), in myometrial tissue samples obtained from women undergoing caesarean deliveries. Data is expressed as the mean contraction % of vehicle-treated samples ± SEM (ns $p>0.05$, *$p<0.05$).

3.5.4 BK channel inhibition via paxilline partially inhibits simvastatin-induced reduction of spontaneous myometrial contractions

Inhibition of BK channels via paxilline (1μM), resulted in the partial inhibition of simvastatin-induced effects on spontaneous contractions and increased the IC_{50} value for simvastatin from 2. 2.91 ± 1.36μM to 4.19 ± 2.18μM (n=7, $p<0.05$). BK channel inhibition in the presence of simvastatin (330μM) increased overall contractility by 20.08% (27.36 ± 4.28% vs. 7.28 ± 3.49%) (n=7, $p<0.05$), compared to tissues exposed to the equivalent simvastatin concentration alone. No significant alteration in contraction amplitude, frequency, or baseline was observed (n=7, $p>0.05$) (**See Figure 3-17**).

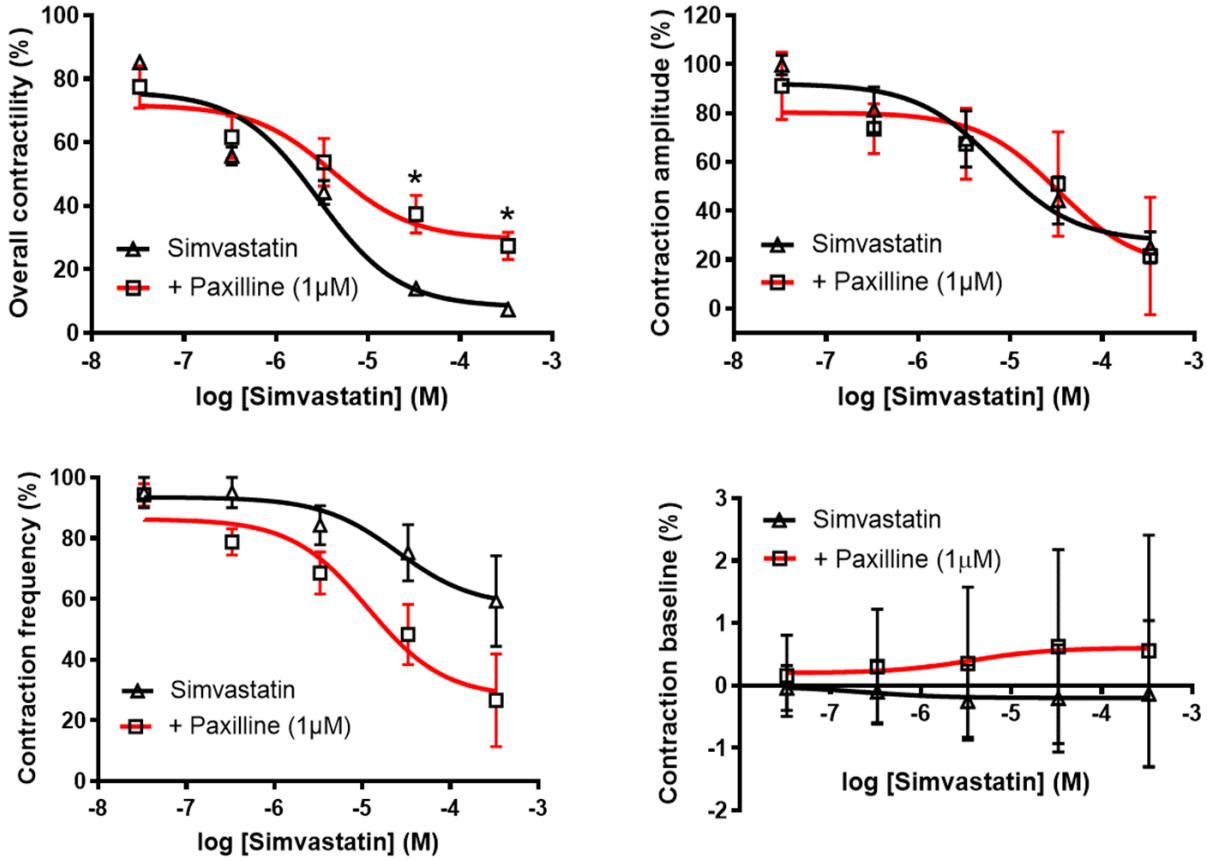


Figure 3-17. Effects of paxilline-induced BK channel inhibition alongside cumulative simvastatin (33nM - 330µM) exposure, on overall spontaneous contractility (n=7), contraction amplitude (n=7), contraction frequency (n=7), and contraction baseline (n=7), in myometrial tissue samples obtained from women undergoing caesarean deliveries. Data is expressed as the mean contraction % of vehicle-treated samples ± SEM (ns $p>0.05$, *$p<0.05$).

3.5.5 Inhibition of SK and BK channels combined enhanced the inhibition of simvastatin-induced effects on spontaneous myometrial contractions

Inhibition of SK and BK channels in combination resulted in a greater inhibition of simvastatin-induced effects on spontaneous contractions. Tissues exposed to simvastatin (330μM) after apamin and paxilline treatment resulted in an increase in overall contractility by 23.14% (30.42 ± 8.42% vs. 7.28 ± 3.49%) (n=5, $p<0.05$), contraction frequency by 38.38% (59.33 ± 8.85% vs. 20.95 ± 6.63%) (n=5, $p<0.05$), and contraction baseline by 6.84% (6.97 ± 0.93 vs. 0.13 ± 0.52%) (n=5, $p<0.05$), compared with exposure to the equivalent simvastatin concentration alone. SK and BK channel inhibition did not alter simvastatin's effects on contraction amplitude, or its IC_{50} value (2.55 ± 3.47μM vs. 2.91 ± 1.36μM) (n=5, $p>0.05$) (**See Figure 3-18**).

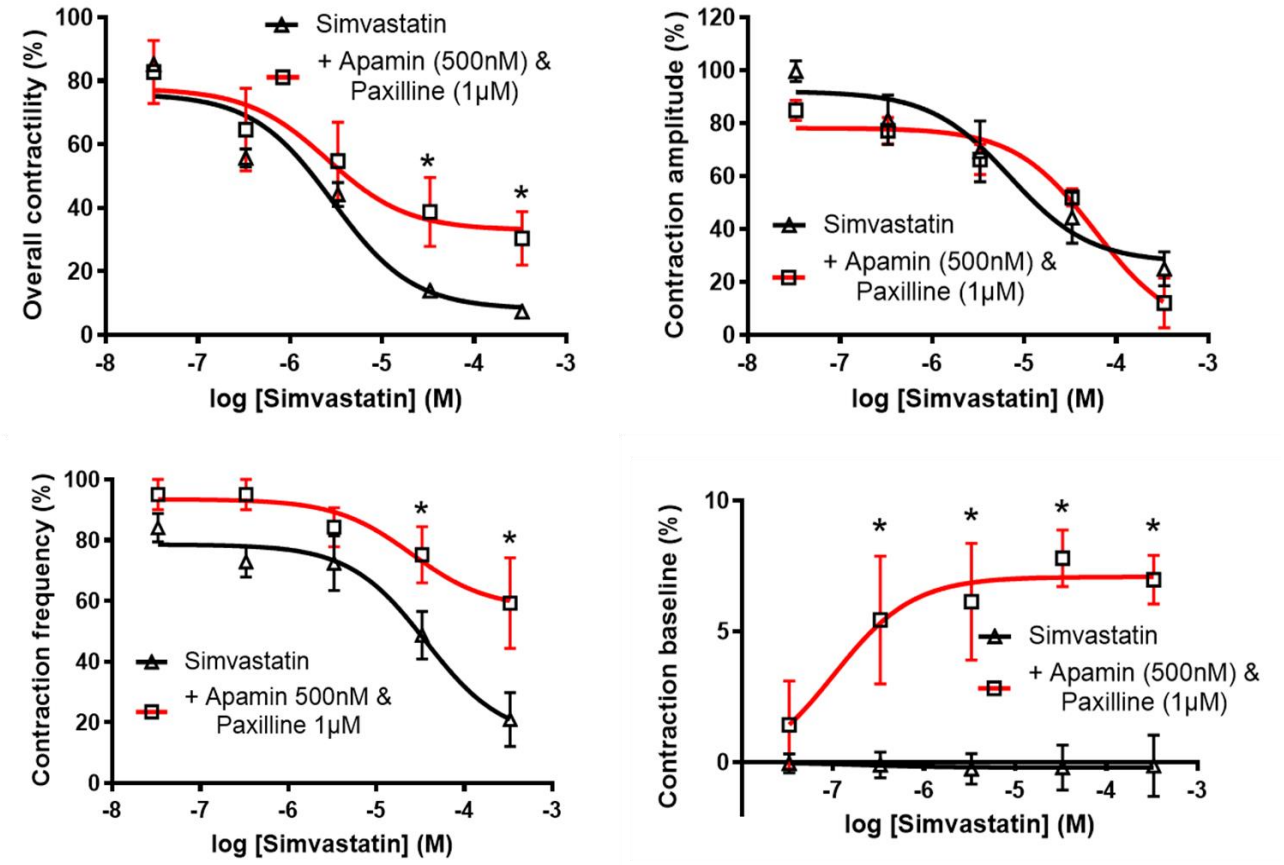


Figure 3-18. Effects of SK and BK channel inhibition alongside cumulative simvastatin (33nM - 330µM) exposure on overall spontaneous contractility (n=6), contraction amplitude (n=6), contraction frequency (n=6), and contraction baseline (n=6), in myometrial tissue samples obtained from women undergoing caesarean deliveries. Data is expressed as the mean contraction % of vehicle-treated samples ± SEM (ns $p>0.05$, *$p<0.05$).

3.5.6 BayK 8644-induced VOCC activation partially inhibited simvastatin-induced reduction of spontaneous myometrial contractions

VOCC activation by BayK 8644 resulted in the partial inhibition of simvastatin-induced reduction of spontaneous contractions. Tissues exposed to simvastatin (330μM) after channel activation resulted in an increase in overall contractility by 41.93% (50.63 ± 10.48 vs. 8.7 ± 2.21%) ($n=5$, $p<0.05$), but no change in contraction frequency or contraction baseline, compared to exposure with the equivalent simvastatin concentration alone ($n=5$, $p>0.05$). VOCC activation caused an increase in contraction amplitude after exposure to simvastatin at concentrations of 3.3μM and 33μM only. This resulted in an increase of 33.94% (96.10 ± 12.29% vs. 62.16 ± 7.89%) and 39.46% (84.31 ± 14.19%, vs. 44.86 ± 5.42%) ($n=5$, $p>0.05$) respectively, compared to exposure with the equivalent concentrations of simvastatin alone. Furthermore, the IC_{50} value for simvastatin did not change after VOCC activation (2.61 ± 3.60μM vs. 2.91 ± 1.36μM) ($n=5$, $p>0.05$) (**See Figure 3-19**).

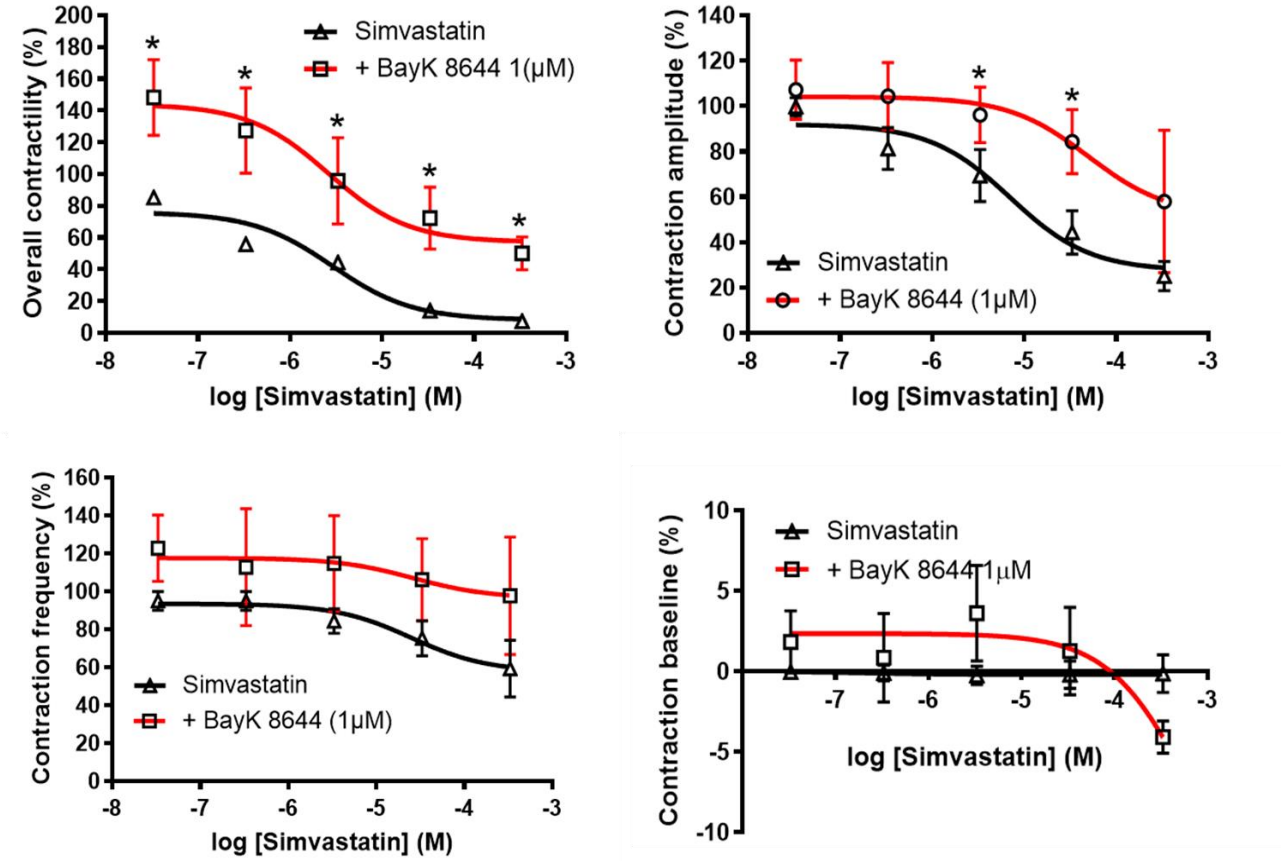


Figure 3-19. Effects of VOCC activation by BayK 8644 alongside cumulative simvastatin (33nM - 330μM) exposure on overall spontaneous contractility (n=5), contraction amplitude (n=5), contraction frequency (n=5), and contraction baseline (n=5), in myometrial tissue samples obtained from women undergoing caesarean deliveries. Data is expressed as the mean contraction % of vehicle-treated samples ± SEM (ns $p>0.05$, *$p<0.05$).

3.5.7 Discussion

Inhibition of voltage-operated K^+ and Ca^{2+}-operated K^+ channels, and selective inhibition of SK, and BK channels resulted in the partial inhibition of simvastatin-induced reduction of spontaneous contractions in myometrial tissues. The inhibition of both SK and BK channels in combination, resulted in enhanced inhibition of simvastatin's effects. These observations suggest that simvastatin may inhibit spontaneous contractility by promoting voltage-operated K^+ and Ca^{2+}-operated K^+ channel activity in the myometrium.

The effects of statins on ion channel activity appear to be tissue dependent, with several studies in different tissue types reporting conflicting observations after statin treatment. In porcine coronary artery smooth muscle cells, simvastatin exposure resulted in the inhibition of both basal BK channel activity and activation by agonists (Seto et al., 2007). Similarly, rat coronary arteries exposed to pravastatin resulted in a similar inhibition of IK channel activity and activation (Bergdhal et al., 2003). However, simvastatin exposure resulted in the activation of SK and BK channels in rat cerebral arteries (McNeish et al., 2012), and human endothelial cells (Kuhlmann et al., 2004). Our data supports the latter two studies, suggesting that simvastatin's effects are likely due to an increase in SK and BK channel activity. The opening of these channels causes an increase in K^+ efflux out the cell, resulting in membrane hyperpolarisation and the inhibition of action potential generation. Myometrial smooth muscle relaxation is achieved by the resultant decrease in $[Ca^{2+}]i$ as VOCCs are closed due to the change in membrane potential (**See Figure 3-20**).

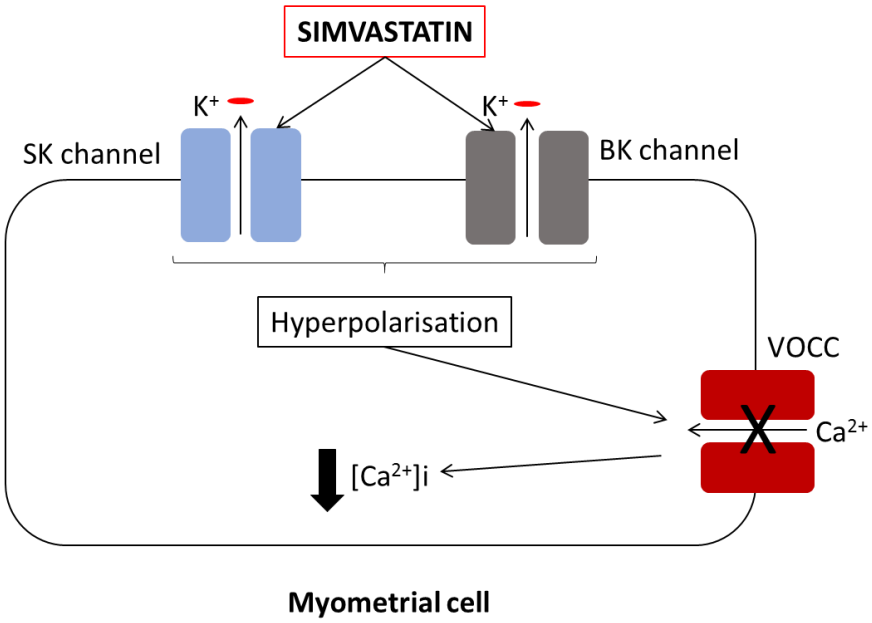


Figure 3-20. Diagram showing simvastatin-induced inhibition of SK and BK channels, resulting in a reduction in $[Ca^{2+}]i$ due to myometrial cell hyperpolarisation and the deactivation of VOCCs.

The activation of VOCCs by BayK 8644 resulted in the partial inhibition of simvastatin-induced reduction in spontaneous myometrial contractility. Our data is consistent with several previous studies showing the modulation of VOCCs in smooth muscle. For example, potassium chloride (KCl)-induced contractions in rat aortic ring smooth muscle were inhibited by simvastatin via inhibition of VOCC opening and activity (Alvarez et al., 2001; Marriot, 1988). This was also observed in rat superior mesenteric arteries, whereby simvastatin exposure inhibited VOCC activation, resulting in a decrease in $[Ca^{2+}]i$ and subsequent reduction in vascular tone and vasoconstriction (de Sotomayor et al., 2005). Similarly, rat pancreatic β-cells (Yada et al., 1999), and basilar artery preparations (Bergdahl et al., 2003b) exposed to simvastatin, and lovastatin respectively resulted in the inhibition of VOCC activity and a reduction in $[Ca^{2+}]i$. These observations suggest that

simvastatin can inhibit VOCC activity in the myometrium, resulting in a reduction in spontaneous myometrial contractions. This is likely due to the resultant decrease in VOCC Ca^{2+} influx causing a reduction $[Ca^{2+}]i$ to promote smooth muscle relaxation (**See Figure 3-21**).

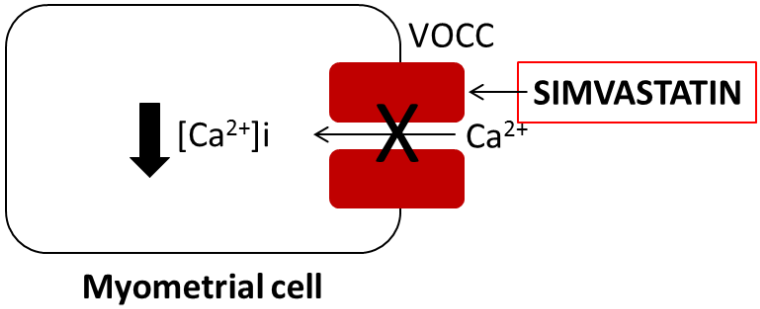


Figure 3-21. Diagram showing simvastatin-induced inhibition of VOCC activity resulting in a reduction in $[Ca^{2+}]i$ due to a decrease in Ca^{2+} influx into the myometrial cell.

3.5.8 Critique and further work

Our findings suggest that simvastatin-induced reduction in spontaneous myometrial contractions may involve the activation of SK and BK channels, and the inhibition of VOCC activity. However, further experiments are required to determine any potential direct changes in ion channel activity and function in the presence of simvastatin.

Electrophysiological recordings can be used to detect changes in electrical activity related to ion channel function during experimental conditions. Individual myometrial cells can be isolated and studied using the patch clamp technique, and single or multiple ion channels can be investigated in the presence of different experimental conditions.

An increase in SK and BK channel activity, and a reduction in VOCC activation after simvastatin exposure would confirm our contractility experiment observations. This would suggest that simvastatin can directly alter ion channel function resulting in the reduction of spontaneous contractions in the myometrium. Furthermore, changes in channel expression and protein concentration in the presence of simvastatin can be quantified using a combination of immunoblotting and immunocytochemical experiments.

Finally, it would be interesting to determine whether other ion channels are modulated in the presence of simvastatin in the myometrium, using a combination of contractility and electrophysiological experiments. These will mainly include ion channels known to be expressed in the myometrium, such as ATP-sensitive K^+ channels, Na^+ channels, Cl^- channels, KCNQ voltage-operated K^+ channel, the two-pore-domain K^+ channels, and hERG channels (Brueggemann et al., 2012; Buxton et al., 2010; Greenwood and Tribe, 2014; McCallum et al., 2011; Patel and Honore, 2002; Zhong et al., 2010).

3.6 Determine the effects of simvastatin on basal and oxytocin-induced $[Ca^{2+}]i$ release in myometrial cells

3.6.1 Aims

These experiments aim to investigate:

a) Whether myometrial cells obtained from pregnant women are sensitive to oxytocin-induced changes in $[Ca^{2+}]i$.

b) Whether simvastatin can affect basal and oxytocin-induced changes in $[Ca^{2+}]i$ in myometrial cells obtained from pregnant women.

3.6.2 Oxytocin increases $[Ca^{2+}]i$ in myometrial cells using the FLUO-4AM® Ca^{2+} assay

Myometrial cells exposed to oxytocin (2μM) resulted in an immediate increase in detected fluorescence, reaching a peak after 8-secs followed by a gradual decrease towards the baseline (**See Figure 3-22**). This resulted in an increase of 104.95% in calculated mean AUC (2.97 ± 0.62 a.u. vs. 0.14 ± 0.62 a.u.) (n=4, $p<0.01$) and 102.86% in peak fluorescence (0.18 ± 0.02 a.u. vs. 0.005 ± 0.003 a.u.) (n=4, $p<0.001$), compared to vehicle-treated cells (**See Figure 3-23**).

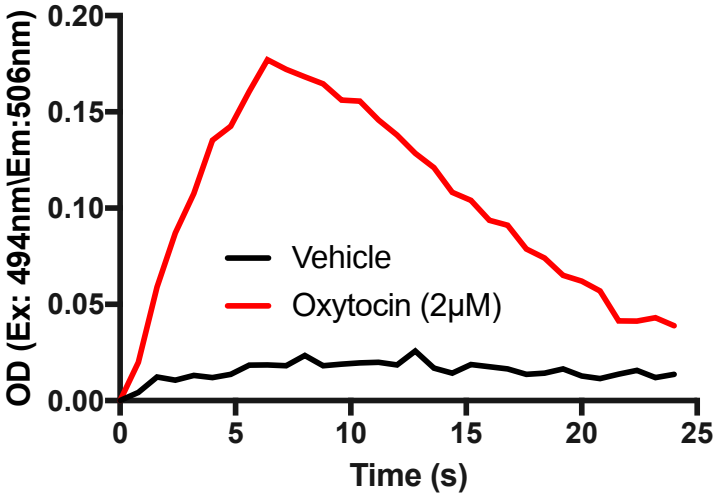


Figure 3-22. Representative trace showing changes in [Ca^{2+}]i-induced FLUO-4AM® fluorescence after exposure to oxytocin (2μM) in myometrial cells obtained from women undergoing caesarean deliveries over time.

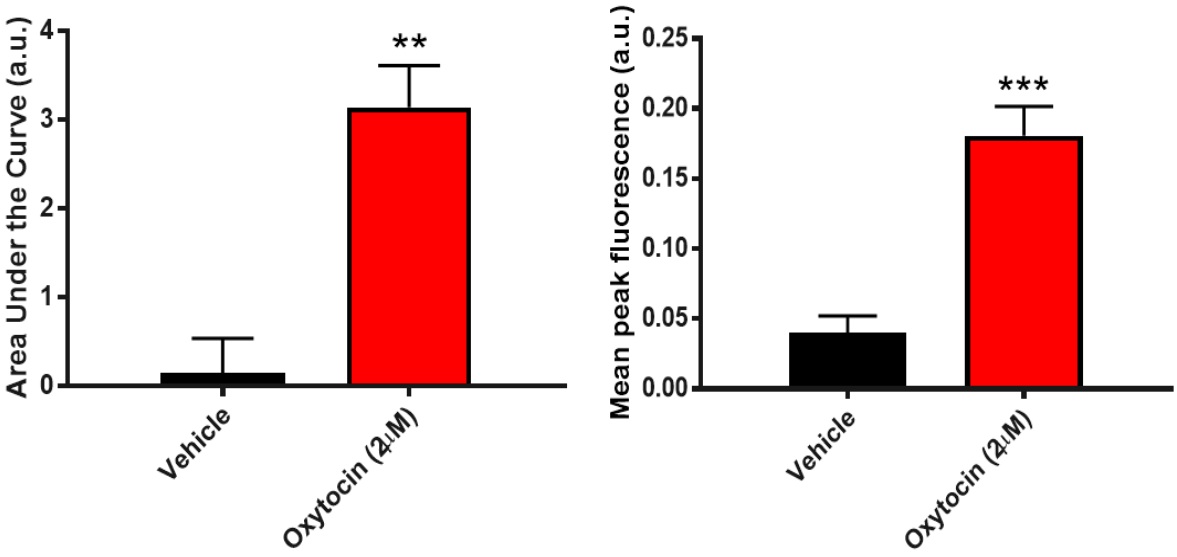


Figure 3-23. Effects of oxytocin (2μM) exposure on [Ca^{2+}]i-induced FLUO-4AM® mean AUC (n=4), and peak fluorescence (n=4). Data is expressed as the mean OD ± SEM (**p<0.01, ***p<0.001).

3.6.3 Simvastatin exposure did not alter $[Ca^{2+}]i$ in myometrial cells using the FLUO-4AM® Ca^{2+} assay

Myometrial cells exposed to simvastatin (3.3μM, 10μM, and 33μM) caused erratic fluctuations in detected fluorescence, with no observable concentration-dependent trend or pattern over time (**See Figure 3-24**). No change in calculated mean AUC or peak fluorescence was observed compared to vehicle-treated cells (n=4, $p>0.05$) (**See Figure 3-25**).

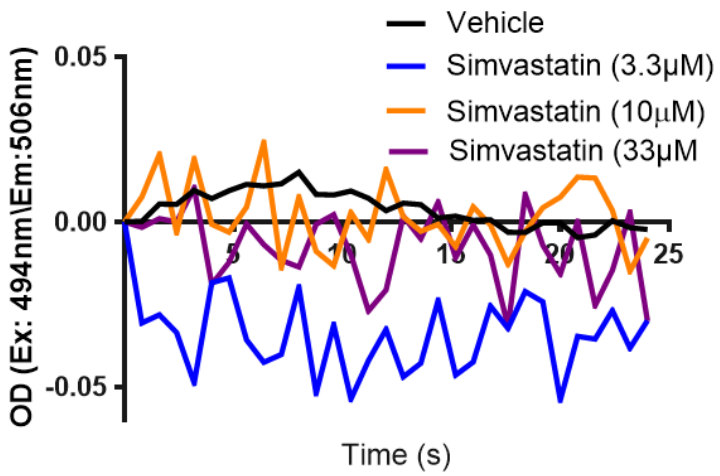


Figure 3-24. Representative trace showing changes in [Ca^{2+}]i-induced FLUO-4AM® fluorescence after exposure to simvastatin (3.3μM, 10μM, and 33μM) in myometrial cells obtained from women undergoing caesarean deliveries over time.

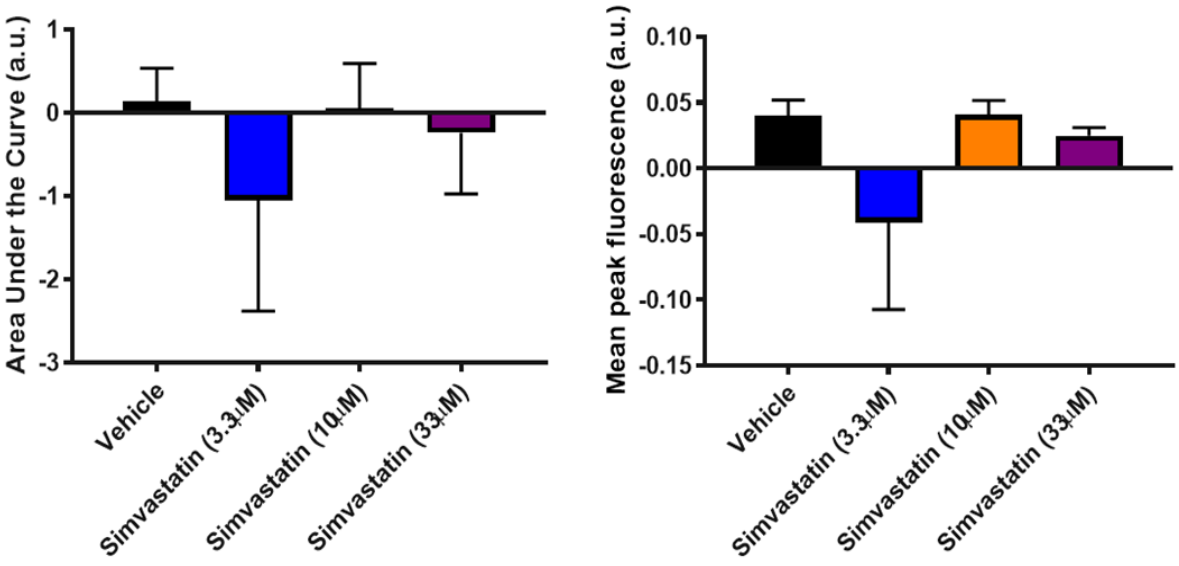


Figure 3-25. Effects of simvastatin (3.3μM, 10μM, and 33μM) exposure on [Ca^{2+}]i-induced FLUO-4AM® mean AUC (n=4) and peak fluorescence (n=4), in myometrial cells obtained from women undergoing caesarean deliveries. Data is expressed as the mean OD ± SEM (ns $p>0.05$).

3.6.4 Simvastatin exposure partially inhibited oxytocin-induced increase in $[Ca^{2+}]i$ in myometrial cells using the FLUO-4AM® Ca^{2+} assay

Myometrial cells exposed to simvastatin (3.3μM, 10μM, and 33μM) immediately after oxytocin (2μM), caused an observable concentration-dependent decrease in detected fluorescence magnitude compared to cells exposed to oxytocin alone (**See Figure 3-26**). This resulted in a decrease of 109.60% in calculated mean AUC (2.97 ± 0.62 a.u. vs. 0.26 ± 0.80 a.u.), and 164.70% in peak fluorescence (0.18 ± 0.02 a.u. vs. 0.07 ± 0.03 a.u.) ($n=4$, $p<0.05$), after exposure to the highest concentration of simvastatin (33μM), compared to cells treated with oxytocin alone. However, changes in fluorescence after exposure to 3.3μM and 10μM concentrations of simvastatin were not statistically significant ($n=4$, $p>0.05$). This is likely due to the variation between replicates at these concentrations (not shown), resulting in visibly large error bars after analysis (**See Figure 3-27**).

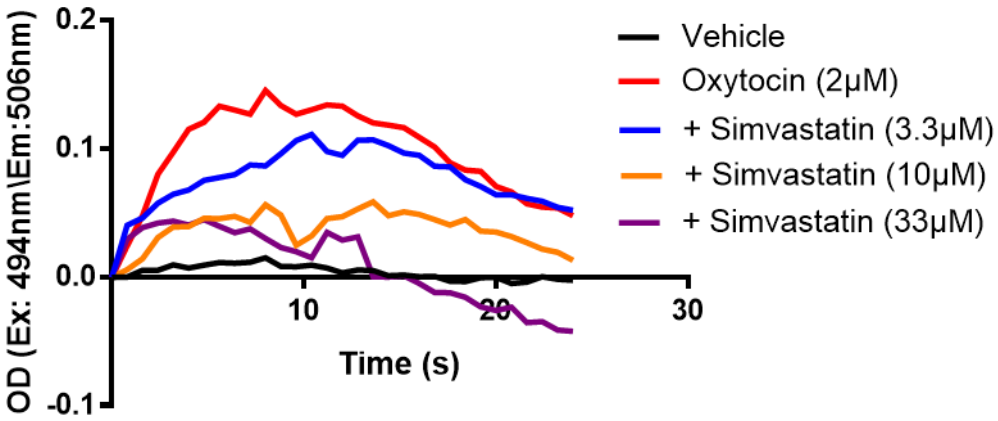


Figure 3-26. Representative trace showing changes in [Ca^{2+}]i-induced FLUO-4AM® fluorescence after exposure to simvastatin (3.3μM, 10μM, and 33μM) immediately after oxytocin (2μM) addition, in myometrial cells obtained from women undergoing caesarean deliveries over time.

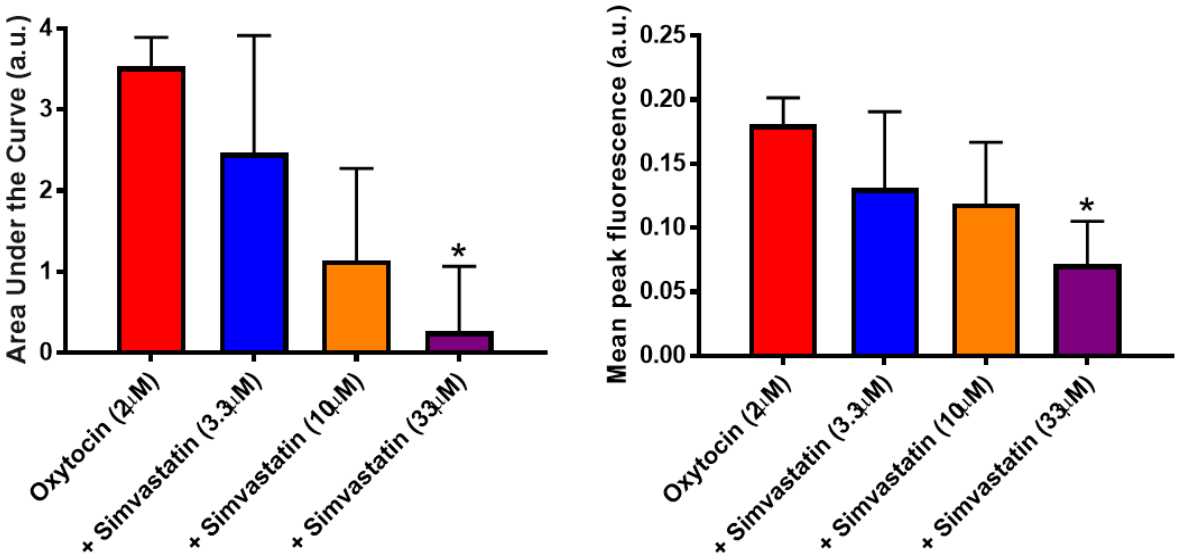


Figure 3-27. Effects of simvastatin (3.3μM, 10μM, and 33μM) exposure, immediately after oxytocin (2μM) addition, on [Ca^{2+}]i-induced FLUO-4AM® mean AUC (n=4), and mean peak fluorescence (n=4) in myometrial cells obtained from women undergoing caesarean deliveries. Data is expressed as the mean OD ± SEM (ns $p>0.05$, *$p<0.05$).

3.6.5 Oxytocin increases $[Ca^{2+}]i$ in myometrial cells using the FLIPR® Ca^{2+} 5 assay

Myometrial cells exposed to oxytocin (10μM) resulted in an immediate increase in detected fluorescence, reaching a peak after 16-secs followed by a decrease back to baseline values (**See Figure 3-28**). Oxytocin exposure caused an increase of 83.19% in calculated mean AUC (1213.294 ± 141.72 a.u. vs. 7219.11 ± 407.50 a.u.) ($n=4$, $p<0.001$), and 99% in peak fluorescence (2.12 ± 0.36 a.u. vs. 210.48 ± 58.38 a.u.) ($n=4$, $p<0.01$), compared to vehicle-treated cells (**See Figure 3-29**).

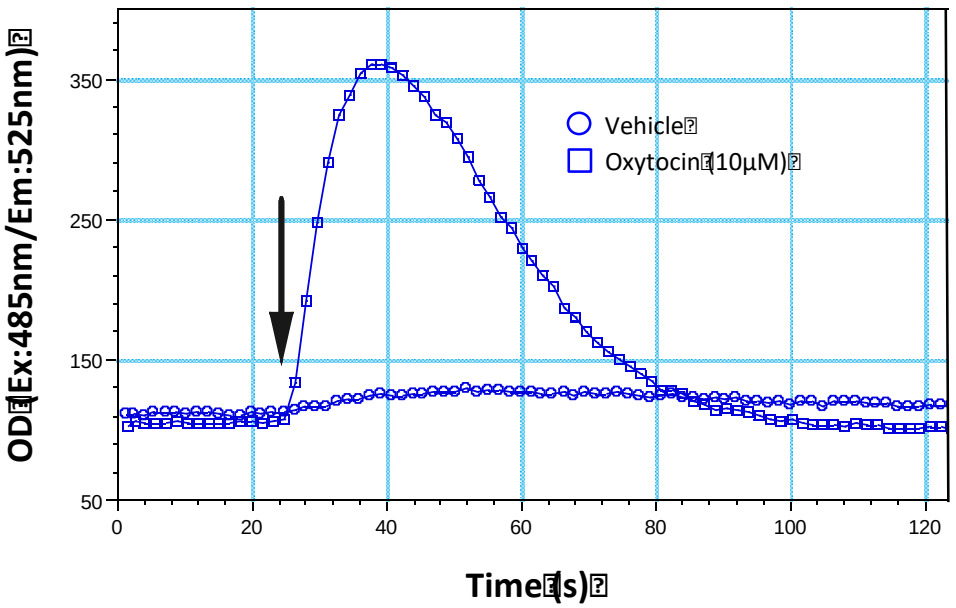


Figure 3-28. Representative trace showing changes in $[Ca^{2+}]$i-induced FLIPR® fluorescence after exposure to oxytocin (10μM) in myometrial cells obtained from women undergoing caesarean deliveries over time (Arrow indicates the time-point at which oxytocin was introduced).

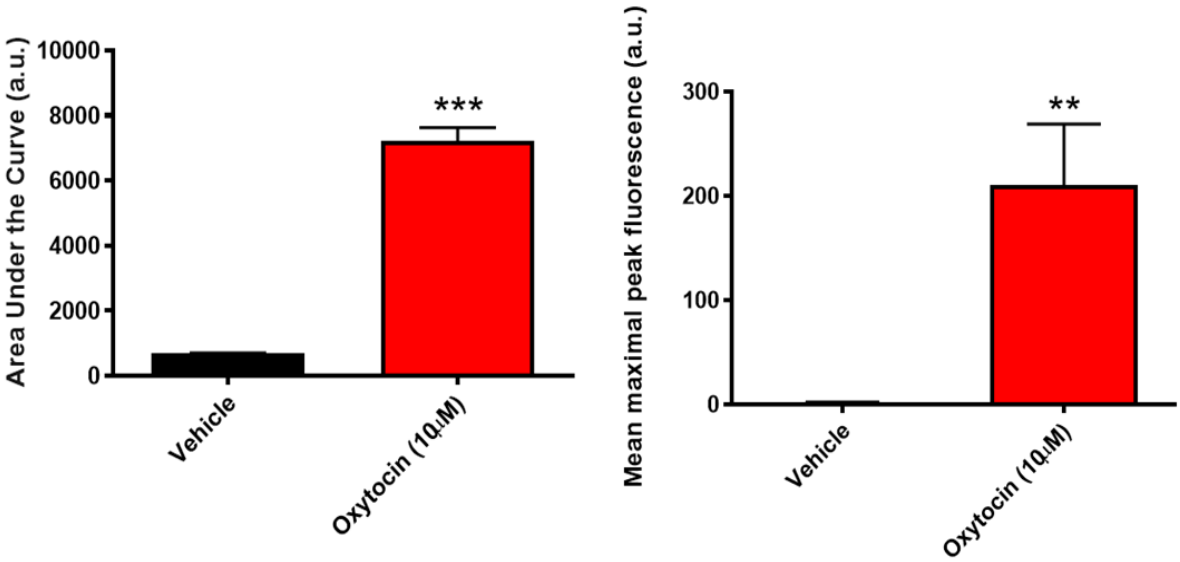


Figure 3-29. Effects of oxytocin (10μM) exposure on $[Ca^{2+}]$i-induced FLIPR® AUC (n=4), and mean peak fluorescence (n=4) in myometrial cells obtained from women undergoing caesarean deliveries. Data is expressed as the mean OD ± SEM (**p<0.01, ***p<0.001).

3.6.6 Myometrial cells pre-incubated with simvastatin for 18-hours inhibited oxytocin-induced increase in $[Ca^{2+}]i$ using the FLIPR® Ca^{2+} 5 assay

Myometrial cells pre-incubated with simvastatin (3.3μM, 10μM, and 33μM) for 18-hours before exposure to oxytocin (10μM), resulted in a concentration-dependent decrease in detected fluorescence magnitude compared to cells treated with oxytocin alone (**See Figure 3-30**). Resultant mean AUC was decreased by 27.95% (5201.60 ± 820.70 a.u.), 32.37% (4881.97 ± 997.38 a.u.), and 37.97% (4477.53 ± 853.46 a.u.), for 3.3μM, 10μM, and 33μM concentrations of simvastatin respectively, compared to oxytocin (7219.11 ± 407.50 a.u.) (n=4, $p<0.01$). Mean peak fluorescence was also significantly decreased by 59.94% (84.31 ± 30.71 a.u.), 67.32% (68.78 ± 24.66 a.u.), and 70.49% (62.10 ± 21.39 a.u.), for 3.3μM, 10μM, and 33μM concentrations of simvastatin respectively, compared to oxytocin (210.48 ± 58.38 a.u.) (n=4, $p<0.01$, $p<0.001$) (**See Figure 3-31**).

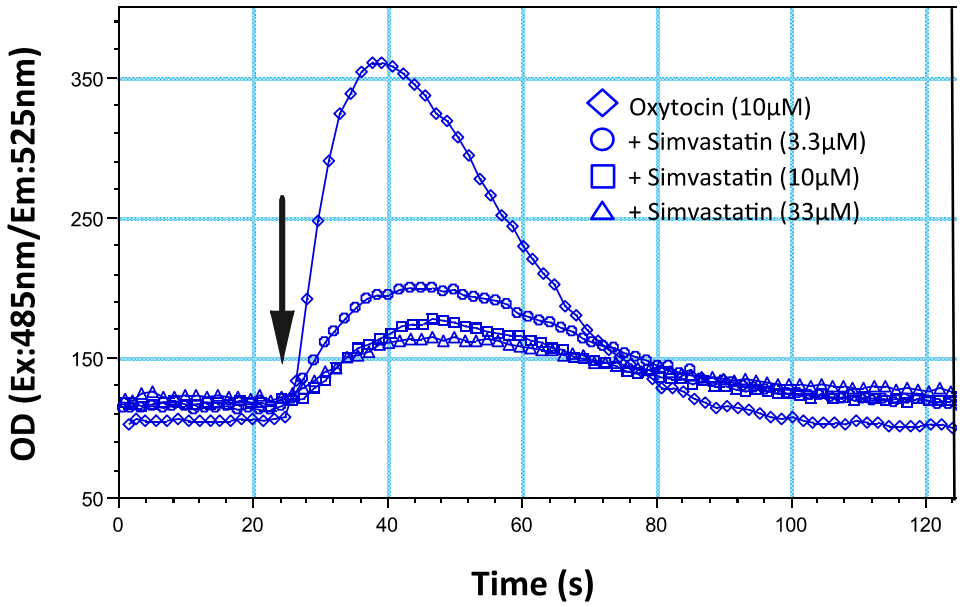


Figure 3-30. Representative trace showing changes in $[Ca^{2+}]$i-induced FLIPR® fluorescence, after pre-incubation with simvastatin (3.3μM, 10μM, and 33μM) for 18-hours, followed by oxytocin (10μM), in myometrial cells obtained from women undergoing caesarean deliveries over time (Arrow indicates the time-point at which oxytocin was introduced).

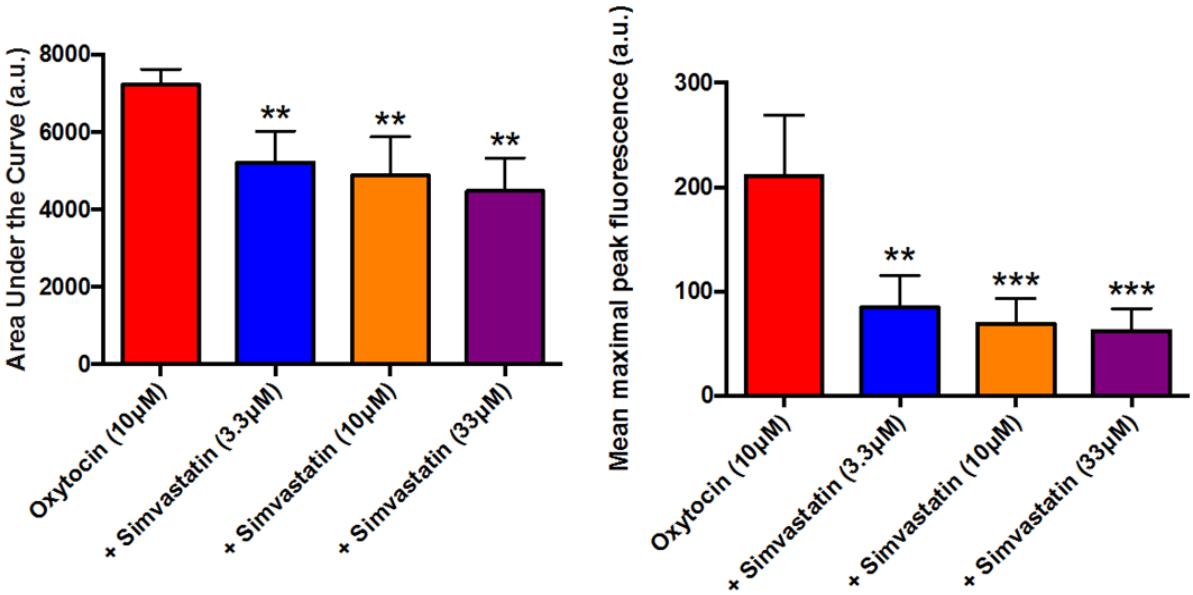


Figure 3-31. Effects of simvastatin (3.3μM, 10μM, and 33μM) pre-incubation for 18-hours, followed by oxytocin (10μM) addition, on $[Ca^{2+}]$i-induced FLIPR® mean AUC (n=4), and peak fluorescence (n=4) in myometrial cells obtained from women undergoing caesarean deliveries. Data is expressed as the mean OD ± SEM (**p<0.01, ***p<0.001).

3.6.7 Discussion

Myometrial cells exposed to simvastatin resulted in the inhibition of oxytocin-induced increase in $[Ca^{2+}]i$. However, simvastatin exposure alone did not alter basal $[Ca^{2+}]i$ in the myometrial cell. These observations support previous studies showing statin-induced modulation of Ca^{2+} homeostasis, and the inhibition of oxytocin-induced Ca^{2+} release (Kang et al., 2014; Marriot, 1998; Alvarez et al., 2001; Yada et al., 1999). However, there are other studies which reported an increase in $[Ca^{2+}]i$ after treatment with fluvastatin and cerivastatin, and had no effect on histamine, and caffeine-induced Ca^{2+} release (Heinke et al., 2004; Liantonio et al., 2007). This is most likely due to a tissue or statin type-dependent variation, and the difference in agonist-induced Ca^{2+} release mechanism investigated.

In the myometrium, exposure to histamine and caffeine results in the release of Ca^{2+} from ryanodine-sensitive stores. This mechanism of Ca^{2+} release is known to play a smaller role in contractility, compared to Ca^{2+} release from internal stores in SR by oxytocin (Taggart & Wray, 1998; Wray et al., 2002). This may explain why other studies have observed no effect on histamine and caffeine-induced Ca^{2+} release, after statin exposure (Heinke et al., 2004; Liantonio et al., 2007). These observations suggest that simvastatin's effects on $[Ca^{2+}]i$ are likely to be tissue dependent, and specific to mechanisms related to oxytocin-induced Ca^{2+} release from the SR.

Simvastatin-induced inhibition of oxytocin-induced Ca^{2+} release was greater with the length of exposure. Myometrial cells exposed to simvastatin for 18-

hours resulted in enhanced inhibition of oxytocin's effects. Furthermore, simvastatin exposure caused a reduction in both total $[Ca^{2+}]i$, and peak $[Ca^{2+}]i$ release after oxytocin treatment, but did not prevent oxytocin's effects completely, indicating that binding between oxytocin and its receptor remain unaffected. These observations suggest that simvastatin is likely to reduce oxytocin-induced activity by competitive with oxytocin for its receptor. Competitive inhibition of the oxytocin receptor prevents the dissociation of the GPCR α-subunit and the activation of PLC, which inhibits the production of IP_3 and DAG from PIP_2. The lack of circulating IP_3 inhibits the activation of IP_3-receptors on the surface of the SR membrane, and therefore the release of Ca^{2+} through these receptors to promote myometrial smooth muscle relaxation (**See Figure 3-32**).

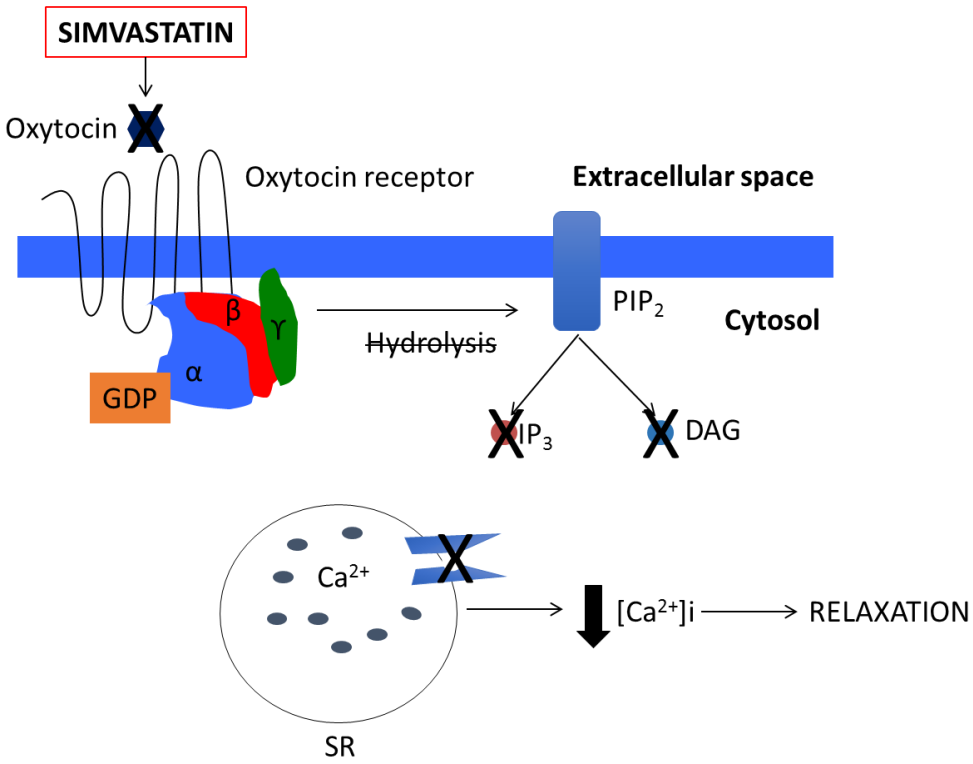


Figure 3-32. Diagram showing simvastatin-induced competitive inhibition of oxytocin for its receptor, resulting in the inhibiting of IP_3 and DAG production and preventing the release of Ca^{2+} from internal SR stores.

3.6.8 Critique and further work

The FLUO-4AM® Ca^{2+} assay was used in tandem with a commercially untested pipette system developed in our lab. These self-made pipette tips, although optimised to pipette the correct volumes, was not designed for the Thermo Fluoroskan Ascent F2 fluorescence plate reader used for detection. There is a possibility that these pipette tips would degrade and become deformed after multiple uses, resulting in potentially incomplete or erroneous transfer of solutions to the treatment plate. Furthermore, the lid of the plate reader was lifted for each treatment addition to reveal the treatment porthole, and exposing parts of the treatment plate to UV light. These technical issues may affect fluorescence measurements and may contribute to variations between experiments observed.

To solve any issues that may arise from using the self-made pipette tips, the effects of simvastatin on oxytocin-induced Ca^{2+} release were also determined using the FLIPR® Ca^{2+} assay, and measured using a FlexStation 3 multi-mode microplate reader (Molecular Devices, UK). The fluorophore used in the FLIPR® Ca^{2+} assay is an enhanced analogue of the FLUO-4AM fluorophore, which is suspended in a masking dye to decrease background fluorescence during detection. The FlexStation 3 microplate reader used for the FLIPR® Ca^{2+} assay was chosen for its automated treatment delivery system, utilising manufactured pipette tips specifically designed for the microplate reader.

During our experiments, we encountered problems relating to the FlexStation 3 microplate reader automated treatment delivery system, resulting in the

functional use of only one delivery pump. Furthermore, the predicted date of repair was beyond our allocated time with the reader. This meant that experiments to determine the effects of immediate simvastatin exposure, rather than over 18-hours, on oxytocin-induced Ca^{2+} release using the FLIPR® Ca^{2+} assay, were not conducted. With more time, it would be useful to repeat these experiments using a fully functional FlexStation 3 microplate reader.

Our FLIPR® Ca^{2+} assay experiments used a 10μM concentration of oxytocin compared to 2μM, as used in our FLUO-4AM® Ca^{2+} assay experiments. During preliminary studies using the FLIPR® Ca^{2+} assay, it was found that at an oxytocin concentration of 2μM resulted in low, erratic, and inconsistent detected fluorescent signals in myometrial cells. These anomalies were not observed when the concentration was increased to 10μM, which showed a consistently strong, and repeatable increase in fluorescent signal immediately after addition. During these studies, we were unable to determine the reason for these anomalies. It was therefore decided that an oxytocin concentration of 10μM would be used in our experiments to progress our investigation.

To further determine the direct effects of simvastatin on oxytocin signalling in the myometrium, tissue contractility experiments can be conducted to assess changes in oxytocin-induced myometrial contractions after simvastatin exposure. A reduction in contractions after simvastatin exposure would further support our conclusion that simvastatin inhibits oxytocin-induced effects in the myometrium. To determine if simvastatin acts as a competitive inhibitor with oxytocin, experiments using enzyme-linked immunosorbent assays (ELISA)

can be conducted. ELISA treatment plates can be coated with human recombinant oxytocin receptor protein and co-incubated with biotinylated-oxytocin, followed by non-biotinylated simvastatin. A reduction in detected biotinylation would indicate that simvastatin competes with oxytocin for the oxytocin receptor.

3.7 Determine the effects of simvastatin on Hoechst 33342 dye tracer permeability in myometrial cells

3.7.1 Aims

These experiments aim to investigate:

a) Whether myometrial cells obtained from pregnant women are permeable to the Hoechst 33342 dye tracer.

b) Whether simvastatin exposure can modulate cell permeability to Hoechst 33342 nuclear dye tracer in myometrial cells obtained from pregnant women.

3.7.2 Myometrial cells are permeable to the Hoechst 33342 dye tracer

Myometrial cells exposed to Hoechst 33342 dye tracer (8μM) resulted in an immediate and sustained increase in detected fluorescence, followed by a gradual decrease after 15-secs (**See Figure 3-33**). This resulted in an increase of 95.39% in mean peak fluorescence (0.39 ± 0.05 a.u. vs. 0.018 ± 0.01 a.u.) (n=5, $p<0.0001$), compared to vehicle-treated cells (**See Figure 3-34**).

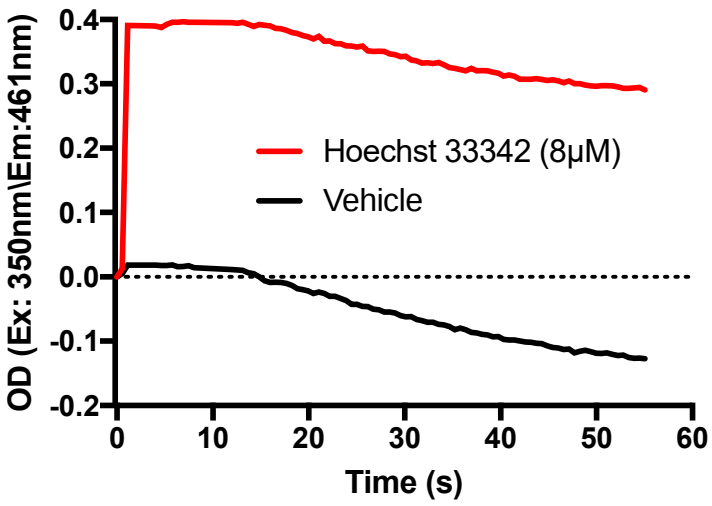


Figure 3-33. Representative trace showing changes in Hoechst 33342-induced fluorescence in myometrial cells obtained from women undergoing caesarean deliveries over time.

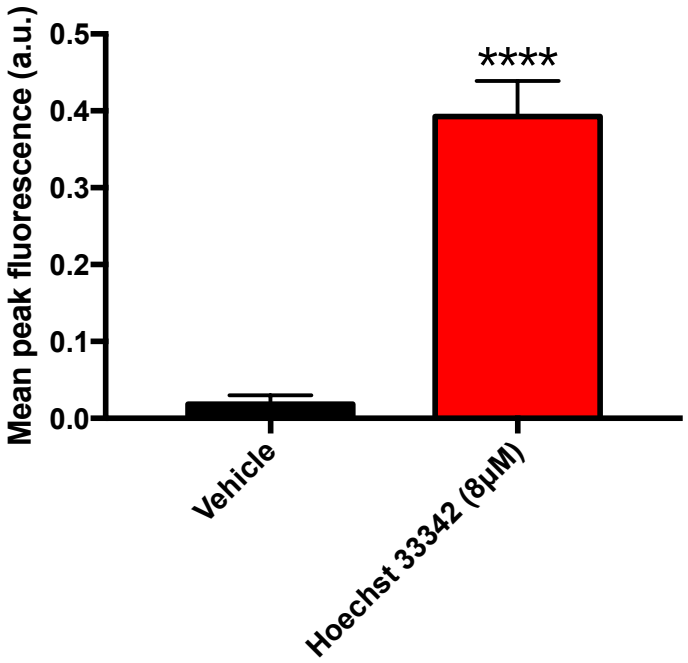


Figure 3-34. Changes in mean peak fluorescence after exposure to Hoechst 33342 dye tracer in myometrial cells obtained from women undergoing caesarean deliveries (n=5). Data is expressed as the mean OD ± SEM (**p<0.01, ****p<0.0001).

3.7.3 Simvastatin increased detected fluorescence in the absence of Hoechst 33342 dye tracer in myometrial cells

In the absence of Hoechst 33342 dye tracer, myometrial cells exposed to simvastatin (3.3μM, 10μM, and 33μM) resulted in a concentration-dependent increase in detected fluorescence, suggesting the possibility of simvastatin-induced auto-fluorescence (**See Figure 3-35**). Cells exposed to the highest concentration of simvastatin (33μM), resulted in a 95.61% (0.018 ± 0.03 a.u. vs. 0.41 ± 0.05 a.u.) *n=5, $p<0.01$) increase in mean peak fluorescence, compared to vehicle-treated cells. Exposure to simvastatin at concentrations of 3.3μM and 10μM also resulted in an observable increase in detected fluorescence, however, these effects were not statistically significant (**See Figure 3-36**).

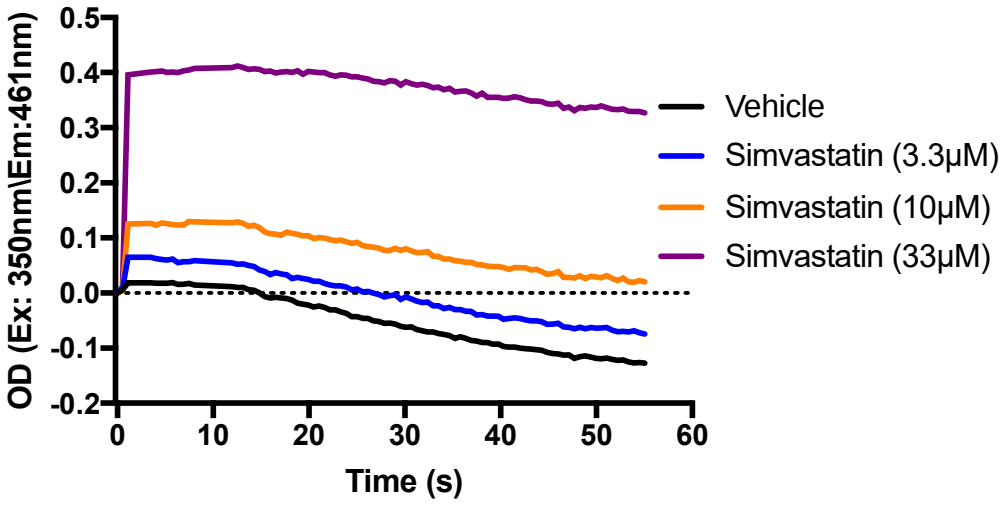


Figure 3-35. Representative trace showing changes in detected auto-fluorescence after exposure to simvastatin (3.3μM, 10μM, and 33μM) in myometrial cells obtained from women undergoing caesarean deliveries over time.

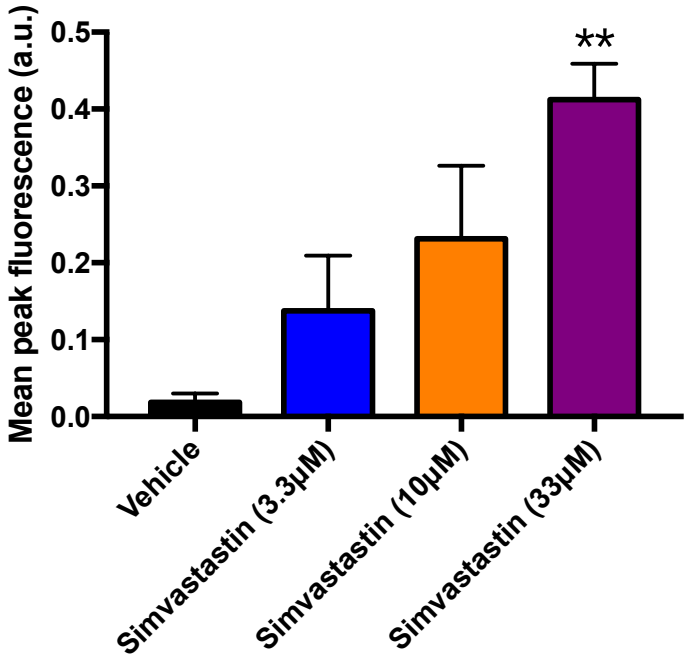


Figure 3-36. Effects of simvastatin (3.3μM, 10μM, and 33μM) exposure on detected mean peak fluorescence (n=5). Data is expressed as the mean OD ± SEM (ns $p>0.05$, **$p<0.01$).

3.7.4 Simvastatin exposure did not alter myometrial cell permeability to Hoechst 33342 dye tracer

Myometrial cells exposed to simvastatin (3.3μM, 10μM, and 33μM) in the presence of Hoechst 33342 dye tracer (8μM), resulted in a concentration-dependent increase in detected fluorescence, with a noticeable increase after exposure to a simvastatin concentration of 33μM (**See Figure 3-37**). However, after normalisation for simvastatin-induced auto-fluorescence, the resultant increase in mean peak fluorescence was not statistically significant compared to cells exposed to the Hoechst 33342 dye tracer alone ($n=5$, $p>0.05$) (**See Figure 3-38**).

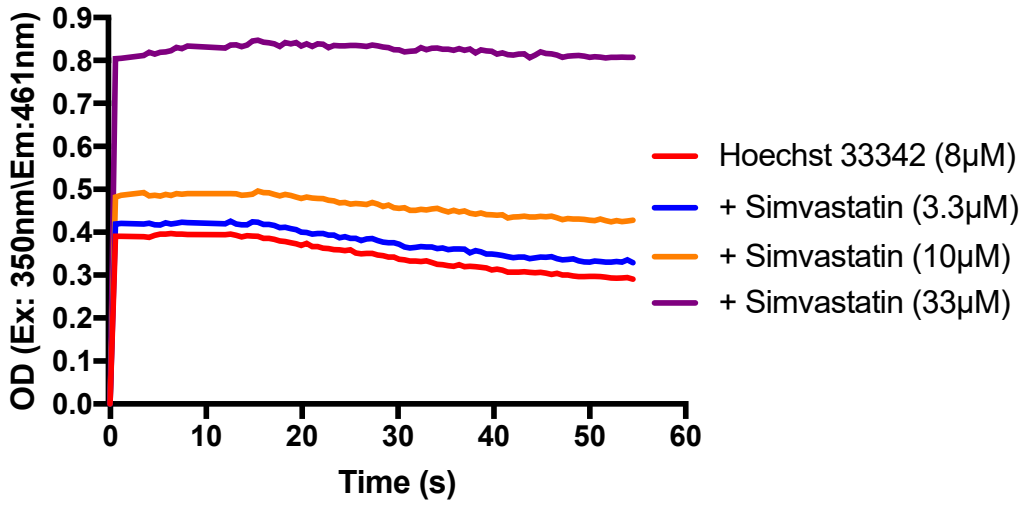


Figure 3-37. Representative tracer showing changes in Hoechst 33342-induced fluorescence after simvastatin (3.3μM, 10μM, and 33μM) exposure in myometrial cells obtained from women undergoing caesarean deliveries over time.

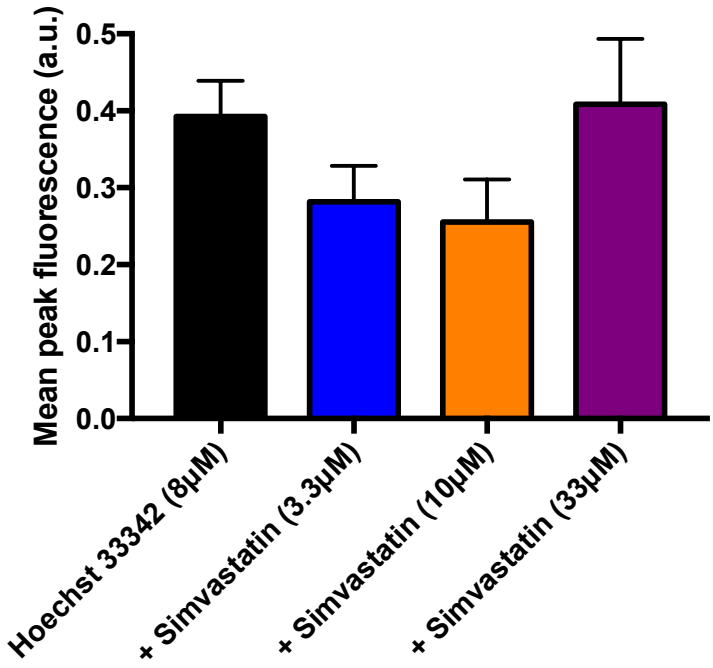


Figure 3-38. Effects of simvastatin (3.3μM, 10μM, and 33μM) exposure in the presence of Hoechst 33342 dye tracer (after normalisation for simvastatin-induced auto-fluorescence) on detected mean peak fluorescence (n=5). Data is expressed as the mean OD ± SEM (ns $p>0.05$).

3.7.5 Discussion

In this investigation, the Hoechst 33342 dye tracer was used to determine changes in myometrial cell permeability in the presence of simvastatin. However, we found that in the absence of the Hoechst 33342 dye tracer, cells exposed to simvastatin alone resulted in a concentration-dependent increase in detected fluorescent signal. After normalising for simvastatin-induced auto-fluorescence, subsequent experiments found no change in myometrial cell permeability to the Hoechst 33342 dye tracer after simvastatin exposure. These experiments suggest that it is unlikely that simvastatin can alter myometrial cell permeability.

The myometrial cell resting membrane potential undergoes rhythmic changes in permeability to Ca^{2+} and K^{+} ions, whereby increases in Ca^{2+} permeability promotes membrane depolarisation, and increases in K^{+} permeability promotes repolarisation or hyperpolarisation (Kao et al., 1989; Marshall, 1990; Parkington & Coleman, 1990; Sanborn, 1995). In our experiments, we hypothesised that simvastatin alters myometrial cell permeability, which in turn may affect the flux of Ca^{2+} and K^{+} ions, and therefore modulate action potential generation and myometrial tissue contractility. Several studies have shown that statins can alter cell and tissue permeability in the blood-brain barrier, the retinal vasculature, and other blood vessels (Mooradian, Haas et al. 2005; Sen, Misra et al. 2002; Gupta, Gupta et al. 2004; Dell'Omo et al., 2000; Wei et al., 2005). However, our data contradicts these previous studies showing no change in permeability in the myometrial cell.

3.7.6 Critique and further work

The evidence of simvastatin-induced auto-fluorescence during our experiments indicates that the Hoechst 33342 dye tracer assay methodology requires further optimisation. It is very likely that this auto-fluorescence masked any detectable simvastatin-induced changes in fluorescent signal during our experiments. The issues with treatment auto-fluorescence may be solved by measuring permeability using non-fluorescent probes. For example, changes in cell permeability can be investigated by detecting changes in electrical resistance, using a transepithelial/transendothelial electrical resistance (TEER) transwell assay, or an electrical cell-substrate impedance sensing (ECIS) assay. Both techniques utilise changes in the electrical resistance produced by a confluent monolayer of cells, to determine modulations in permeability.

3.8 Determine the effects of simvastatin on the expression of caveolae cholesterol binding protein caveolin-1 in the myometrial cell

3.8.1 Aims

These experiments aim to investigate:

a) Evidence of endogenous caveolin-1 protein expression in myometrial cells obtained from women undergoing caesarean deliveries.
b) Changes in caveoin-1 and α-actin protein expression after simvastatin, and MCD exposure over time in myometrial cells obtained from women undergoing caesarean deliveries.

3.8.2 Identification of myometrial cells in culture

Myometrial cells were isolated from myometrial tissue samples obtained from pregnant women and cultured for 18-hours before preparation for visualisation under light and fluorescent microscopy. Representative phase-contrast images showed a collection of elongated and spindle-shaped cells, typical of myometrial smooth muscle cells in culture conditions. Representative immunofluorescent images of myometrial cells cultured for 18-hours showed evidence of α-actin staining, appearing as networks of filament bundles that are indicative of the cytoskeletal structures in smooth muscle cells (**See Figure 3-39**).

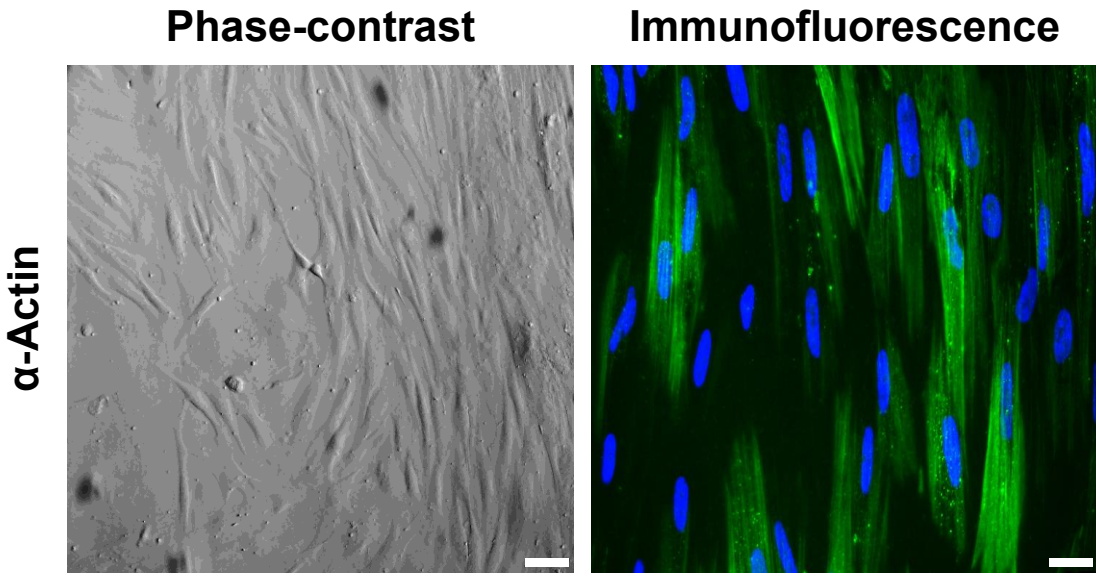


Figure 3-39. Representative phase-contrast and immunofluorescent images of myometrial cells cultured for 18-hours, isolated from samples obtained from women undergoing caesarean deliveries. Staining: α-actin/DAPI (Scale bar = 100μm).

3.8.3 Caveolin-1 is expressed in myometrial cells

Representative immunofluorescent images show evidence of caveolin-1 protein expression in myometrial cells taken from pregnant women. Caveolin-1 appears to be expressed around the nucleus in separate intracellular compartments (white arrow), within the nucleus itself (red arrow), and around the cell body, possibly in the cell membrane (orange arrow). These observations were consistent with both un-treated and vehicle-treated cells cultured for 18-hours, with no obvious change in caveolin-1 expression between the two groups (**See Figure 3-40**).

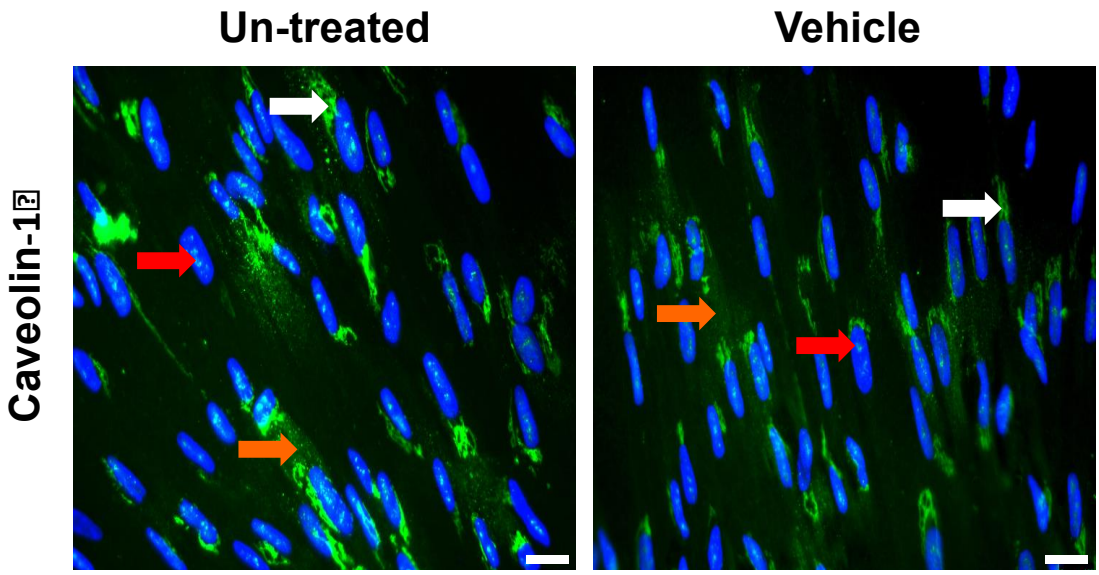


Figure 3-40. Representative phase-contrast and immunofluorescent images showing evidence of caveolin-1 protein expression in un-treated and vehicle-treated myometrial cells cultured for 18-hours, isolated from samples obtained from women undergoing caesarean deliveries(n=4). Caveolin-1 expression localised in: intracellular compartments around the nucleus (white arrow), within the nucleus (red arrow), and around the cell body (orange arrow). Staining: Caveolin-1/DAPI (Scale bar = 100µm).

3.8.4 Simvastatin exposure did not alter α-actin expression in myometrial cells

Myometrial cells exposed to simvastatin (3.3μM, 10μM, and 33μM) resulted in no observable change in α-actin expression after 24-hours. However, cells exposed to MCD (330μM) resulted in the complete disruption of α-actin staining, with evidence of nuclei rounding and blebbing after 24-hours (n=4) (**See Figure 3-41**).

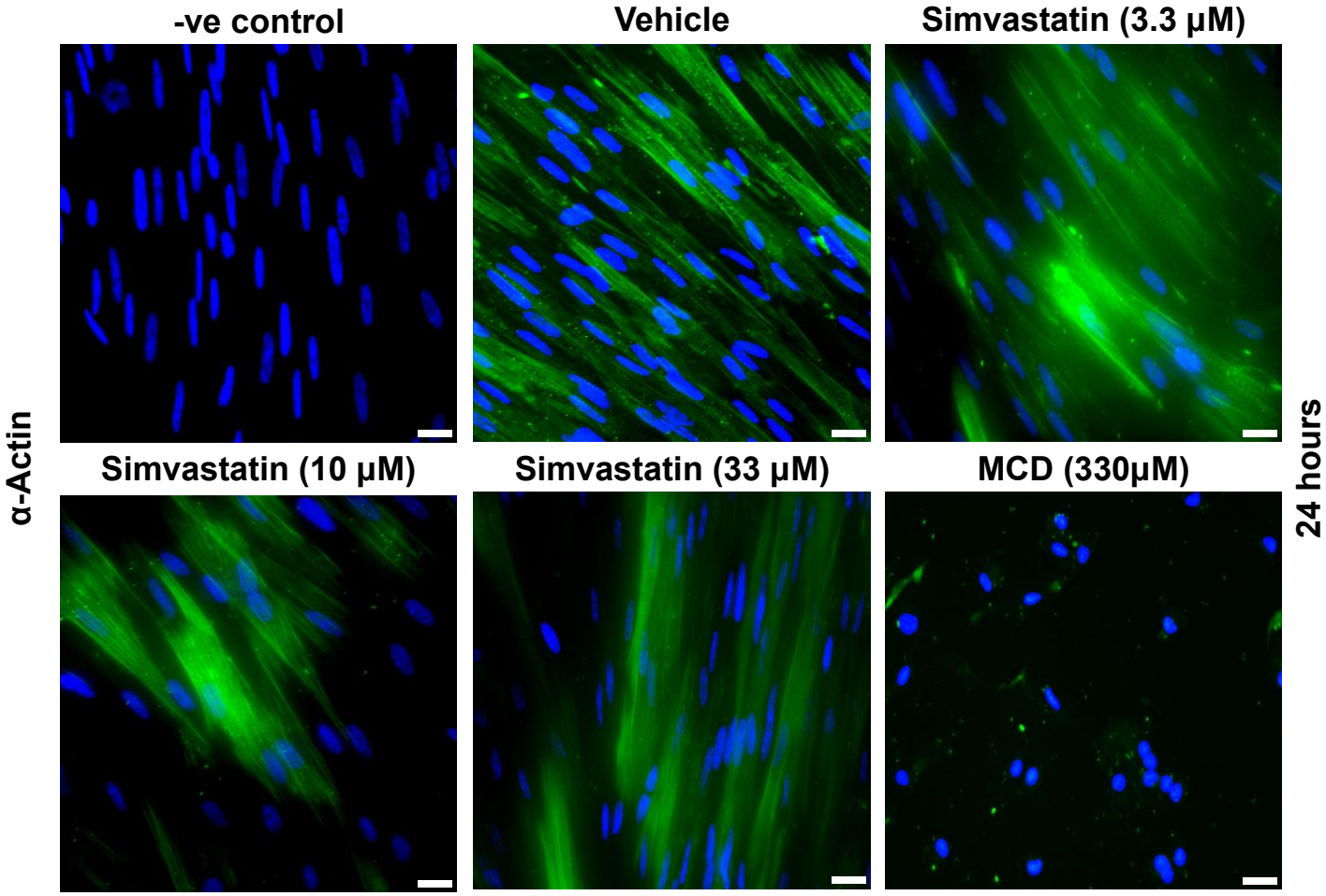


Figure 3-41. Representative immunofluorescent images showing the effects of simvastatin (3.3μM, 10μM, and 33μM) and MCD (300μM) exposure on α-actin protein expression in myometrial cells after 24-hours. Cells were isolated from samples obtained from women undergoing caesarean deliveries (n=4). Staining: α-actin/DAPI (Scale bar = 100μm).

3.8.5 Simvastatin and MCD exposure disrupted caveolin-1 expression in myometrial cells over time

Myometrial cells exposed to simvastatin (3.3μM, 10μM, and 33μM) resulted in a gradual decrease in caveolin-1 expression over time. After 45 mins (**See Figure3-42**) and 4-hours (**See Figure 3-43**), caveoline-1 expression remained intact but appeared to diminish in intensity, with a visible loss in staining in areas around the nucleus and cell body. After 24-hours (**See Figure 3-44**), caveolin-1 expression appeared to be present in only a small number of cells, with the complete absence of staining in areas around the cell body and within the nucleus. Cell exposed to MCD (330μM) resulted in the complete disruption of caveolin-1 staining immediately after 45-mins, persisting after 4-hours or 24-hours of exposure.

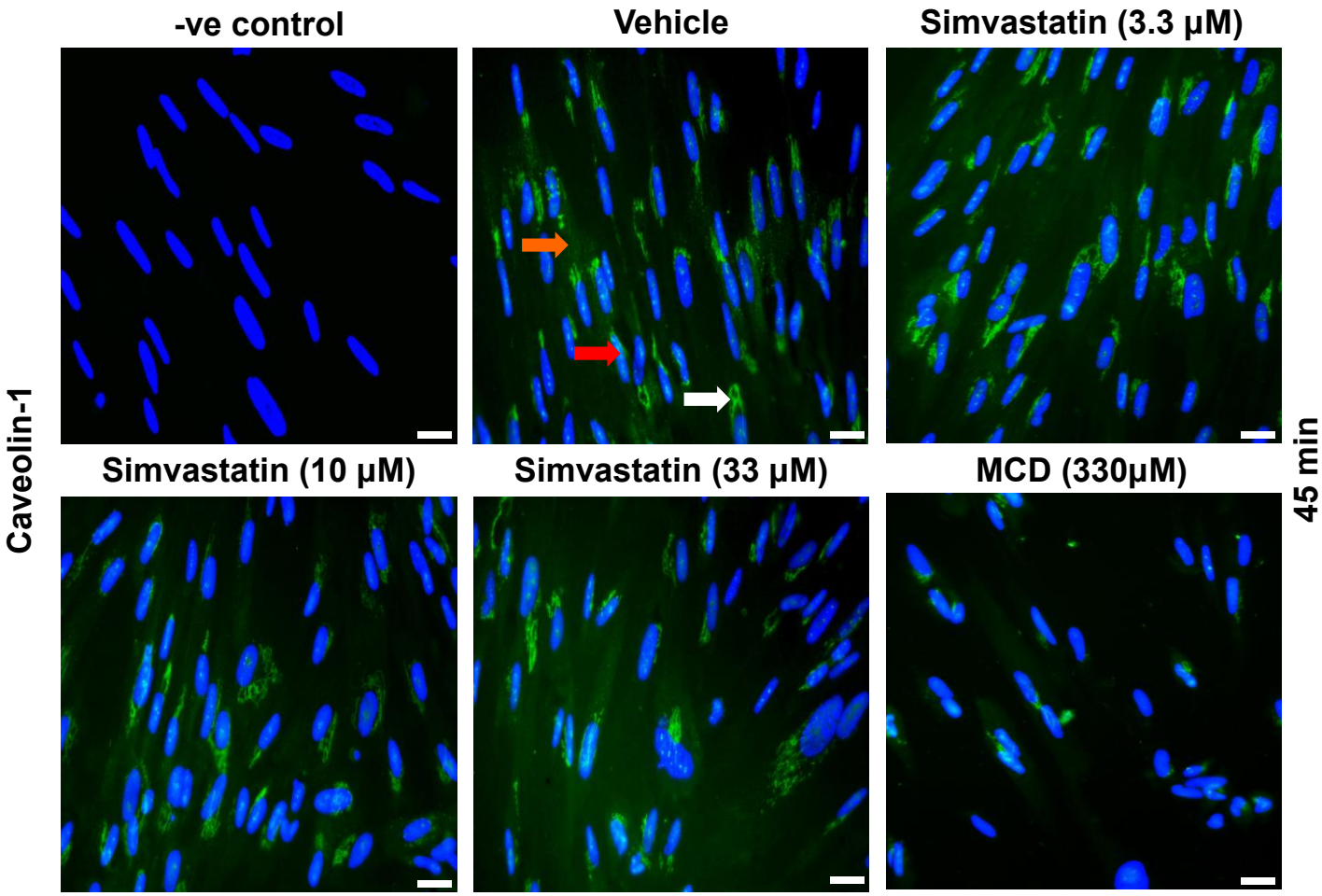


Figure 3-42. Representative immunofluorescent images showing the effects of simvastatin (3.3µM, 10µM, and 33µM) and MCD (300µM) exposure on caveolin-1 protein expression after 45-mins, in myometrial cells isolated from samples obtained from women undergoing caesarean deliveries. Caveolin-1 expression localised in: intracellular compartments around the nucleus (white arrow), within the nucleus (red arrow), and around the cell body (orange arrow) (n=4). Staining: Caveolin-1/DAPI (Scale bar = 100µm).

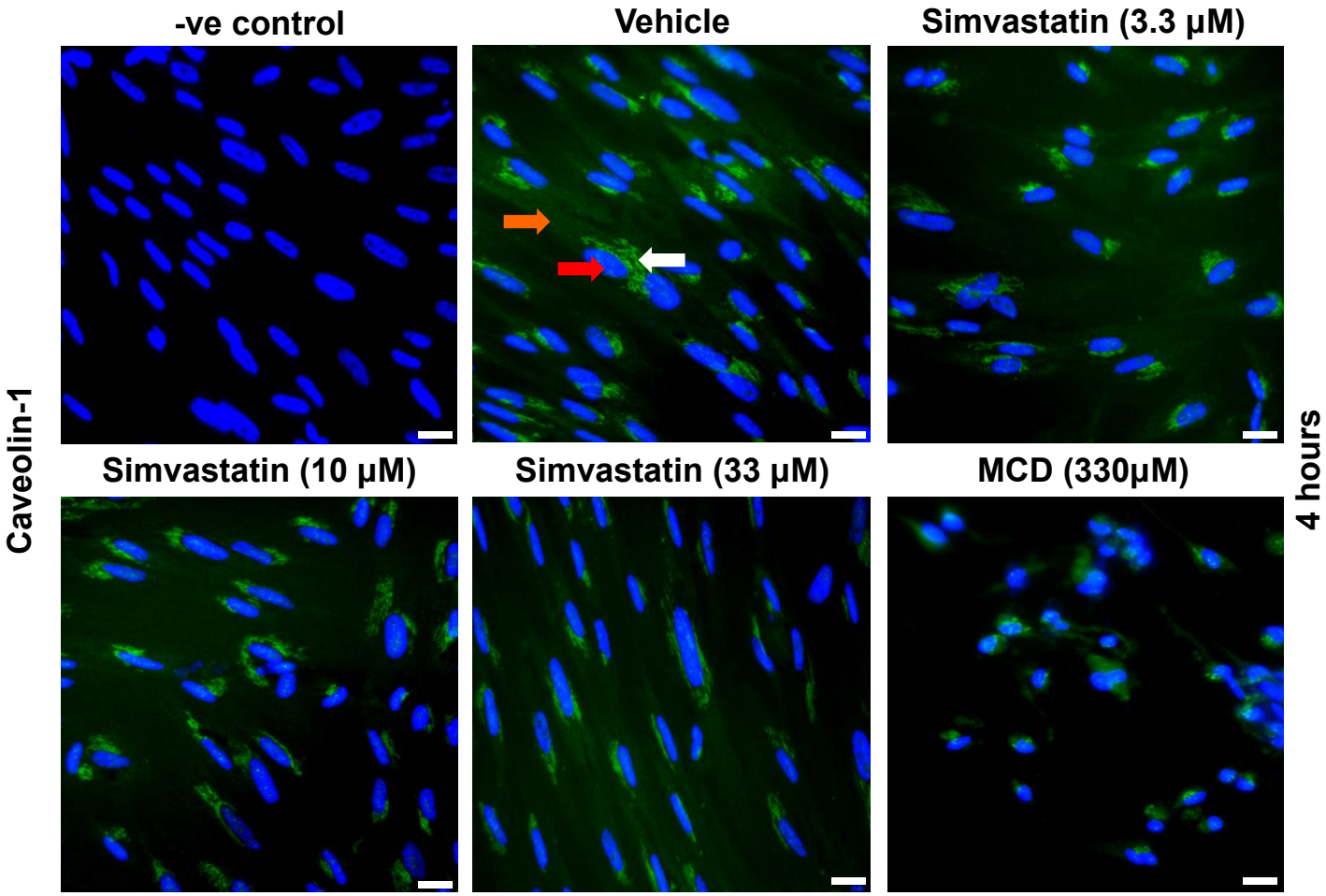


Figure 3-43. Representative immunofluorescent images showing the effects of simvastatin (3.3μM, 10μM, and 33μM) and MCD (300μM) exposure on caveolin-1 protein expression after 4-hours, in myometrial cells isolated from samples obtained from women undergoing caesarean deliveries. Caveolin-1 expression localised in: intracellular compartments around the nucleus (white arrow), within the nucleus (red arrow), and around the cell body (orange arrow) (n=4). Staining: Caveolin-1/DAPI (Scale bar = 100μm).

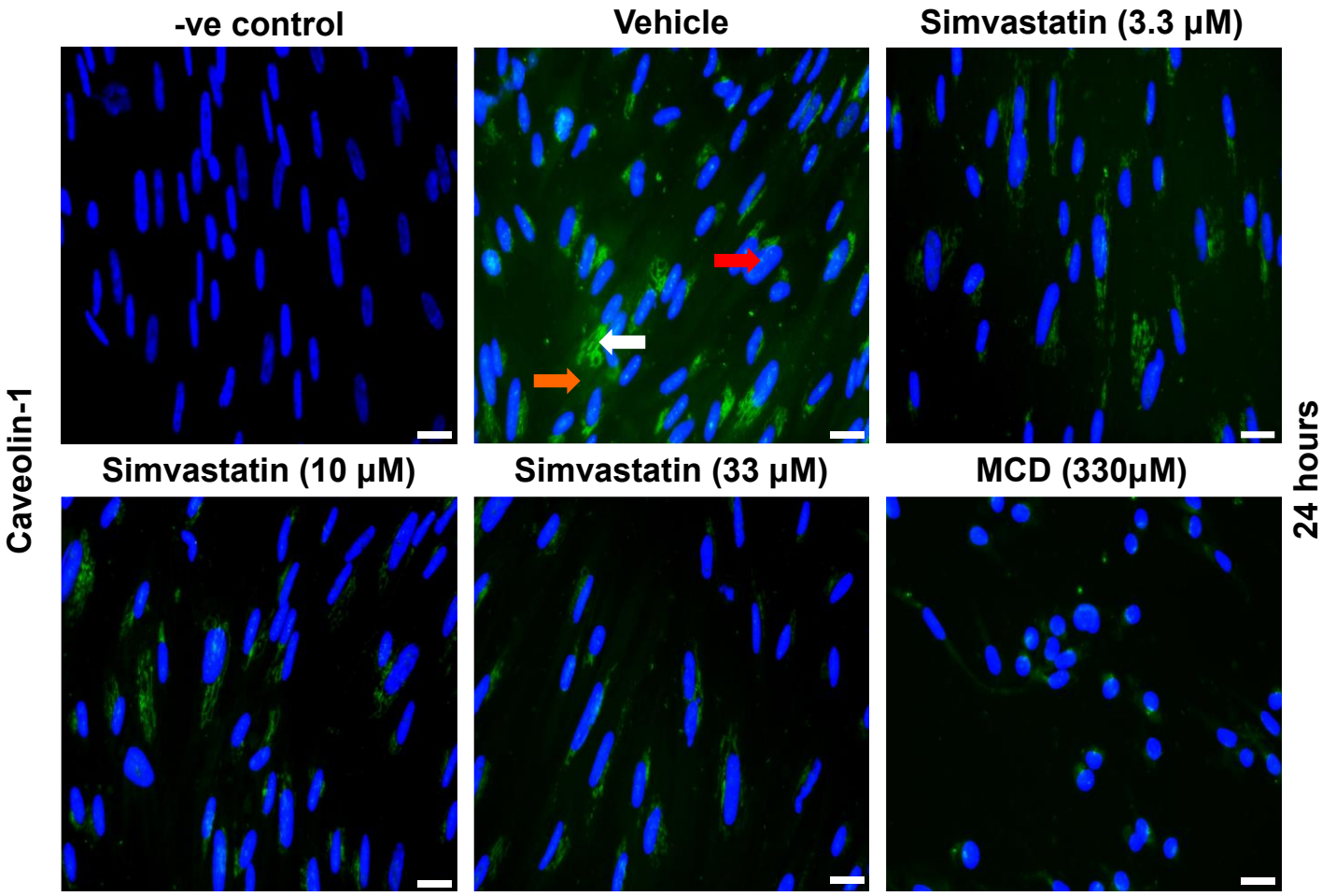


Figure 3-44. Representative immunofluorescent images showing the effects of simvastatin (3.3µM, 10µM, and 33µM) and MCD (300µM) exposure on caveolin-1 protein expression after 24-hours, in myometrial cells isolated from samples obtained from women undergoing caesarean deliveries. Caveolin-1 expression localised in: intracellular compartments around the nucleus (white arrow), within the nucleus (red arrow), and around the cell body (orange arrow) (n=4). Staining: Caveolin-1/DAPI (Scale bar = 100µm).

Exposure to simvastatin after 45-mins resulted in a reduction in percentage nuclear and extra-nuclear caveolin-1 expression per cell over time. Myometrial cell nuclear caveolin-1 expression was reduced by 20.98% and 25.50%, after exposure to simvastatin at concentrations of 10μM (64.35 ± 8.32%) ($n=4$, $p<0.05$), and 33μM (59.82 ± 6.24%) ($n=4$, $p<0.01$) respectively, compared to vehicle-treated cells. Extra-nuclear expression of caveolin-1 was also reduced by 22.48% (44.22 ± 5.83%) ($n=4$, $p<0.0001$), but only after 33μM. Cells exposed to MCD resulted in a greater reduction of 45.02% (40.31 ± 5.12%) ($n=4$, $p<0.01$) in nuclear, and 56.99% (9.72 ± 3.23%) ($n=4$, $p<0.0001$) in extra-nuclear caveolin-1 expression than simvastatin, compared to vehicle-treated cells (**See Figure 3-45**).

A similar reduction in both percentage nuclear and extra-nuclear caveolin-1 expression, was observed in myometrial cells after 4-hours and 24-hours of simvastatin and MCD exposure. Nuclear and extra-nuclear expression of caveolin-1 after 4-hours, was reduced by 13.15% (70.85 ± 3.28%) ($n=4$, $p<0.05$) and 16.95% (50.31 ± 8.74%) ($n=4$, $p<0.001$) respectively. After 24-hours, this was reduced by 21.78% (62.22 ± 4.06%) ($n=4$, $p<0.01$) and 23.51% (43.75 ± 7.79%) ($n=4$, $p<0.0001$), compared to vehicle-treated cells. In comparison, cells exposed to MCD for 4-hours resulted in a reduction of 37.81% (46.19 ± 3.74%) ($n=4$, $p<0.0001$) and 52.11% (15.16 ± 6.97%) ($n=4$, $p<0.0001$) in nuclear and extra-nuclear caveolin-1 expression respectively, compared to vehicle-treated cells (**See Figure 3-45**).

After 24-hours, simvastatin caused a further decrease in nuclear and extra-nuclear caveolin-1 expression. Myometrial cell nuclear caveolin-1 expression was decreased after exposure to 3.3μM (45.30 ± 5.9%), 10μM (29.71 ± 4.48%), and 33μM (23.36 ± 4.23%) concentrations of simvastatin, resulting in reductions of 29.05%, 44.64%, and 50.99% respectively compared to vehicle-treated cells (n=4, $p<0.001$, $p<0.0001$). Similarly, extra-nuclear caveolin-1 expression was also reduced after exposure to 3.3μM (22.38 ± 0.83%), 10μM (12.25 ± 3.63%), and 33μM (8.13 ± 1.74%) concentrations of simvastatin, resulting in reduction of 39.43%, 49.56%, and 53.67% respectively (n=4, $p<0.0001$). After 24-hours, cells exposed to MCD caused further reductions in both nuclear (9.29 ± 6.60%) and extra-nuclear (4.45 ± 1.60%) caveolin-1 expression, resulting in decrease of 65.06% and 57.36% respectively, compared to vehicle-treated cells (n=4, $p<0.0001$) (**See Figure 3-45**).

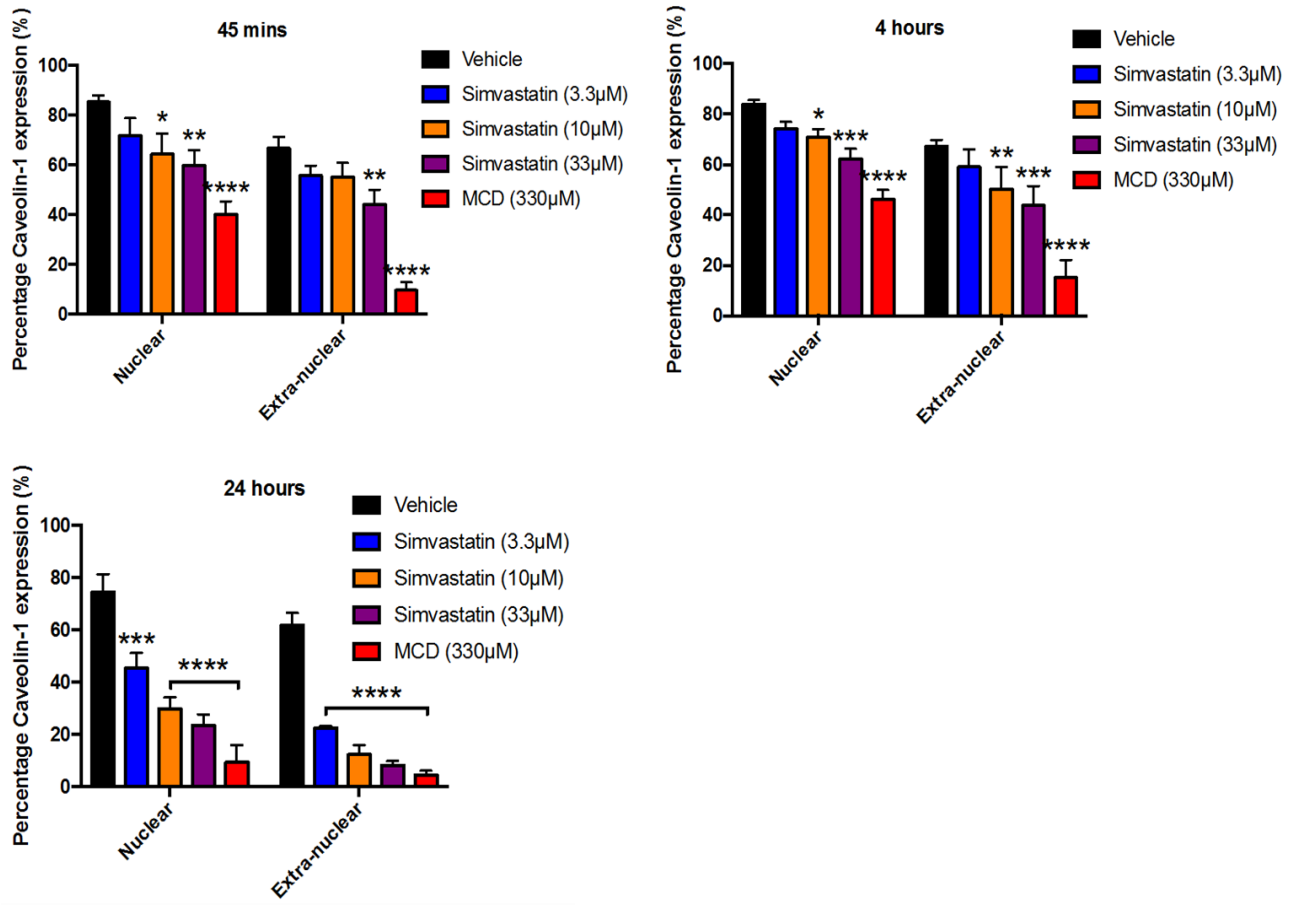


Figure 3-45. Effects of simvastatin (3.3μM, 10μM, and 33μM) and MCD (330μM) exposure over 45-mins, 4-hours, and 24-hours on percentage nuclear and extra-nuclear caveolin-1 expression, in myometrial cells obtained from women undergoing caesarean deliveries (n=4). Data is expressed as the mean caveolin-1 expression % of vehicle-treated samples ± SEM (ns $p>0.05$, *$p<0.05$, **$p<0.01$, ***$p<0.001$, ****$p<0.0001$).

3.8.6 Discussion

Exposure to simvastatin did not alter α-actin expression in myometrial cells after 24-hours. However, cells exposed to MCD resulted in the complete disruption of α-actin staining, with evidence of nuclear rounding and blebbing after 24-hours. Simvastatin caused a concentration-dependent reduction in caveolin-1 expression over time, with a visible decrease in staining intensity in areas surrounding the nucleus, within the nucleus, and around the cell.

In contrast, cells exposed to MCD resulted in the complete disruption and loss of caveolin-1 staining, with evidence of nuclear rounding and blebbing after 45-mins of exposure. These results indicate that simvastatin can modulate the caveolin-1 cholesterol-binding protein**,** resulting in a gradual decrease in its expression without affecting the myometrial cell cytoskeleton This decrease may contribute to simvastatin-induced reduction of spontaneous myometrial contractions. In comparison, MCD's disruption of both caveolin-1 and the myometrial cell cytoskeleton after 45-mins may contribute to MCD-induced increase of spontaneous myometrial contraction frequency.

Caveolae lipid-raft structures have been identified as small invaginations in the myometrial cell membrane under transmission electron microscopy (Taggart et al., 2000; England et al., 2000; Riley et al., 2005). Functionally, caveolae appear to be recruitment platforms, co-localising proteins such as BK and L-type Ca^{2+} channels to the cell membrane (Chanrachakul et al., 2004**;** Brainard et al., 2005). The modulation of caveolae structures by cholesterol-manipulating agents, have been shown to affect the function of

these ion channels, and resulting in changes in smooth muscle contractility (Brainard et al., 2009; Dreja et al., 2002; Kendrick et al., 2004; Shmygol et al., 2007; Smith et al., 2005; Taggart et al., 2000). For example, caveolae disruption in rat uterine tissues by MCD enhanced spontaneous contractility and VOCC activity (Kendrick et al., 2004; Smith et al., 2005). MCD exposure was also observed to inhibit BK channel activity in the human myometrium, resulting in an increase in spontaneous contractions (Shmygol & Wray, 2005). These observations are consistent with data from our experiments, showing both an increase in spontaneous myometrial contractility and the disruption of caveolin-1 in myometrial cells, in the presence of MCD. Furthermore, the contrasting effects between simvastatin and MCD exposure on caveolin-1 expression in the myometrium, suggests that simvastatin-induced reduction of spontaneous contractions is unlikely to involve the complete disruption of caveolae. It is possible that simvastatin disrupts and reduces caveolin-1 without affecting cholesterol.

Several studies have shown that caveolin-1 can directly reduce NO activity, by forming am inhibitory complex with eNOS in several different tissue types. The caveolin-1 scaffolding domain amino acid sequence has been shown to interact with a binding motif found in the eNOS oxygenase domain, resulting in the inhibition eNOS function. Evidence of this complex has been found in the inner leaflet of the caveolae membrane (Bucci et al., 2000; Frank et al., 2003; Gratton et al., 2004; Garcia Cardena et al., 1997; Michel et al., 1997). The disruption of this caveolin-eNOS inhibitory complex by caveolin-1 removal, has been shown to restore eNOS activity, resulting in the

upregulation of NO (Drab et al., 2001; Razani et al., 2001; Zhao et al., 2002; Kwok et al., 2009) via the PKG activation dependent pathways mentioned previously (**See Chapter 3.4.3**). It is possible that the gradual reduction in caveolin-1 expression in the myometrial cell after simvastatin exposure, corresponds to the disruption of caveolin-1 in these inhibitory complexes, thereby releasing eNOS and promoting NO-induced myometrial smooth muscle relaxation via PKG activation (Norman, 1996; Ramsay et al., 1996) (**See Figure 3-46**).

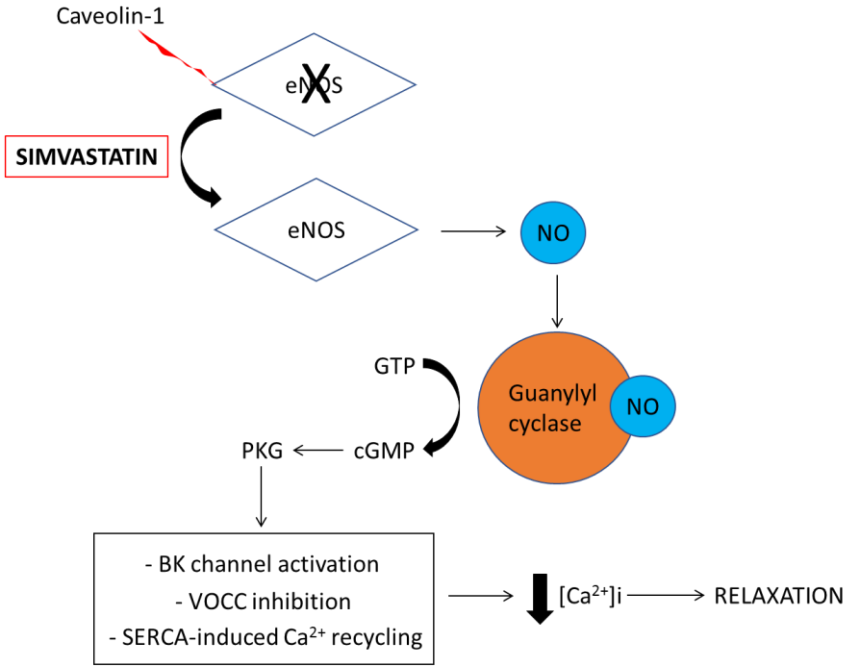


Figure 3-46. Diagram showing simvastatin-induced disruption of the eNOS-caveolin-1 inhibitory complex by caveolin-1 modulation, resulting in the release of eNOS from its inhibitory state and promoting NO-induced smooth muscle relaxation via PKG activation.

There is evidence to suggest that caveolin-1 can also form functional complexes other proteins, such as RhoA (Shaul et al., 1998). However, rather than inhibit RhoA activity, caveolin-1 binding causes an increase in RhoA activity to promote smooth muscle contractility via MLCP inhibition (Kimura et

al., 1996; Kureishi et al., 1997). For example, in human mesenteric resistance arteries, the RhoA-caveolin-1 complex was disrupted by inhibiting RhoA activation, resulting in the subsequent reduction in vessel contraction and tone (Dubroca et al., 2006). It is possible that simvastatin-induced reduction of caveolin-1 expression in the myometrium can also disrupt the formation of the RhoA-caveolin-1 complex, resulting in the reduction of RhoA activity and the inhibition of RhoA-induced smooth muscle contractility (**See Figure 3-47**).

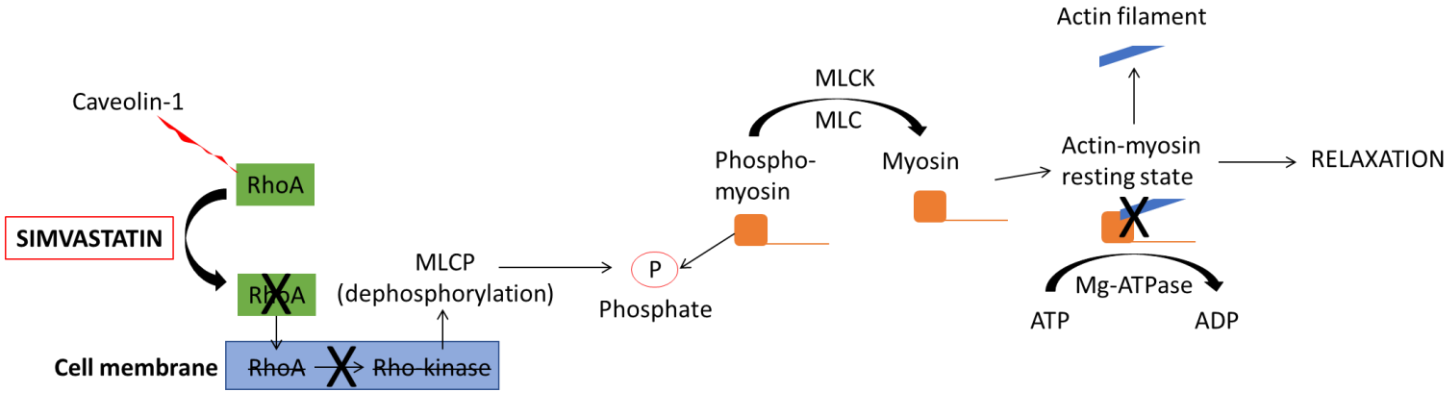


Figure 3-47. Diagram showing simvastatin disruption of the RhoA-caveolin-1 complex, resulting in the activation of MLCP and return of the actin-myosin cross bridge to its resting state to promote smooth muscle relaxation.

3.8.7 Critique and further work

Our experiments used changes in myometrial cell caveolin-1 staining as a marker for the modulation of caveolae structures, in the presence of simvastatin. However, to determine whether simvastatin can directly alter caveolae structures in the myometrium, changes in the quantity or morphology of individual caveolae can be identified using more sophisticated imaging techniques, such as transmission and scanning electron microscopy (Taggart et al., 2000). The evidence of physical changes in caveolae structure morphology or concentration in the presence of simvastatin, would indicate

the possibility that simvastatin's effects on spontaneous myometrial contractility involves the direct modification of caveolae.

To determine whether the eNOS-caveolin-1 inhibitory complex is present in the myometrium, further immunocytochemical and immunohistochemical experiments can be conducted to identify changes in eNOS and caveolin-1 expression in the myometrial cell. Evidence of staining co-localisation would indicate the presence of the eNOS-caveolin-1 complex in the myometrium. Furthermore, a reduction in staining intensity or alteration in staining pattern in the presence of simvastatin would suggest the possible disruption of the complex. Similar investigations can also be conducted to determine the presence of the RhoA-caveolin-1 complex. These experiments can be further supplemented using immunoblotting techniques, to determine evidence of complex formation, disruption, and changes in the complex protein expression in the presence of simvastatin.

4 Conclusions

Spontaneous preterm labour is the leading cause of premature delivery (Goldenberg et al., 2008), which remains the leading contributor of global neonatal mortality and morbidity (WHO, 1992). This is due in part, to an incomplete understanding of the mechanisms responsible for these conditions, resulting in therapeutic strategies that provide symptomatic relief without disease prevention. Recently, studies have shown the disruption of cholesterol-containing caveolae structures by membrane cholesterol manipulation, resulting in changes to spontaneous and agonist-induced myometrial contractions (Brainard et al., 2009; Dreja et al., 2002; Smith et al., 2005; Shmygol et al., 2007; Taggart et al., 2000). These observations indicate a functional role for cholesterol, beyond the development of the fetus during gestation, and highlights the therapeutic potential of cholesterol-manipulating agents in pregnancy complications related to myometrial dysfunction.

Studies investigating the effects of statins on smooth muscle function have observed reductions in smooth muscle contractions. Furthermore, these effects appear to be independent of cholesterol inhibition (Bergdahl et al., 2003b; de Sotomayor et al., 2005; Laufs et al., 1998 Yada et al., 1999). More recently, the effects of statins have been determined in an inflammation-based model of preterm labour, which showed a reduction in C5a-induced human myometrial contractions after incubation with simvastatin incubation overnight (Gonzalez et al., 2014). To date, changes in spontaneous myometrial contractions after statin exposure, statin's effects on myometrial cholesterol concentrations, evidence of statin-induced HMG-CoA reductase

inhibition, and the presence of statin's cholesterol-independent pathways in the human myometrium, are not known.

In this study, we have shown that the cumulative addition of simvastatin caused a reduction spontaneous myometrial contractions, in the absence of cholesterol modulation. This reduction was partially inhibited by L-NAME, suggesting that simvastatin's effects may involve the promotion of eNOS activity, possibly by upregulating eNOS mRNA and protein expression to promote NO-induced smooth muscle relaxation via PKG activation (Kosmidou et al., 2007; Norman, 1996; Ramsay et al., 1996). We have also reported evidence for the absence of the HMG-CoA reductase pathway in the myometrium, evident after replenishment with mevalonate and GGPP failed to inhibit simvastatin-induced reduction in spontaneous contractions. These observations suggest that simvastatin's effects are likely to involve pathways independent of the HMG-CoA reductase pathway and subsequent cholesterol modulation.

Experiments investigating the effects of ion channel modulation on simvastatin's effects suggests a combination of SK and BK channel activation, and VOCC inhibition, resulting in a reduction of $[Ca^{2+}]i$ in myometrial cells to promote smooth muscle relaxation (Kuhlmann et al., 2004; McNeish et al., 2012; Yada et al., 1999). This is likely supplemented by the inhibition of oxytocin-induced Ca^{2+} release from the SR, causing a further reduction in $[Ca^{2+}]i$ and therefore Ca^{2+}-induced smooth muscle contractility pathways.

Finally, although our tissue contractility and cholesterol measurements experiments indicate an absence of cholesterol modulation, our immunocytochemical data showed a gradual concentration-dependent reduction in the expression of the caveolae cholesterol-binding protein, caveolin-1. However, due to the contrasting nature of caveolin-1 reductions between simvastatin and MCD treatment, it is likely that simvastatin can disrupt and reduce the caveolin-1 protein, without modulating cholesterol. Simvastatin-induced reduction in spontaneous contractions can therefore occur by disruption of the eNOS-caveolin-1 inhibitory (Drab et al., 2001; Feron et al., 1996; Garcia Cardena et al., 1996; Razani et al., 2001; Zhao et al., 2002) and RhoA-caveolin-1 complexes, resulting in the promotion of NO-induced relaxation, and the inhibition of RhoA-induced contractions respectively. All the proposed mechanisms associated with simvastatin-induced reduction in myometrial contractility investigated in this study are summarised in the diagram below (**See Figure 4-1**):

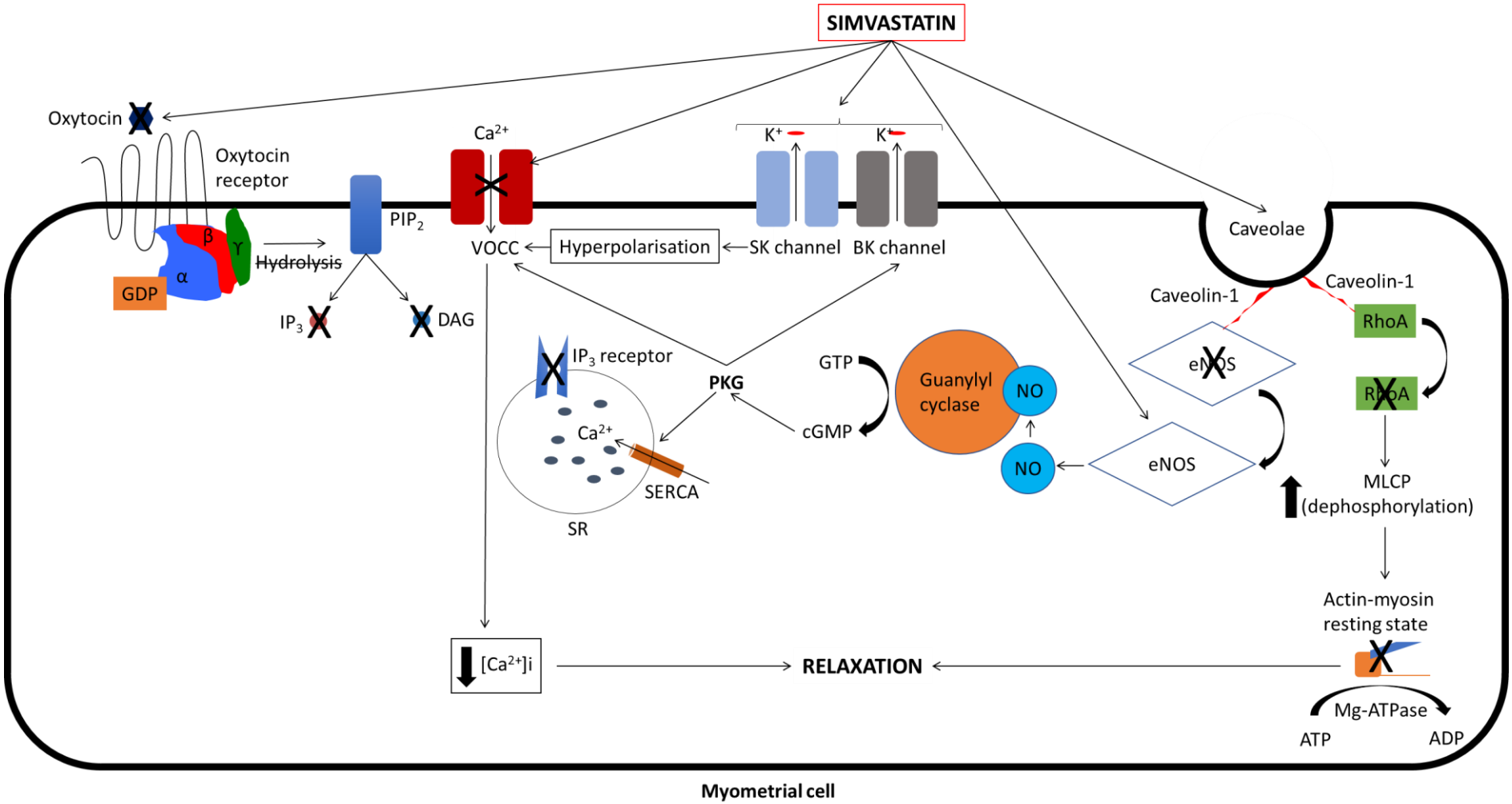


Figure 4-1. Diagram showing the mechanisms proposed to be involved in simvastatin-induced reduction of myometrial tissue contractility. In our study, simvastatin can modulate the activity of VOCC, SK and BK channels to decrease $[Ca^{2+}]i$, which is further promoted by the activation of PKG, via a combination of eNOS activity upregulation and the disruption of the eNOS-caveolin-1 inhibitory complex. Simvastatin can also compete with oxytocin for its receptor, resulting in the inhibition of IP_3 production and therefore Ca^{2+} release from SR internal stores via IP_3 receptors. It is also possible that PKG activation can promote the activity of SERCA to induce Ca^{2+} recycling back into the SR internal stores. Finally, simvastatin-induced disruption of the RhoA-caveolin-1 complex inhibits the activation of RhoA, and subsequent smooth muscle contractility by preventing MLCP inhibition. These mechanisms all reduce myometrial cell $[Ca^{2+}]i$, resulting in the promotion of smooth muscle relaxation and uterine quiescence.

Based on simvastatin's effects on spontaneous myometrial contractions, our data highlights the potential use of statins as a tocolytic agent for the treatment of preterm labour. Despite current health care guidelines preventing statin use during pregnancy and breastfeeding, there are numerous studies and reviews that found no increased risk of adverse pregnancy outcomes, or congenital defects after statin treatment (Kusters et al., 2014; Manson et al., 1996; Pollack et al., 2005; Taguchi et al., 2008; Winterfeld et al., 2012). However, the comparably higher experimental concentrations used in our study compared to those found in patient serum after statin administration (Bjorkhem-Bergman et al., 2011), indicates a need for additional experiments at therapeutic concentrations, before the application of statins for preterm labour treatment can be considered.

This study has shown that our understanding of cholesterol and the effects of statins on the myometrium are incomplete. Simvastatin's effects on the myometrium are complex, involving several different mechanisms that in combination results in the reduction of spontaneous contractions. Furthermore, these pathways appear to be independent of cholesterol modulation, despite the properties of statins as lipid-lowering drugs. Additional independent investigations into each pathway are required to fully understand the extent of simvastatin's mechanisms in the myometrium. With regards to the potential application of statins as tocolytic agents, it is our opinion that any therapeutic considerations without further investigations using therapeutic concentrations are currently premature. However, once these studies are

complete, simvastatin may become a promising alternative to current tocolytic therapies in the management of preterm labour.

5 Appendix

5.1 Experimental formulations

Physiological salt solution
119mM NaCl, 4.7mM KCl, 25mM $NaHCO_3$, 2.5mM $MgSO_4$, 1.6mM $CaCl_2$, 1.2mM KH_2PO_4, 5.5mM glucose, 0.034mM EDTA. pH 7.4 achieved with 1M NaOH and stored at 4ºC for up to 1 month.

High K^+ salt solution
60mM KCl, 25mM $NaHCO_3$, 2.5mM $MgSO_4$, 3.2mM $CaCl_2$, 1.2mM KH_2PO_4, 5.5mM glucose, 0.034mM EDTA. pH 7.4 achieved with 1M NaOH and stored at 4ºC for up to 1 month.

Myometrial cell lysis buffer
100mM Tris, 150mM NaCl, 1mM EGTA, 1mM EDTA, 1% Triton X-100, 0.5% sodium deoxycholate, 1% phosphatase/protease inhibitor cocktail containing 1mM PMSF. pH 7.4 achieved with 1M NaOH and stored at 4ºC for up to 1 month.

Amplex red® cholesterol assay reagents and protocol
Amplex red® reaction (MW= ~257), DMOS, HRP, H_2O_2, 5X reaction buffer (0.5M KH_2PO_4, 0.25M Ba Cl, 25mM cholic acid, 0.5% Triton X-100), cholesterol oxidase from *Streptomyces*, cholesterol esterase from *Pseudomonas*, cholesterol reference standard (MW=387), resorufin sodium salt (MW=235).
(Protocol: https://tools.thermofisher.com/content/sfs/manuals/mp12216.pdf).

FLUO-4AM CA^{2+} assay reagents and protocol
FLUO-4 direct calcium assay reagent, 250mM water-soluble probenecid stock diluted in HBSS, FLUO-4 direct calcium assay buffer.
(Protocol: https://tools.thermofisher.com/content/sfs/manuals/mp10471.pdf).

FLIPR Ca^{2+} 5 assay reagents and protocol
Component A, component B (1X HBSS, 20mM HEPES solution), 250mM water-soluble probenecid stock diluted in HBSS.
(Protocol:
http://mdc.custhelp.com/euf/assets/content/product_insert_D5001069[1].D.pdf
)

4% w/v paraformaldehyde
4g PFA was dissolved in dH_2O at 60ºC. pH 7.4 achieved with 1M NaOH and stored at -20ºC for up to 3 months

5% normal goat serum working solution
Normal goat serum (0.5mL), ddH_2O (10mL).

0.1% BSA/PBS buffer
BSA (1g), 1X PBS (100mL)

0.5% Igepal
Igepal (50µL), ddH_2O (10mL).

0.1% DMSO vehicle
DMSO (1µL), PSS (900µL)

5.2 Example of patient study consent forms and information sheet

The University of Nottingham

Derby Hospitals NHS
NHS Foundation Trust

CONSENT FORM: PREGNANCY
(Version 2- 12/2009)

Title of Study: Studies of Human Pregnancy and Preterm Birth

REC ref: 09/H0401/90

Name of Researcher: Dr Raheela Khan

Name of Participant: **Please initial box**

1. I confirm that I have read and understand the information sheet version number 2 dated 12/2009 for the above study and have had the opportunity to ask questions. ☐

2. I understand that my participation is voluntary and that I am free to withdraw at any time, without giving any reason, and without my medical care of legal rights being affected. I understand that should I withdraw then the information collected so far cannot be erased and that this information may still be used to the project analysis. ☐

3. I understand that relevant sections of my medical notes and data collected in the study may be looked at by authorised individuals from the University of Nottingham, the research group and regulatory authorities where it is relevant to my taking part in this study. I give permission for these individuals to have access to these records and to collect, store, analyse and publish information obtained from my participation in this study. I understand that my person details will be kept confidential. ☐

4. I understand and agree to a myometrial ☐ placental ☐ and cord blood ☐ sample to be taken for research investigations.

5. I agree to the storage of uterine, placental and cord blood samples for any future, as yet, unspecified research studies relating to the study of pregnancy and pregnancy related disorders. ☐

6. I agree to take part in the above study. ☐

Name of Participant	Date	Signature
Name of Participant	Date	Signature
Name of Participant	Date	Signature

CONSENT FORM: HYSTERECTOMY
(Version 2- 12/2009)

Title of Study: Studies of Human Pregnancy and Preterm Birth

REC ref: 09/H0401/90

Name of Researcher: Dr Raheela Khan

Name of Participant: **Please initial box**

7. I confirm that I have read and understand the information sheet version number 2 dated 12/2009 for the above study and have had the opportunity to ask questions. ☐

8. I understand that my participation is voluntary and that I am free to withdraw at any time, without giving any reason, and without my medical care of legal rights being affected. I understand that should I withdraw then the information collected so far cannot be erased and that this information may still be used to the project analysis. ☐

9. I understand that relevant sections of my medical notes and data collected in the study may be looked at by authorised individuals from the University of Nottingham, the research group and regulatory authorities where it is relevant to my taking part in this study. I give permission for these individuals to have access to these records and to collect, store, analyse and publish information obtained from my participation in this study. I understand that my person details will be kept confidential. ☐

10. I understand and agree to a myometrial ☐ and cord blood sample ☐ to be taken for research investigations.

11. I agree to the storage of uterine, placental and cord blood samples for any future, as yet, unspecified research studies relating to the study of pregnancy and pregnancy related disorders. ☐

12. I agree to take part in the above study. ☐

Name of Participant	Date	Signature
Name of Participant	Date	Signature
Name of Participant	Date	Signature

Derby Hospitals NHS
NHS Foundation Trust

The University of Nottingham

Patient Information Sheet

Studies of Human Pregnancy and Preterm Birth

You are being invited to take part in a research study of the University of Nottingham being carried out in Derby. Before you decide it is important for you to understand why the research is being done and what it will involve. Please take time to read the following information carefully. Talk to others about the study if you wish.

1. What is the purpose of the study?

The switch from pregnancy to labour and how the uterus contracts for delivery is not understood. In some cases, labour may begin too early when the baby is not ready to be born (preterm). Preterm birth is delivery occurring before 37 completed weeks of pregnancy and affects about 8% of all pregnancies in the UK. Preterm labour is a factor in approximately 40% of all preterm deliveries. Two other pregnancy-specific disorders preeclampsia (high blood pressure with protein in the urine) and intrauterine growth restriction IUGR), where babies are born small for their size, may also lead to preterm birth. To date, there are still no effective drugs to treat preterm birth due to preterm labour nor any reliable markers that allow these disorders to be monitored throughout pregnancy.

Here at the Royal Derby Hospital, we are carrying out research into term and preterm birth with the aim of improving our understanding of the causes of preterm birth. We hope that new information from our studies will pave the way for the future development of new drugs and new ways designed to reduce the incidence of preterm delivery. The three projects we are involved with are as follows:

Project 1: *Inflammation in pregnancy:* The uterus produces many important proteins which play a role in pregnancy and labour. It is thought that infection or inflammation of the female reproductive tract may activate the process of labour too early by causing uterine contractions through molecules produced by the placenta and cord blood.

Project 2: *Lipid-protein interactions in the pregnant human uterus:* In recent years, there has been great interest in how certain fats affect pregnancy. We are studying how these fats (also known as lipids) present in the uterus (womb) influence labour. In addition, we know that the location of these lipids within cells may also indirectly activate pathways that control the production of proteins in the uterus.

Project 3: *Vascular problems in pregnancy:* During pregnancy, blood flow to the baby provides food and oxygen essential to baby's growth and development. In some 10% of cases, poor blood flow to the placenta (afterbirth) may mean that the baby does not develop or grow properly, a condition known as intra-uterine growth restriction (IUGR). In addition, 1-2% of pregnancies result in preeclampsia, a leading cause of high blood pressure in pregnancy, which may endanger both mother's and baby's health if left undiagnosed. The aim of our project is to study the properties

of the blood vessels in the uterus and placentae of women with preeclampsia or a growth-restricted pregnancy to identify whether blood vessel function is changed in these disorders compared with vessels of women with a normal pregnancy.

2. Why have you been invited?

We are recruiting patients from four different groups. You have been chosen as somebody who falls into one of the four following groups: (a) normal non-labouring, term pregnancy (b) labouring pregnancy, or have been diagnosed with (c) a growth-restricting pregnancy, (d) preeclampsia. The 'normal pregnancy' group is a control group and including patients from this group will allow us to compare normal versus potentially difficult pregnancies. The normal pregnancy groups will be divided further into term or preterm. We are recruiting patients for all three projects and it is likely that your tissue and cord blood samples will be used for any one of these 3 projects. We expect to recruit 3000 women in five years. There will be no direct benefit to you from this study but your participation may significantly aid our understanding of pregnancy and birth thus enabling us to make advances in the field of female and fetal health.

3. Do I have to take part?

No. It is up to you to decide whether or not to take part. If you do, you will be given this information sheet to keep and be asked to sign a consent form. You are free to withdraw at any time and without giving a reason. A decision to withdraw at any time, or a decision not to take part, will not affect the standard or care you receive. Any stored tissue samples that can still be identified as yours will be destroyed if you wish.

4. What will happen to me if I take part?

Should you decide to take part, if you will be undergoing a caesarean section, you may be asked to provide a myometrial (uterine muscle) biopsy which will be taken either at caesarean section from the site of the operation, or post operatively. The biopsy is ~2g in weight and the size of a thumb tip. We will also ask you if we can take your placenta for research if applicable. In the case of a normal delivery, we will ask you to consider providing a placental and cord blood sample only after you baby has been delivered. Cord blood samples collected will not be available for any clinical needs such as subsequent treatment of your baby or other investigations. All samples will be taken after delivery of the baby. There is no further follow-up in relation to our study. This investigation is laboratory-based therefore samples will be taken to the lab and analysed using a variety of experimental techniques. We would also wish to store any unused tissue and blood samples obtained from you for future unspecified research. Samples will only be used for studies approved by a research ethics committee. If however, you change your mind later about having your tissues stored for future research, then you can withdraw at any time without providing a reason. This should be done by contacting the Chief Investigator (contact details at the bottom of this sheet).

5. What are the other possible disadvantages and risks of taking part?

There is minimal risk from taking the uterine muscle biopsy over and above that associated with the caesarean section. Taking the sample at caesarean section will not harm your baby, nor prolong the operation and will not affect the normal healing of your uterus. Nor will there be any effect on the structure or function of your uterus afterwards, your future fertility or any risk to baby as the biopsy will be taken after delivery of your baby. If it is felt by the clinical in charge of your care that taking a uterine muscle biopsy is not appropriate, the sample will not be taken. Your wellbeing and that of your baby is paramount. There is no risk to you or your baby from the use of placental samples.

6. What are the possible benefits of taking part?
There is no direct benefit to you or your baby in taking part in this study. However, the information obtained from using your uterine muscle biopsy and placenta may enable us to identify possible new pathways that will improve our understanding of uterine function.

7. What happens when the research study stops?
The data collected will be analysed and prepared for scientific publication. We would hope to expand the study to understand more about the functions of the human uterus in normal and abnormal conditions. Participants will not be identified in any report, presentation or publication.

8. Will my taking part in the study be kept confidential?
Yes. All the information about your participation in this study will be kept confidential. If you consent to take part in the research, any of your medical records may be inspected by researchers directly involved with the project for purposes of analysing the results and all details will remain strictly confidential. They may also be looked at by people from regulatory authorities to check that the study is being carried out correctly.

9. Who is organising and funding the research?
This study is being funded through various sources including the Wellcome Trust, the Medical Research Council, British Heart Foundation and the University of Nottingham. The research is sponsored by the University of Nottingham.

10. Who has reviewed the study?
All research in the NHS is looked at by an independent group of people, called a Research Ethics Committee, to protect your interests. This study has been reviewed and given favourable opinion by the Derbyshire Research Ethics Committee.

Complaints:
If you have a concern about any aspect of this study, you should ask to speak with the researchers who will do their best to answer your questions (Dr Raheela Khan 01332 724664; raheela.khan@nottingham.ac.uk). If you remain unhappy and wish to complain formally, you can do this through the NHS Complaints Procedure or details can be obtained from the Royal Derby Hospital Patient Advice and Liaison Service (Uttoxeter Road, DE1 2QY Derby; pals@derbyhospitals.nhs.uk; tel: 01332 785156).

Contact for Further Information
Dr Raheela N Khan 01332 724664; bleep 1208; email: raheela.khan@nottingham.ac.uk
Mr Daniel Hay 01332 724668; email: Daniel.hay@Nottingham.ac.uk

For further information on the research of the group:
http://www.nottingham.ac.uk/GEM/Research/og.aspx

Thank you for taking the time to read this.

6 Bibliography

Aguilar, H.N., & B.F. Mitchell. 2010. Physiological pathways and molecular mechanisms regulating uterine contractility. *Hum Reprod Update*. 16(6):725-44.

Ahyayauch, H., M. Bennouna, A. Alonso, and F.M. Goni. 2010. Detergent effects on membranes at subsolubilizing concentrations: transmembrane lipid motion, bilayer permeabilization, and vesicle lysis/reassembly are independent phenomena. *Langmuir*. 26:7307-7313.

Alexander, S.P.H., A Mathie and J.A. Peters. 2001. Guide to Receptors and Channels (GRAC) 5th Edition. *BJP*.

Ali, B.R., I. Nouvel, K.F. Leung, A.N. Hume, and M.C. Seabra. 2010. A novel statin-mediated "prenylation block-and-release" assay provides insight into the membrane targeting mechanisms of small GTPases. *Biochem Biophys Res Commun*. 397:34-41.

Ali, O.F., E.J. Growcott, G.S. Butrous, and J. Wharton. 2011. Pleiotropic effects of statins in distal human pulmonary artery smooth muscle cells. *Respir Res*. 12:137.

Alioua, A., P. Higgins, E. Rousseau. 1995. PKG-I phosphorylates the α-subunit and upregulates reconstituted GK_{Ca} channels in trachel smooth muscle cells. *Am J Physiol Lung Cell Mo Physiol.* 268:L1057-L1063.

Alvarez de Sotomayor, M., C. Perez-Guerrero, M.D. Herrera, and E. Marhuenda. 1999. Effects of chronic treatment with simvastatin on endothelial dysfunction in spontaneously hypertensive rats. *J Hypertens*. 17:769-776.

Alvarez de Sotomayor, M., C. Perez-Guerrero, M.D. Herrera, and E. Marhuenda. 2001. Effect of simvastatin on vascular smooth muscle responsiveness: involvement of Ca(2+) homeostasis. *Eur J Pharmacol*. 415:217-224.

Alvarez, J.J., A. Montelongo, A. Iglesias, M.A. Lasuncion, and E. Herrera. 1996. Longitudinal study on lipoprotein profile, high density lipoprotein subclass, and postheparin lipases during gestation in women. *J Lipid Res*. 37:299-308.

Amano, M., M. Ito, K. Kimura, Y. Fukata, K. Chihara, T. Nakano, Y. Matsuura, and K. Kaibuchi. 1996. Phosphorylation and activation of myosin by Rho-associated kinase (Rho-kinase). *J Biol Chem*. 271:20246-20249.

Amedee, T., C. Mironneau, and J. Mironneau. 1986. Isolation and contractile responses of single pregnant rat myometrial cells in short-term primary culture and the effects of pharmacological and electrical stimuli. *Br J Pharmacol*. 88:873-880.

Amedee, T., C. Mironneau, and J. Mironneau. 1987. The calcium channel current of pregnant rat single myometrial cells in short-term primary culture. *J Physiol*. 392:253-272.

Anderson, N.C., Jr. 1969. Voltage-clamp studies on uterine smooth muscle. *J Gen Physiol*. 54:145-165.

Anderson, T.J., I.T. Meredith, A.C. Yeung, B. Frei, A.P. Selwyn, and P. Ganz. 1995. The effect of cholesterol-lowering and antioxidant therapy on endothelium-dependent coronary vasomotion. *N Engl J Med*. 332:488-493.

Andersson, K.E. 1982. Pharmacological inhibition of uterine activity. *Acta Obstet Gynecol Scand Suppl*. 108:17-23.

Archerm S.L., J.M.C. Huang, V. Hampl, D.P. Nelson, P.J. Shultz, and E.K. Weir. 1994. Nitric oxide and cGMP cause vasorelaxation by activation of a charybdotoxin-sensitive K channel by cGMP-dependent protein kinase. *Proc Natl Acad Sci USA.* 91:7583-7587.

Arnaudeau, S., N. Lepretre, and J. Mironneau. 1994a. Chloride and monovalent ion-selective cation currents activated by oxytocin in pregnant rat myometrial cells. *Am J Obstet Gynecol*. 171:491-501.

Arnaudeau, S., N. Lepretre, and J. Mironneau. 1994c. Oxytocin mobilizes calcium from a unique heparin-sensitive and thapsigargin-sensitive store in single myometrial cells from pregnant rats. *Pflugers Arch*. 428:51-59.

Ashcroft, F.M. 1988. Adenosine 5'-triphosphate-sensitive potassium channels. *Annu Rev Neurosci*. 11:97-118.

Astolfi, P. and Zonta, L.A. 1999. Risks of preterm derlivery and association with maternal age, birth order, and fetal gender. *Hum Reprod.* 14(11):2891-2894.

Baardman, M.E., W.S. Kerstjens-Frederikse, R.M. Berger, M.K. Bakker, R.M. Hofstra, and T. Plosch. 2013. The role of maternal-fetal cholesterol transport in early fetal life: current insights. *Biol Reprod*. 88:24.

Balasubramanian, K., and A.J. Schroit. 2003. Aminophospholipid asymmetry: A matter of life and death. *Annu Rev Physiol*. 65:701-734.

Benkusky, N.A., V.P. Korovkina, A.M. Brainard, and S.K. England. 2002. Myometrial maxi-K channel beta1 subunit modulation during pregnancy and after 17beta-estradiol stimulation. *FEBS Lett*. 524:97-102.

Bennet, J.H. 1872. On the External and Internal Orifices of the Uterus: Their Anatomy, Physiology, and Pathology. *Br Med J*. 2:321-323.

Bergdahl, A., M.F. Gomez, K. Dreja, S.Z. Xu, M. Adner, D.J. Beech, J. Broman, P. Hellstrand, and K. Sward. 2003a. Cholesterol depletion impairs vascular reactivity to endothelin-1 by reducing store-operated Ca2+ entry dependent on TRPC1. *Circ Res*. 93:839-847.

Bergdahl, A., E. Persson, P. Hellstrand, and K. Sward. 2003b. Lovastatin induces relaxation and inhibits L-type Ca(2+) current in the rat basilar artery. *Pharmacol Toxicol*. 93:128-134.

Berridge, M.J. 1993a. Cell signalling. A tale of two messengers. *Nature*. 365:388-389.

Berridge, M.J. 1993b. Inositol trisphosphate and calcium signalling. *Nature*. 361:315-325.

Bjorkhem-Bergman, L, J. Lindh, and P. Bergman. 2011. What is a relevant statin concentration in cell experiments claiming pleiotrophic effects?. *Br J Clin Pharmacol.* 72(1):164-165.

Blatz, A.L., and K.L. Magleby. 1986. Single apamin-blocked Ca-activated K+ channels of small conductance in cultured rat skeletal muscle. *Nature*. 323:718-720.

Bond, C.T., J. Maylie, and J.P. Adelman. 2005. SK channels in excitability, pacemaking and synaptic integration. *Curr Opin Neurobiol*. 15:305-311.

Boog, G., M.B. Brahim, and R. Gandar. 1975. Beta-mimetic drugs and possible prevention of respiratory distress syndrome. *Br J Obstet Gynaecol*. 82:285-288.

Bowden, S.E., S. Fletcher, D.J. Loane, and N.V. Marrion. 2001. Somatic colocalization of rat SK1 and D class (Ca(v)1.2) L-type calcium channels in rat CA1 hippocampal pyramidal neurons. *J Neurosci.* 21:RC175.

Boyle, M.B., N.J. MacLusky, F. Naftolin, and L.K. Kaczmarek. 1987. Hormonal regulation of K+-channel messenger RNA in rat myometrium during oestrus cycle and in pregnancy. *Nature*. 330:373-375.

Brainard, A.M., V.P. Korovkina, and S.K. England. 2007. Potassium channels and uterine function. *Semin Cell Dev Biol*. 18:332-339.

Brainard, A.M., V.P. Korovkina, and S.K. England. 2009. Disruption of the maxi-K-caveolin-1 interaction alters current expression in human myometrial cells. *Reprod Biol Endocrinol*. 7:131.

Brainard, A.M., A.J. Miller, J.R. Martens, and S.K. England. 2005. Maxi-K channels localize to caveolae in human myometrium: a role for an actin-channel-caveolin complex in the regulation of myometrial smooth muscle K+ current. *Am J Physiol Cell Physiol*. 289:C49-57.

Braveman, F.R. 2006. Pregnancy in patients of advanced maternal age. *Anestesiol Clin.* 24(3):637-46.

Brown, D.A., and E. London. 1998. Functions of lipid rafts in biological membranes. *Annu Rev Cell Dev Biol*. 14:111-136.

Brownfoot, F., S. Tong, N. Hannan, N. Binder, S. Walker, P. Cannon, R.Hastie, K. Onda, T. Kaitu'u-Lino. 2015. Effects of Pravastatin on human placenta, endothelium and women with severe preeclampsia. *Hypertension.* 66(3):687-97.

Brueggemann, L.I., P.P. Kakad, R.B. Love, J. Solway, M.L. Dowell, L.L. Cribbs, and K.L. Byron. 2012. Kv7 potassium channels in airway smooth muscle cells: signal transduction intermediates and pharmacological targets for bronchodilator therapy. *Am J Physiol Lung Cell Mol Physiol*. 302:L120-132.

Burgess, G.M., M. Claret, and D.H. Jenkinson. 1981. Effects of quinine and apamin on the calcium-dependent potassium permeability of mammalian hepatocytes and red cells. *J Physiol*. 317:67-90.

Buxton, I.L., C.A. Singer, and J.N. Tichenor. 2010. Expression of stretch-activated two-pore potassium channels in human myometrium in pregnancy and labor. *PLoS One*. 5:e12372.

Casey, M.L., and P.C. MacDonald. 1997. The endocrinology of human parturition. *Ann N Y Acad Sci*. 828:273-284.

Casey, P.J. 1992. Biochemistry of protein prenylation. *J Lipid Res*. 33:1731-1740.

Catov J, Bodnar L, Kip K. 2007. Early pregnancy lipid concentrations and spontaneous preterm birth. *Am J Obstet Gynecol* 2007:197:610.e1-e7.

Chiang, A., M. Yang, J. Hun, P. Chou, S. Shyn, H. Ng. 1995. Alterations of serum lipid levels and their biological relevances during and after pregnancy. *Life Sci.*56:2367-75.

Chanrachakul, B., N. Matharoo-Ball, A. Turner, G. Robinson, F. Broughton Pipkin, S. Arulkumaran, RN. Khan. Immunolocalization and protein expression of the alpha subunit of the large-cinductance calcium-activated potassium channel in human myometrium. *Reproduction.* 126(1):43-8.

Chanrachakul, B., F. Broughton Pipkin, and R.N. Khan. 2004. Contribution of coupling between human myometrial beta2-adrenoreceptor and the BK(Ca) channel to uterine quiescence. *Am J Physiol Cell Physiol*. 287:C1747-1752.

Chatterjee, J., J. Gullam, M. Vatish, and S. Thornton. 2007. The management of preterm labour. *Arch Dis Child Fetal Neonatal Ed*. 92:F88-93.

Chen, T.Y., and K.W. Yau. 1994. Direct modulation by Ca(2+)-calmodulin of cyclic nucleotide-activated channel of rat olfactory receptor neurons. *Nature*. 368:545-548.

Cheuk, J.M., M. Hollingsworth, S.J. Hughes, I.T. Piper, and M.J. Maresh. 1993. Inhibition of contractions of the isolated human myometrium by potassium channel openers. *Am J Obstet Gynecol*. 168:953-960.

Chvapil, M., J.B. Ulreich, K. O'Dea, K. Betts, and W. Droegemueller. 1980. Studies on nonoxynol-9. III. Effect on fibroblasts and spermatozoa. *Fertil Steril*. 33:521-525.

Coleman, H.A., and H.C. Parkington. 1987. Single channel Cl- and K+ currents from cells of uterus not treated with enzymes. *Pflugers Arch*. 410:560-562.

Copaja, M., D. Venegas, P. Aranguiz, J. Canales, R. Vivar, M. Catalan, I. Olmedo, A.E. Rodriguez, M. Chiong, L. Leyton, S. Lavandero, and G. Diaz-Araya. 2011. Simvastatin induces apoptosis by a Rho-dependent mechanism in cultured cardiac fibroblasts and myofibroblasts. *Toxicol Appl Pharmacol*. 255:57-64.

Copper, R.L., R.L. Goldenberg, A. Das, N. Elder, M. Swain, G. Norman, R. Ramsey, P. Cotroneo, B.A. Collins, F. Johnson, P. Jones, and A.M. Meier. 1996. The preterm prediction study: maternal stress is associated with spontaneous preterm birth at less than thirty-five weeks' gestation. National Institute of Child Health and Human Development Maternal-Fetal Medicine Units Network. *Am J Obstet Gynecol*. 175:1286-1292.

Cuello, A.C., J.V. Priestley, and M.V. Sofroniew. 1983. Immunocytochemistry and neurobiology. *Q J Exp Physiol*. 68:545-578.

D'Ercole, C., F. Bretelle, R. Shojai, R. Desbriere, and L. Boubli. 2002. [Tocolysis: indications and contraindications. When to start and when to stop]. *J Gynecol Obstet Biol Reprod (Paris)*. 31:5S84-95.

Dabelea, D., R. L. Hanson, R. S. Lindsay. 2000. Intrauterine exposure to diabetes conveys risks for type 2 diabetes and obesity: a study of discordant sibships. *Diabetes.* 49:2208-2211.

Darios, E.S., B. Seitz, and S.W. Watts. 2012. Smooth muscle pharmacology in the isolated virgin and pregnant rat uterus and cervix. *J Pharmacol Exp Ther*. 341:587-596.

De Preval, C., J.R. Pink, and C. Milstein. 1970. Variability of interchain binding of immunoglobulins. Interchain bridges of mouse IgG2a and IgG2b. *Nature*. 228:930-932.

de Sotomayor, M.A., C. Perez-Guerrero, M.D. Herrrera, L. Jimenez, R. Marin, E. Marhuenda, and R. Andriantsitohaina. 2005. Improvement of age-related endothelial dysfunction by simvastatin: effect on NO and COX pathways. *Br J Pharmacol*. 146:1130-1138.

Degani, S., Z. Leibovitz, I. Shapiro, R. Gonen, and G. Ohel. 1998. Myometrial thickness in pregnancy: longitudinal sonographic study. *J Ultrasound Med*. 17:661-665.

Dehelean, C.A., S. Feflea, J. Molnar, I. Zupko, and C. Soica. 2012. Betulin as an antitumor agent tested in vitro on A431, HeLa and MCF7, and as an angiogenic inhibitor in vivo in the CAM assay. *Nat Prod Commun*. 7:981-985.

Dell'Omo, G., S. Bandinelli, G. Penno, R. Pedrinelli, and M. Mariani. 2000. Simvastatin, capillary permeability, and acetylcholine-mediated vasomotion in atherosclerotic, hypercholesterolemic men. *Clin Pharmacol Ther*. 68:427-434.

DeVivo, M., and R. Iyengar. 1994. G protein pathways: signal processing by effectors. *Mol Cell Endocrinol*. 100:65-70.

Di Angelantonio, E., N. Sarwar, P. Perry, S. Kaptoge, K.K. Ray, A. Thompson, A.M. Wood, S. Lewington, N. Sattar, C.J. Packard, R. Collins, S.G. Thompson, and J. Danesh. 2009. Major lipids, apolipoproteins, and risk of vascular disease. *JAMA*. 302:1993-2000.

Downing, S.J., and M. Hollingsworth. 1991. Antagonism of relaxin by glibenclamide in the uterus of the rat in vivo. *Br J Pharmacol*. 104:71-76.

Dreja, K., M. Voldstedlund, J. Vinten, J. Tranum-Jensen, P. Hellstrand, and K. Sward. 2002. Cholesterol depletion disrupts caveolae and differentially impairs agonist-induced arterial contraction. *Arterioscler Thromb Vasc Biol*. 22:1267-1272.

Dubuis, E., N. Rockliffe, M. Hussain, M. Boyett, D. Wray, and D. Gawler. 2006. Evidence for multiple Src binding sites on the alpha1c L-type Ca2+ channel and their roles in activity regulation. *Cardiovasc Res*. 69:391-401.

Edelman, G.M., B.A. Cunningham, W.E. Gall, P.D. Gottlieb, U. Rutishauser, and M.J. Waxdal. 1969. The covalent structure of an entire gammaG immunoglobulin molecule. *Proc Natl Acad Sci U S A*. 63:78-85.

Edison, R., & M. Muenke. 2004. Mechanistic and epidemiologic considerations in the evaluation of adverse birth outcomes following gestational exposure to statins. 2004. *Am J Med Genet.* 131(3):287-98.

Edison, R., & M. Muenke. 2004. Central nervosu system and limb anomalies in case reports of first-trimester statin exposure. 2004. *N Engl J Med.* 350(15):1579-82.

Eghbali, M., L. Toro, and E. Stefani. 2003. Diminished surface clustering and increased perinuclear accumulation of large conductance Ca2+-activated K+ channel in mouse myometrium with pregnancy. *J Biol Chem*. 278:45311-45317.

Elias, E.R., R.M. Hansen, M. Irons, N.B. Quinn, and A.B. Fulton. 2003. Rod photoreceptor responses in children with Smith-Lemli-Opitz syndrome. *Arch Ophthalmol*. 121:1738-1743.

Ellenberg, J.H., and K.B. Nelson. 1979. Birth weight and gestational age in children with cerebral palsy or seizure disorders. *Am J Dis Child*. 133:1044-1048.

Engelman, J.A., C. Chu, A. Lin, H. Jo, T. Ikezu, T. Okamoto, D.S. Kohtz, and M.P. Lisanti. 1998. Caveolin-mediated regulation of signaling along the p42/44 MAP kinase cascade in vivo. A role for the caveolin-scaffolding domain. *FEBS Lett*. 428:205-211.

Ewang-Emukowhate, M., and A.S. Wierzbicki. 2013. Lipid-lowering agents. *J Cardiovasc Pharmacol Ther*. 18:401-411.

Faber, E.S., and P. Sah. 2003. Calcium-activated potassium channels: multiple contributions to neuronal function. *Neuroscientist*. 9:181-194.

Fanelli, F., P. Barier, D. Zanchetta, P.G. De Benedetti and B. Chini. 1999. Activation mechanism of human oxytocin receptor: a combined study of experimental and computer-simulated mutagenesis. *Mol Pharmacol.* 56:214-225.

Ferguson, J.J., I.F. Durr, and H. Rudney. 1959. The Biosynthesis of Mevalonic Acid. *Proc Natl Acad Sci U S A*. 45:499-504.

Folander, K., J.S. Smith, J. Antanavage, C. Bennett, R.B. Stein, and R. Swanson. 1990. Cloning and expression of the delayed-rectifier IsK channel from neonatal rat heart and diethylstilbestrol-primed rat uterus. *Proc Natl Acad Sci U S A*. 87:2975-2979.

Formoso, C. 1973. The interaction of -cyclodextrin with nucleic acid monomer units. *Biochem Biophys Res Commun*. 50:999-1005.

Freyburger, W.A., C.C. Gruhzit, B.R. Rennick, and G.K. Moe. 1950. Action of tetraethylammonium on pressor response to asphyxia. *Am J Physiol*. 163:554-560.

Fuchs, A.R., M.J. Fields, S. Freidman, M. Shemesh, and R. Ivell. 1995. Oxytocin and the timing of parturition. Influence of oxytocin receptor gene expression, oxytocin secretion, and oxytocin-induced prostaglandin F2 alpha and E2 release. *Adv Exp Med Biol*. 395:405-420.

Fukao, M., H.S. Mason, F.C. Britton, J.L Kenyon, G. Horowitz and K.D. Keef. 1999. Cyclic GMP-dependent protein kinase activates cloned BK_{Ca} channels expressed in mammalian cells by direct phosphorylation at serine 1072. *J Biol Chem*. 274:10927-10935.

Fujisawa, K., P. Madaule, T. Ishizaki, G. Watanabe, H. Bito, Y. Saito, A. Hall, and S. Narumiya. 1998. Different regions of Rho determine Rho-selective binding of different classes of Rho target molecules. *J Biol Chem*. 273:18943-18949.

Futerman, A.H., and Y.A. Hannun. 2004. The complex life of simple sphingolipids. *EMBO Rep*. 5:777-782.

Ghidini, A., S. Sicherer, J. Willner. 1992. Congenital abnormalities (VATER) in baby born to mother using lovastatin. *Lancet.* 339(8806):1416-7.

Gleason, A., S.A. Back. 2005. Developmental physiology of the central nervous system. In: Tauesch H.W., R.A. Ballard, C.A Gleason Avery's Disease of the Newborn, Philadelphia, PA. Elsvier Saunders pp 903-907.

Goepfert, A.R., and R.L. Goldenberg. 1996. Prediction of prematurity. *Curr Opin Obstet Gynecol*. 8:417-427.

Goldenberg, R.L., and J.F. Culhane. 2005. Prepregnancy health status and the risk of preterm delivery. *Arch Pediatr Adolesc Med*. 159:89-90.

Goldenberg, R.L., J.F. Culhane, J.D. Iams, and R. Romero. 2008. Epidemiology and causes of preterm birth. *Lancet*. 371:75-84.

Goldenberg, R.L., A.R. Goepfert, and P.S. Ramsey. 2005. Biochemical markers for the prediction of preterm birth. *Am J Obstet Gynecol*. 192:S36-46.

Goldenberg, R.L., J.D. Iams, M. Miodovnik, J.P. Van Dorsten, G. Thurnau, S. Bottoms, B.M. Mercer, P.J. Meis, A.H. Moawad, A. Das, S.N. Caritis, and D. McNellis. 1996. The preterm prediction study: risk factors in twin gestations. National Institute of Child Health and Human Development Maternal-Fetal Medicine Units Network. *Am J Obstet Gynecol*. 175:1047-1053.

Goldstein, J.L., and M.S. Brown. 1990. Regulation of the mevalonate pathway. *Nature*. 343:425-430.

Gonzalez, J., S. Pedroni, G. Girardi. 2014. Statins prevent cervical remodeling, myometrial contractions and preterm labour through a mechanism that involves hemoxygenase-1 and complement inhibition. *Mol Hum Reprod.* 20(6):579-89.

Greenwood, I.A., and R.M. Tribe. 2014. Kv7 and Kv11 channels in myometrial regulation. *Exp Physiol*. 99:503-509.

Groome, L.J., R.L. Goldenberg, S.P. Cliver, R.O. Davis, and R.L. Copper. 1992. Neonatal periventricular-intraventricular hemorrhage after maternal beta-sympathomimetic tocolysis. The March of Dimes Multicenter Study Group. *Am J Obstet Gynecol*. 167:873-879.

Gyetvai, K., M.E. Hannah, E.D. Hodnett, and A. Ohlsson. 1999. Tocolytics for preterm labor: a systematic review. *Obstet Gynecol*. 94:869-877.

Hamada, Y., Y. Nakaya, S. Hamada, M. Kamada, and T. Aono. 1994. Activation of K+ channels by ritodrine hydrochloride in uterine smooth muscle cells from pregnant women. *Eur J Pharmacol*. 288:45-51.

Harder, T. 2003. Formation of functional cell membrane domains: the interplay of lipid- and protein-mediated interactions. *Philos Trans R Soc Lond B Biol Sci*. 358:863-868.

Harder, T., E. Rodekamp, K. Schellong. 2007. Birth weight and subsequent risk of type 2 diabetes: a meta-analysis. *AmJ Epidemiol.* 165:849-857.

Harkness, M.L., R.D. Harkness, and B.E. Moralee. 1956. Loss of collagen from the uterus of the rat after ovariectomy and from the non-pregnant horn after parturition. *Q J Exp Physiol Cogn Med Sci*. 41:254-262.

Harootunian, A.T., J.P. Kao, S. Paranjape, S.R. Adams, B.V. Potter, and R.Y. Tsien. 1991. Cytosolic Ca2+ oscillations in REF52 fibroblasts: Ca(2+)-stimulated IP3 production or voltage-dependent Ca2+ channels as key positive feedback elements. *Cell Calcium*. 12:153-164.

Haug, T., R. Olcese, L. Toro, and E. Stefani. 2004. Regulation of K+ flow by a ring of negative charges in the outer pore of BKCa channels. Part II: Neutralization of aspartate 292 reduces long channel openings and gating current slow component. *J Gen Physiol*. 124:185-197.

Heaton, R.C., S. Wray, and D.A. Eisner. 1993. Effects of metabolic inhibition and changes of intracellular pH on potassium permeability and contraction of rat uterus. *J Physiol*. 465:43-56.

Hedin, K.E., K. Duerson, and D.E. Clapham. 1993. Specificity of receptor-G protein interactions: searching for the structure behind the signal. *Cell Signal*. 5:505-518.

Hendler, I., R.L. Goldenberg, B.M. Mercer, J.D. Iams, P.J. Meis, A.H. Moawad, C.A. MacPherson, S.N. Caritis, M. Miodovnik, K.M. Menard, G.R. Thurnau, and Y. Sorokin. 2005. The Preterm Prediction Study: association between maternal body mass index and spontaneous and indicated preterm birth. *Am J Obstet Gynecol*. 192:882-886.

Herrera, E. 2002. Lipid metabolism in pregnancy and its consequences in the fetus and newborn. *Endocrine*. 19:43-55.

Hodgkin, A.L., A.F. Huxley, and B. Katz. 1952. Measurement of current-voltage relations in the membrane of the giant axon of Loligo. *J Physiol*. 116:424-448.

Hofmann, F., A. Ammendola and J. Scholossmann. 2000. Rising behind NO: cGMP-dependent protein kinase. *J Cell Sci.* 113:1671-1676.

Hollingsworth, M., T. Amedee, D. Edwards, J. Mironneau, J.P. Savineau, R.C. Small, and A.H. Weston. 1987. The relaxant action of BRL 34915 in rat uterus. *Br J Pharmacol*. 91:803-813.

Honda, Y. 1971. [The effects of some ganglion stimulants and ganglion blockers upon the electrical activity of rabbit retinas in vitro]. *Nihon Ganka Gakkai Zasshi*. 75:1299-1308.

Honore, E., T. Amedee, C. Martin, C. Dacquet, C. Mironneau, and J. Mironneau. 1989. Calcium channel current and its sensitivity to (+) isradipine in cultured pregnant rat myometrial cells. An electrophysiological and a binding study. *Pflugers Arch*. 414:477-483.

Hooper, N.M. 1999. Detergent-insoluble glycosphingolipid/cholesterol-rich membrane domains, lipid rafts and caveolae (review). *Mol Membr Biol*. 16:145-156.

Hosono, T., M. Suzuki, and Y. Chiba. 2001. Contraindication of magnesium sulfate in a pregnancy complicated with late-onset diabetes mellitus and sensory deafness due to mitochondrial myopathy. *J Matern Fetal Med*. 10:355-356.

Hubbard, K.S., I.M. Gut, S.M. Scheeler, M.E. Lyman, and P.M. McNutt. 2012. Compatibility of SYTO 13 and Hoechst 33342 for longitudinal imaging of neuron viability and cell death. *BMC Res Notes*. 5:437.

Hugues, M., G. Romey, D. Duval, J.P. Vincent, and M. Lazdunski. 1982a. Apamin as a selective blocker of the calcium-dependent potassium channel in neuroblastoma cells: voltage-clamp and biochemical characterization of the toxin receptor. *Proc Natl Acad Sci U S A*. 79:1308-1312.

Hugues, M., H. Schmid, G. Romey, D. Duval, C. Frelin, and M. Lazdunski. 1982b. The Ca2+-dependent slow K+ conductance in cultured rat muscle cells: characterization with apamin. *EMBO J*. 1:1039-1042.

Hulsey, T.C., G.R. Alexander, P.Y. Robillard, D.J, A. Keenan. 1993. Hyaline membrane disease. The role of ethnicity and maternal risk characteristics. *Am J Obstet Gynecol.* 168(2):572-576.

Ikezu, T., B.D. Trapp, K.S. Song, A. Schlegel, M.P. Lisanti, and T. Okamoto. 1998. Caveolae, plasma membrane microdomains for alpha-secretase-mediated processing of the amyloid precursor protein. *J Biol Chem*. 273:10485-10495.

Inoue, Y., K. Nakao, K. Okabe, H. Izumi, S. Kanda, K. Kitamura, and H. Kuriyama. 1990. Some electrical properties of human pregnant myometrium. *Am J Obstet Gynecol*. 162:1090-1098.

Inoue, Y., and N. Sperelakis. 1991. Gestational change in Na+ and Ca2+ channel current densities in rat myometrial smooth muscle cells. *Am J Physiol*. 260:C658-663.

Istvan, E.S., and J. Deisenhofer. 2000. The structure of the catalytic portion of human HMG-CoA reductase. *Biochim Biophys Acta*. 1529:9-18.

Istvan, E.S., and J. Deisenhofer. 2001. Structural mechanism for statin inhibition of HMG-CoA reductase. *Science*. 292:1160-1164.

Istvan, E.S., M. Palnitkar, S.K. Buchanan, and J. Deisenhofer. 2000. Crystal structure of the catalytic portion of human HMG-CoA reductase: insights into regulation of activity and catalysis. *EMBO J*. 19:819-830.

Ivell, R., W. Rust, A. Einspanier, S. Hartung, M. Fields, and A.R. Fuchs. 1995. Oxytocin and oxytocin receptor gene expression in the reproductive tract of the pregnant cow: rescue of luteal oxytocin production at term. *Biol Reprod*. 53:553-560.

Janmey, P.A., and P.K. Kinnunen. 2006. Biophysical properties of lipids and dynamic membranes. *Trends Cell Biol*. 16:538-546.

Jirapinyo, M., P. Thuvasethakul, and S. Leelaphiwat. 1990. Prospective study on premature labor with magnesium sulfate. *Asia Oceania J Obstet Gynaecol*. 16:91-96.

Jmari, K., C. Mironneau, and J. Mironneau. 1987. Selectivity of calcium channels in rat uterine smooth muscle: interactions between sodium, calcium and barium ions. *J Physiol*. 384:247-261.

Jones, K., A. Shmygol, S. Kupittayanant, and S. Wray. 2004. Electrophysiological characterization and functional importance of calcium-activated chloride channel in rat uterine myocytes. *Pflugers Arch*. 448:36-43.

Kakei, M., A. Noma, and T. Shibasaki. 1985. Properties of adenosine-triphosphate-regulated potassium channels in guinea-pig ventricular cells. *J Physiol*. 363:441-462.

Kao, C.Y., and J.R. McCullough. 1975. Ionic currents in the uterine smooth muscle. *J Physiol*. 246:1-36.

Kenny, L.C., P.N. Baker, D.A. Kendall, M.D. Randall, and W.R. Dunn. 2002. The role of gap junctions in mediating endothelium-dependent responses to bradykinin in myometrial small arteries isolated from pregnant women. *Br J Pharmacol*. 136:1085-1088.

Khan, R.N., J.J. Morrison, S.K. Smith, and M.L. Ashford. 1998. Activation of large-conductance potassium channels in pregnant human myometrium by pinacidil. *Am J Obstet Gynecol*. 178:1027-1034.

Khan, R.N., S.K. Smith, J.J. Morrison, and M.L. Ashford. 1993. Properties of large-conductance K+ channels in human myometrium during pregnancy and labour. *Proc Biol Sci*. 251:9-15.

Khan, R.N., S.K. Smith, J.J. Morrison, and M.L. Ashford. 1997. Ca2+ dependence and pharmacology of large-conductance K+ channels in nonlabor and labor human uterine myocytes. *Am J Physiol*. 273:C1721-1731.

Khoury J, Henriksen T, Christophersen B, Tonstad S. 2005. Effect of a cholesterol-lowering diet on maternal, cord, and neonatal lipids, and pregnancy outcome: a randomized clinical trial. *Am J Obstet Gynecol* 193:1292–301.

Kimura, K., M. Ito, M. Amano, K. Chihara, Y. Fukata, M. Nakafuku, B. Yamamori, J. Feng, T. Nakano, K. Okawa, A. Iwamatsu, and K. Kaibuchi. 1996a. Regulation of myosin phosphatase by Rho and Rho-associated kinase (Rho-kinase). *Science*. 273:245-248.

Kimura, T., M. Takemura, S. Nomura, T. Nobunaga, Y. Kubota, T. Inoue, K. Hashimoto, I. Kumazawa, Y. Ito, K. Ohashi, M. Koyama, C. Azuma, Y. Kitamura, and F. Saji. 1996b. Expression of oxytocin receptor in human pregnant myometrium. *Endocrinology*. 137:780-785.

Kinsella, B.T., and W.A. Maltese. 1992. rab GTP-binding proteins with three different carboxyl-terminal cysteine motifs are modified in vivo by 20-carbon isoprenoids. *J Biol Chem*. 267:3940-3945.

Knaus, H.G., O.B. McManus, S.H. Lee, W.A. Schmalhofer, M. Garcia-Calvo, L.M. Helms, M. Sanchez, K. Giangiacomo, J.P. Reuben, A.B. Smith, 3rd, and et al. 1994. Tremorgenic indole alkaloids potently inhibit smooth muscle high-conductance calcium-activated potassium channels. *Biochemistry*. 33:5819-5828.

Knowles, R.G., M. Palacios, R.M. Palmer, and S. Moncada. 1989. Formation of nitric oxide from L-arginine in the central nervous system: a transduction mechanism for

stimulation of the soluble guanylate cyclase. *Proc Natl Acad Sci U S A*. 86:5159-5162.

Koh, C.M. 2013. Preparation of Cells for Microscopy using Cytospin. *Methods Enzymol*. 533:235-240.

Kohler, M., B. Hirschberg, C.T. Bond, J.M. Kinzie, N.V. Marrion, J. Maylie, and J.P. Adelman. 1996. Small-conductance, calcium-activated potassium channels from mammalian brain. *Science*. 273:1709-1714.

Kosterin, S.A., N.N. Slinchenko, and G.L. Gergalova. 1994. [Energy characteristics of an ATP-hydrolase reaction catalyzed by solubilized Ca2+,Mg2+-ATPase from smooth muscle cell membrane]. *Biokhimiia*. 59:889-904.

Krantz, K.E., and W.P. Phillips. 1962. Anatomy of the human uterine cervix, gross and microscopic. *Ann N Y Acad Sci*. 97:551-563.

Krapivinsky, G., E.A. Gordon, K. Wickman, B. Velimirovic, L. Krapivinsky, and D.E. Clapham. 1995. The G-protein-gated atrial K+ channel IKACh is a heteromultimer of two inwardly rectifying K(+)-channel proteins. *Nature*. 374:135-141.

Krueger, J.K., R.C. Padre, and J.T. Stull. 1995. Intrasteric regulation of myosin light chain kinase. *J Biol Chem*. 270:16848-16853.

Ku, C.Y., A. Qian, Y. Wen, K. Anwer, and B.M. Sanborn. 1995. Oxytocin stimulates myometrial guanosine triphosphatase and phospholipase-C activities via coupling to G alpha q/11. *Endocrinology*. 136:1509-1515.

Kumar, D., J.J. Russell, and A.C. Barnes. 1961. Basic observations on the physiology of the human myometrium during pregnancy. *JAMA*. 178:827-830.

Kumasawa, K., M. Ikawa, H. Kidoya, H. Hasuwa, M. Okabe. 2011. Pravastatin induces placental growth factor (PGF) and ameliorates preeclampsia in a mouse model. *Proc Natl Acad Sci.* 108(4):1451-5.

Kyozuka, M., J. Crankshaw, and E.E. Daniel. 1987. Calcium channels in isolated cells and strips of longitudinal muscle of rat myometrium. *Can J Physiol Pharmacol*. 65:1976-1981.

Lachance, V., A. Cartier, S. Genier, S. Munger, P. Germain, P. Labrecque, and J.L. Parent. Regulation of beta2-adrenergic receptor maturation and anterograde trafficking by an interaction with Rab geranylgeranyltransferase: modulation of Rab geranylgeranylation by the receptor. *J Biol Chem*. 286:40802-40813.

Lajat, S., Z. Tanfin, G. Guillon, and S. Harbon. 1996. Modulation of phospholipase C pathway and level of Gq alpha/G11 alpha in rat myometrium during gestation. *Am J Physiol*. 271:C895-904.

Lalande, M.E., V. Ling, and R.G. Miller. 1981. Hoechst 33342 dye uptake as a probe of membrane permeability changes in mammalian cells. *Proc Natl Acad Sci U S A*. 78:363-367.

Lampinen, R., Vebvilainen-Julkunen K, Kankkunen P. 2009. A review of pregnancy in women over 3 years of age. *Open Nurs J.* 3:33-38.

Laufs, U., V. La Fata, J. Plutzky, and J.K. Liao. 1998. Upregulation of endothelial nitric oxide synthase by HMG CoA reductase inhibitors. *Circulation*. 97:1129-1135.

Laufs, U., and J.K. Liao. 1998. Post-transcriptional regulation of endothelial nitric oxide synthase mRNA stability by Rho GTPase. *J Biol Chem*. 273:24266-24271.

Lawn, J.E., K. Wilczynska-Ketende, and S.N. Cousens. 2006. Estimating the causes of 4 million neonatal deaths in the year 2000. *Int J Epidemiol*. 35:706-718.

Lee, S.E., D.S. Ahn, and Y.H. Lee. 2009. Role of T-type Ca Channels in the Spontaneous Phasic Contraction of Pregnant Rat Uterine Smooth Muscle. *Korean J Physiol Pharmacol*. 13:241-249.

Lincolm, T.M and P. Komalavilas. 2000. Cyclic GMP-mediated signaling mechanisms in smooth muscle. *Nitric Oxide,* ed Ignarro LJ. Academic, New York, pp401-4425.

Liu, L., H.L. Johnson, S. Cousens, J. Perin, S. Scott, J.E. Lawn, I. Rudan, H. Campbell, R. Cibulskis, M. Li, C. Mathers, R.E. Black, W.H.O. Child Health Epidemiology Reference Group of, and Unicef. 2012. Global, regional, and national causes of child mortality: an updated systematic analysis for 2010 with time trends since 2000. *Lancet*. 379:2151-2161.

Liu, L., S. Oza, D. Hogan, J. Perin, I. Rudan, J.E. Lawn, S. Cousens, C. Mathers, and R.E. Black. 2015. Global, regional, and national causes of child mortality in 2000-13, with projections to inform post-2015 priorities: an updated systematic analysis. *Lancet*. 385:430-440.

Low, J.A., R.S. Galbraith, D.W. Muir, H.L. Killen, E.A. Pater, and E.J. Karchmar. 1985. The relationship between perinatal hypoxia and newborn encephalopathy. *Am J Obstet Gynecol*. 152:256-260.

Luckas, M.J., M.J. Taggart, and S. Wray. 1999. Intracellular calcium stores and agonist-induced contractions in isolated human myometrium. *Am J Obstet Gynecol*. 181:468-476.

Lustig, K.D., B.R. Conklin, P. Herzmark, R. Taussig, and H.R. Bourne. 1993. Type II adenylylcyclase integrates coincident signals from Gs, Gi, and Gq. *J Biol Chem*. 268:13900-13905.

Madan, a., W.V. Good. Disorders of the eye. In: H.W. Taeush, R.A Ballard, C.A. Gleason editors. Avery's Diseasesof the Newborn. Philadelphia, PA. Elsevier Sauders. 2005. pp1471-1483.

MacKinnon, K., and M. McIntyre. 2006. From Braxton Hicks to preterm labour: the constitution of risk in pregnancy. *Can J Nurs Res*. 38:56-72.

Manson, J., C. Freyssinges, M. Ducrocq, W. Stephenson. 1996. Postmarketing surveillance of lovastatin and simvastatin exposure during pregnancy. *Reprof Toxicol.* 10(6):439-46.

Marty, A., and E. Neher. 1985. Potassium channels in cultured bovine adrenal chromaffin cells. *J Physiol*. 367:117-141.

Marty, A., Y.P. Tan, and A. Trautmann. 1984. Three types of calcium-dependent channel in rat lacrimal glands. *J Physiol*. 357:293-325.

Matharoo-Ball, B., M.L. Ashford, S. Arulkumaran, and R.N. Khan. 2003. Down-regulation of the alpha- and beta-subunits of the calcium-activated potassium channel in human myometrium with parturition. *Biol Reprod*. 68:2135-2141.

McMallum L., S. Pierce, S. England, I.Greenwood, R. Tribe. 2011. THe contribution of Kv7 channels to pregnant mouse and human myometrial contractility. *J Cell Mol Med.* 15(3):577-86.

Mershon, J.L., G. Mikala, and A. Schwartz. 1994. Changes in the expression of the L-type voltage-dependent calcium channel during pregnancy and parturition in the rat. *Biol Reprod*. 51:993-999.

Milstein, C., and J.R. Pink. 1970. Structure and evolution of immunoglobulins. *Prog Biophys Mol Biol*. 21:209-263.

Minsker, D., J. MacDonald, R. Robertson, D. Bokelman. 1983. Mevalonate supplementation in pregnant rats suppresses the teratogenicity of mevionolinic acid, an inhibitor of 3-hydroxy-3-methylblutaryl-coenzyme a reductase. *Teratology.* 28(£): 449-56.

Mollard, P., J. Mironneau, T. Amedee, and C. Mironneau. 1986. Electrophysiological characterization of single pregnant rat myometrial cells in short-term primary culture. *Am J Physiol*. 250:C47-54.

Moomaw, J.F., and P.J. Casey. 1992. Mammalian protein geranylgeranyltransferase. Subunit composition and metal requirements. *J Biol Chem*. 267:17438-17443.

Mooradian, A.D., M.J. Haas, O. Batejko, M. Hovsepyan, and S.S. Feman. 2005. Statins ameliorate endothelial barrier permeability changes in the cerebral tissue of streptozotocin-induced diabetic rats. *Diabetes*. 54:2977-2982.

Moore, P.K., O.A. al-Swayeh, N.W. Chong, R.A. Evans, and A. Gibson. 1990. L-NG-nitro arginine (L-NOARG), a novel, L-arginine-reversible inhibitor of endothelium-dependent vasodilatation in vitro. *Br J Pharmacol*. 99:408-412.

Morrison, J.J., M.L. Ashford, R.N. Khan, and S.K. Smith. 1993. The effects of potassium channel openers on isolated pregnant human myometrium before and after the onset of labor: potential for tocolysis. *Am J Obstet Gynecol*. 169:1277-1285.

Newburn-Cook, C.V. and Onyskiw, J.E. 2005. Is older maternal age a risk factor for preterm birth and fetal growth restriction? A systematic review. *Health Care Women Int.* 26(9):852-75.

Noble, K., R. Floyd, A. Shmygol, A. Mobasheri, and S. Wray. 2010. Distribution, expression and functional effects of small conductance Ca-activated potassium (SK) channels in rat myometrium. *Cell Calcium*. 47:47-54.

Noma, A. 1983. ATP-regulated K+ channels in cardiac muscle. *Nature*. 305:147-148.

O'Driscoll, G., D. Green, and R.R. Taylor. 1997. Simvastatin, an HMG-coenzyme A reductase inhibitor, improves endothelial function within 1 month. *Circulation*. 95:1126-1131.

Ohkubo, T., T. Kawarabayashi, Y. Inoue, and K. Kitamura. 2005. Differential expression of L- and T-type calcium channels between longitudinal and circular muscles of the rat myometrium during pregnancy. *Gynecol Obstet Invest*. 59:80-85.

Ohya, Y., and N. Sperelakis. 1989. Fast Na+ and slow Ca2+ channels in single uterine muscle cells from pregnant rats. *Am J Physiol*. 257:C408-412.

Okamoto, T., A. Schlegel, P.E. Scherer, and M.P. Lisanti. 1998. Caveolins, a family of scaffolding proteins for organizing "preassembled signaling complexes" at the plasma membrane. *J Biol Chem*. 273:5419-5422.

Orio, P., Y. Torres, P. Rojas, I. Carvacho, M.L. Garcia, L. Toro, M.A. Valverde, and R. Latorre. 2006. Structural determinants for functional coupling between the beta and alpha subunits in the Ca2+-activated K+ (BK) channel. *J Gen Physiol*. 127:191-204.

Orlov, S.N., A.V. Sitozhevskii, N.I. Pokudin, and V.M. Agnaev. 1985. [Mechanism of the effect of EGTA on the affinity to calcium of Ca-transporting and Ca-binding cell systems]. *Biokhimiia*. 50:1920-1925.

Packard, C. 2000. Lipid-lowering drug therapies: the evidence. *Proc Nutr Soc*. 59:423-424.

Palinski, W. 2009. Maternal-fetal cholesterol transport in the placenta.*Circ Res.* 104@569-71.

Parkington, H.C., and H.A. Coleman. 2001. Excitability in uterine smooth muscle. *Front Horm Res*. 27:179-200.

Patel, A., and E. Honore. 2002. The TREK two P domain K+ channels. *J Physiol*. 539:647.

Perez-Guerrero, C., M. Alvarez de Sotomayor, M.D. Herrera, and E. Marhuenda. 2000. Endothelium modulates contractile response to simvastatin in rat aorta. *Z Naturforsch C*. 55:121-124.

Perney, T.M., and L.K. Kaczmarek. 1991. The molecular biology of K+ channels. *Curr Opin Cell Biol*. 3:663-670.

Pettitt, D. J., H. R. Baird, K. A. Aleck. 1983. Excessive obesity in offspring of Pima Indian women with diabetes during pregnancy. *N Engl J Med.* 208:242-245.

Phaneuf, S., G.N. Europe-Finner, M.P. Carrasco, C.H. Hamilton, and A. Lopez Bernal. 1995a. Oxytocin signalling in human myometrium. *Adv Exp Med Biol*. 395:453-467.

Phaneuf, S., G.N. Europe-Finner, I.Z. MacKenzie, S.P. Watson, and A. Lopez Bernal. 1995b. Effects of oestradiol and tamoxifen on oxytocin-induced phospholipase C activation in human myometrial cells. *J Reprod Fertil*. 103:121-126.

Phillippe, M., and A. Basa. 1996. The effects of ruthenium red, an inhibitor of calcium-induced calcium release, on phasic myometrial contractions. *Biochem Biophys Res Commun*. 221:656-661.

Piechota, W., and A. Staszewski. 1992. Reference ranges of lipids and apolipoproteins in pregnancy. *Eur J Obstet Gynecol Reprod Biol*. 45:27-35.

Pierce, S.L., J.D. Kresowik, K.G. Lamping, and S.K. England. 2008. Overexpression of SK3 channels dampens uterine contractility to prevent preterm labor in mice. *Biol Reprod*. 78:1058-1063.

Piper, I., E. Minshall, S.J. Downing, M. Hollingsworth, and H. Sadraei. 1990. Effects of several potassium channel openers and glibenclamide on the uterus of the rat. *Br J Pharmacol*. 101:901-907.

Plagemann, A., T. Harder, R. Kohlhoff. 1997. Overweight and obesity in infants of mothers with long-term insulin-dependent diabetes or gestational diabetes. *Int J Obes Relat Metab Discord.* 21:451-456.

Pollack, P., K. Shields, D. Burnett, M. Osborne, M. Cunningham, M. Stepanavage. 2005. Pregnancy outcomes after maternal exposure to simvastatin and lovastatin. *Birth Defects Res A Clin Mol Teratol.* 73:(11):888-96

Pragnell, M., K.J. Snay, J.S. Trimmer, N.J. MacLusky, F. Naftolin, L.K. Kaczmarek, and M.B. Boyle. 1990. Estrogen induction of a small, putative K+ channel mRNA in rat uterus. *Neuron*. 4:807-812.

Pralle, A., P. Keller, E.L. Florin, K. Simons, and J.K. Horber. 2000. Sphingolipid-cholesterol rafts diffuse as small entities in the plasma membrane of mammalian cells. *J Cell Biol*. 148:997-1008.

Preiss, D., and N. Sattar. 2009. Lipids, lipid modifying agents and cardiovascular risk: a review of the evidence. *Clin Endocrinol (Oxf)*. 70:815-828.

Ramon y Cajal, J., M. Pocovi, M.A. Romero, D. Jimenez, H. Martinez, and F. Grande. 1988. Plasma lipids and high density lipoprotein cholesterol in maternal and umbilical vessels in twin pregnancies. *Artery*. 15:109-117.

Rattan, S. 2010. 3-Hydroxymethyl coenzyme A reductase inhibition attenuates spontaneous smooth muscle tone via RhoA/ROCK pathway regulated by RhoA prenylation. *Am J Physiol Gastrointest Liver Physiol*. 298:G962-969.

Reynolds, S.R. 1946. The relation of hydrostatic conditions in the uterus to the size and shape of the conceptus during pregnancy; a concept of uterine accommodation. *Anat Rec*. 95:283-296.

Reynolds, S.R. 1947. Relation of maternal blood-flow within the uterus to change in shape and size of the conceptus during pregnancy; physiological basis of uterine accommodation. *Am J Physiol*. 148:77-85.

Richter, O.N., C. Bartz, J. Dowaji, M. Kupka, J. Reinsberg, U. Ulrich, and W. Rath. 2006. Contractile reactivity of human myometrium in isolated non-pregnant uteri. *Hum Reprod*. 21:36-45.

Riley, M., P.N. Baker, R.M. Tribe, and M.J. Taggart. 2005. Expression of scaffolding, signalling and contractile-filament proteins in human myometria: effects of pregnancy and labour. *J Cell Mol Med*. 9:122-134.

Robier, C., F. Quehenberger, M. Neubauer, M. Stettin, and F. Rainer. 2013. The cytospin technique improves the detection of calcium pyrophosphate crystals in synovial fluid samples with a low leukocyte count. *Rheumatol Int*.

Rodal, S.K., G. Skretting, O. Garred, F. Vilhardt, B. van Deurs, and K. Sandvig. 1999. Extraction of cholesterol with methyl-beta-cyclodextrin perturbs formation of clathrin-coated endocytic vesicles. *Mol Biol Cell*. 10:961-974.

Romey, G., M. Hugues, H. Schmid-Antomarchi, and M. Lazdunski. 1984. Apamin: a specific toxin to study a class of Ca2+-dependent K+ channels. *J Physiol (Paris)*. 79:259-264.

Rosenbaum, S.T., J. Svalo, K. Nielsen, T. Larsen, J.C. Jorgensen, and P. Bouchelouche. 2012. Immunolocalization and expression of small-conductance calcium-activated potassium channels in human myometrium. *J Cell Mol Med*. 16:3001-3008.

Ruan, B., W.K. Wilson, J. Pang, and G.J. Schroepfer, Jr. 2000. Synthesis of [3alpha-3H]cholesta-5,8-dien-3beta-ol and tritium-labeled forms of other sterols of potential importance in the Smith-Lemli-Optiz syndrome. *Steroids*. 65:29-39.

Sah, P., and E.S. Faber. 2002. Channels underlying neuronal calcium-activated potassium currents. *Prog Neurobiol*. 66:345-353.

Sailer, C.A., H. Hu, W.A. Kaufmann, M. Trieb, C. Schwarzer, J.F. Storm, and H.G. Knaus. 2002. Regional differences in distribution and functional expression of small-conductance Ca2+-activated K+ channels in rat brain. *J Neurosci*. 22:9698-9707.

Sampaio, J.L., M.J. Gerl, C. Klose, C.S. Ejsing, H. Beug, K. Simons, and A. Shevchenko. 2011. Membrane lipidome of an epithelial cell line. *Proc Natl Acad Sci U S A*. 108:1903-1907.

Samsonov, A.V., I. Mihalyov, and F.S. Cohen. 2001. Characterization of cholesterol-sphingomyelin domains and their dynamics in bilayer membranes. *Biophys J*. 81:1486-1500.

Sanborn, B.M., C.Y. Ku, S. Shlykov, and L. Babich. 2005. Molecular signaling through G-protein-coupled receptors and the control of intracellular calcium in myometrium. *J Soc Gynecol Investig*. 12:479-487.

Savalli, N., A. Kondratiev, S.B. de Quintana, L. Toro, and R. Olcese. 2007. Modes of operation of the BKCa channel beta2 subunit. *J Gen Physiol*. 130:117-131.

Schramm, M., G. Thomas, R. Towart, and G. Franckowiak. 1983a. Activation of calcium channels by novel 1,4-dihydropyridines. A new mechanism for positive inotropics or smooth muscle stimulants. *Arzneimittelforschung*. 33:1268-1272.

Schramm, M., G. Thomas, R. Towart, and G. Franckowiak. 1983c. Novel dihydropyridines with positive inotropic action through activation of Ca2+ channels. *Nature*. 303:535-537.

Seto, S.W., A.L. Au, T.Y. Lam, S.S. Chim, S.M. Lee, S. Wan, D.C. Tjiu, N. Shigemura, A.P. Yim, S.W. Chan, S.K. Tsui, G.P. Leung, and Y.W. Kwan. 2007. Modulation by simvastatin of iberiotoxin-sensitive, Ca2+-activated K+ channels of porcine coronary artery smooth muscle cells. *Br J Pharmacol*. 151:987-997.

Shmygol, A., K. Noble, and S. Wray. 2007. Depletion of membrane cholesterol eliminates the Ca2+-activated component of outward potassium current and decreases membrane capacitance in rat uterine myocytes. *J Physiol*. 581:445-456.

Shmygol, A., and S. Wray. 2005. Modulation of agonist-induced Ca2+ release by SR Ca2+ load: direct SR and cytosolic Ca2+ measurements in rat uterine myocytes. *Cell Calcium*. 37:215-223.

Shynlova, O., A. Oldenhof, A. Dorogin, Q. Xu, J. Mu, N. Nashman, and S.J. Lye. 2006. Myometrial apoptosis: activation of the caspase cascade in the pregnant rat myometrium at midgestation. *Biol Reprod*. 74:839-849.

Simons, K., and J.L. Sampaio. 2011. Membrane organization and lipid rafts. *Cold Spring Harb Perspect Biol*. 3:a004697.

Simmons, L.E., C.E. Rubens, G.L. Darmstadt, M.G. Garvett. 2010. Preventing preterm birth and neonatal mortality: exploring the epidemiology, causes, and interventions. *Semin Perinatol.* 34(6):408-15.

Sinclair, J.C. 1972. Neonatal acidosis and respiratory distress syndrome in the preterm infant: role of early pH correction with bicarbonate. *J Pediatr*. 81:1188-1189.

Skarra, D.V., T. Cornwell, V. Solodushko, A. Brown, and M.S. Taylor. 2011. CyPPA, a positive modulator of small-conductance Ca(2+)-activated K(+) channels, inhibits phasic uterine contractions and delays preterm birth in mice. *Am J Physiol Cell Physiol*. 301:C1027-1035.

Smith, J.D., C. Waelde, A. Horwitz, and P. Zheng. 2002. Evaluation of the role of phosphatidylserine translocase activity in ABCA1-mediated lipid efflux. *J Biol Chem*. 277:17797-17803.

Smith, K.B & Smith, M.S 2016. Obesity statistics. *Prim Care. 43:121-135.*

Smith, R.D., E.B. Babiychuk, K. Noble, A. Draeger, and S. Wray. 2005. Increased cholesterol decreases uterine activity: functional effects of cholesterol alteration in pregnant rat myometrium. *Am J Physiol Cell Physiol*. 288:C982-988.

Soloff, M.S., Y.J. Jeng, M. Ilies, S.L. Soloff, M.G. Izban, T.G. Wood, N.I. Panova, G.V. Velagaleti, and G.D. Anderson. 2004. Immortalization and characterization of human myometrial cells from term-pregnant patients using a telomerase expression vector. *Mol Hum Reprod*. 10:685-695.

Sotgia, F., B. Razani, G. Bonuccelli, W. Schubert, M. Battista, H. Lee, F. Capozza, A.L. Schubert, C. Minetti, J.T. Buckley, and M.P. Lisanti. 2002. Intracellular retention of glycosylphosphatidyl inositol-linked proteins in caveolin-deficient cells. *Mol Cell Biol*. 22:3905-3926.

Speert, H. 1956. John Braxton Hicks, bipolar version, and the contractions of the pregnant uterus. *J Obstet Gynaecol Br Emp*. 63:268-271.

Sperelakis, N., Y. Inoue, and Y. Ohya. 1992a. Fast Na+ channels and slow Ca2+ current in smooth muscle from pregnant rat uterus. *Mol Cell Biochem*. 114:79-89.

Sperelakis, N., Y. Inoue, and Y. Ohya. 1992d. Fast Na+ channels in smooth muscle from pregnant rat uterus. *Can J Physiol Pharmacol*. 70:491-500.

Spruce, A.E., N.B. Standen, and P.R. Stanfield. 1987. Studies of the unitary properties of adenosine-5'-triphosphate-regulated potassium channels of frog skeletal muscle. *J Physiol*. 382:213-236.

Stanley, F.J. 1981. Spastic cerebral palsy: changes in birthweight and gestational age. *Early Hum Dev*. 5:167-178.

Steer, P.J. 1990. The endocrinology of parturition in the human. *Baillieres Clin Endocrinol Metab*. 4:333-349.

Stocker, M., M. Krause, and P. Pedarzani. 1999. An apamin-sensitive Ca2+-activated K+ current in hippocampal pyramidal neurons. *Proc Natl Acad Sci U S A*. 96:4662-4667.

Stocker, M., and P. Pedarzani. 2000. Differential distribution of three Ca(2+)-activated K(+) channel subunits, SK1, SK2, and SK3, in the adult rat central nervous system. *Mol Cell Neurosci*. 15:476-493.

Stroes, E. 2005. Statins and LDL-cholesterol lowering: an overview. *Curr Med Res Opin*. 21 Suppl 6:S9-16.

Taggart, M.J., P. Leavis, O. Feron, and K.G. Morgan. 2000. Inhibition of PKCalpha and rhoA translocation in differentiated smooth muscle by a caveolin scaffolding domain peptide. *Exp Cell Res*. 258:72-81.

Taggart, M.J., and S. Wray. 1998. Contribution of sarcoplasmic reticular calcium to smooth muscle contractile activation: gestational dependence in isolated rat uterus. *J Physiol*. 511 (Pt 1):133-144.

Taguchi, N., E. Rubin, A. Hosokawa, J. Choi, A. Ying, M. Moretti, G. Koren, S. Ito. 2008. Prenatal exposure to HMG-CoA reductase inhibitors: effects on fetal and neonatal outcomes. *Reprod Toxicol.* 26(2): 175-7.

Tansey, M.G., K. Luby-Phelps, K.E. Kamm, and J.T. Stull. 1994. Ca(2+)-dependent phosphorylation of myosin light chain kinase decreases the Ca2+ sensitivity of light chain phosphorylation within smooth muscle cells. *J Biol Chem*. 269:9912-9920.

Trautmann, A., and A. Marty. 1984. Activation of Ca-dependent K channels by carbamoylcholine in rat lacrimal glands. *Proc Natl Acad Sci U S A*. 81:611-615.

Treasure, C.B., J.L. Klein, W.S. Weintraub, J.D. Talley, M.E. Stillabower, A.S. Kosinski, J. Zhang, S.J. Boccuzzi, J.C. Cedarholm, and R.W. Alexander. 1995. Beneficial effects

of cholesterol-lowering therapy on the coronary endothelium in patients with coronary artery disease. *N Engl J Med*. 332:481-487.

Turi, A., A.L. Kiss, and N. Mullner. 2001. Estrogen downregulates the number of caveolae and the level of caveolin in uterine smooth muscle. *Cell Biol Int*. 25:785-794.

Vabratian, A. 2009. Prevalence of overweight and obesity among women of childbearing age. *Matern Child Health.* 13:268-273.

Uldbjerg, N., G. Ekman, A. Malmstrom, K. Olsson, and U. Ulmsten. 1983a. Ripening of the human uterine cervix related to changes in collagen, glycosaminoglycans, and collagenolytic activity. *Am J Obstet Gynecol*. 147:662-666.

Uldbjerg, N., U. Ulmsten, and G. Ekman. 1983b. The ripening of the human uterine cervix in terms of connective tissue biochemistry. *Clin Obstet Gynecol*. 26:14-26.

Ulloa, A., A.L. Gonzales, M. Zhong, Y.S. Kim, J. Cantlon, C. Clay, C.Y. Ku, S. Earley, and B.M. Sanborn. 2009. Reduction in TRPC4 expression specifically attenuates G-protein coupled receptor-stimulated increases in intracellular calcium in human myometrial cells. *Cell Calcium*. 46:73-84.

Urban, N.H., K.M. Berg, and P.H. Ratz. 2003. K+ depolarization induces RhoA kinase translocation to caveolae and Ca2+ sensitization of arterial muscle. *Am J Physiol Cell Physiol*. 285:C1377-1385.

Urbina, P., M. Flores-Diaz, A. Alape-Giron, A. Alonso, and F.M. Goni. 2011. Effects of bilayer composition and physical properties on the phospholipase C and sphingomyelinase activities of Clostridium perfringens alpha-toxin. *Biochim Biophys Acta*. 1808:279-286.

Valnes, K., and P. Brandtzaeg. 1982. Comparison of paired immunofluorescence and paired immunoenzyme staining methods based on primary antisera from the same species. *J Histochem Cytochem*. 30:518-524.

Van Aelst, L., and C. D'Souza-Schorey. 1997. Rho GTPases and signaling networks. *Genes Dev*. 11:2295-2322.

Vater, W., G. Kroneberg, F. Hoffmeister, H. Saller, K. Meng, A. Oberdorf, W. Puls, K. Schlossmann, and K. Stoepel. 1972. [Pharmacology of 4-(2'-nitrophenyl)-2,6-dimethyl-1,4-dihydropyridine-3,5-dicarboxylic acid dimethyl ester (Nifedipine, BAY a 1040)]. *Arzneimittelforschung*. 22:1-14.

Waldenstrom, U., S. Cnattingius, L. Vixner, M. Norman. 2016. Advanced maternal age increases the risk of very preterm brith, irrespective of parity: a population-based register study. *BJOG.* 1111:1471-0528.

Wei, H., L. Fang, J. Song, and S. Chatterjee. 2005. Statin-inhibited endothelial permeability could be associated with its effect on PECAM-1 in endothelial cells. *FEBS Lett*. 579:1272-1278.

Weitz-Schmidt, G., K. Welzenbach, V. Brinkmann, T. Kamata, J. Kallen, C. Bruns, S. Cottens, Y. Takada, and U. Hommel. 2001. Statins selectively inhibit leukocyte function antigen-1 by binding to a novel regulatory integrin site. *Nat Med*. 7:687-692.

White, R.E., A.B. Lee, A.D. Shcherbatko, T.M. Lincoln, A. Schonbrunn, and D.L. Armstrong. 1993. Potassium channel stimulation by natriuretic peptides through cGMP-dependent dephosphorylation. *Nature*. 361:263-266.

Whitley, E., and J. Ball. 2002. Statistics review 4: sample size calculations. *Crit Care*. 6:335-341.

Whittaker, M., E.M. Wilson-Kubalek, J.E. Smith, L. Faust, R.A. Milligan, and H.L. Sweeney. 1995. A 35-A movement of smooth muscle myosin on ADP release. *Nature*. 378:748-751.

Wickman, K.D., and D.E. Clapham. 1995. G-protein regulation of ion channels. *Curr Opin Neurobiol*. 5:278-285.

Williams, E., J. Cooper, W. Stillwell, L. Jenski. 2000. The curvature and cholesterol content of phospholipid bilayers alter the transbilayer distribution of specific molecular species of phosphatidylethanolamine. *Mol Membr Biol.* 12(3): 157-64.

Winterfeld, U., A. Allignol, A. Panchaud, L. Rothuizen, P, Merlob, B. Cuppers-Maarschalkerweerd, T,. Vial, S. Stephens, T. Buclin. Pregnancy outcomes following maternal exposure to statins: a multicentre prospective study. 2013. *BJOG*. 120(4):463-71.

Word, R.A., D.C. Tang, and K.E. Kamm. 1994. Activation properties of myosin light chain kinase during contraction/relaxation cycles of tonic and phasic smooth muscles. *J Biol Chem*. 269:21596-21602.

Wray, S., K. Jones, S. Kupittayanant, Y. Li, A. Matthew, E. Monir-Bishty, K. Noble, S.J. Pierce, S. Quenby, and A.V. Shmygol. 2003. Calcium signaling and uterine contractility. *J Soc Gynecol Investig*. 10:252-264.

Wray, S., and A. Shmygol. 2007. Role of the calcium store in uterine contractility. *Semin Cell Dev Biol*. 18:315-320.

Wynn, RM., J, WP. 2013. Biology of the Uterus (2nd Edition). USA, Springer, Plenum Medical Book Company.

Yada, T., M. Nakata, T. Shiraishi, and M. Kakei. 1999. Inhibition by simvastatin, but not pravastatin, of glucose-induced cytosolic Ca2+ signalling and insulin secretion due to blockade of L-type Ca2+ channels in rat islet beta-cells. *Br J Pharmacol*. 126:1205-1213.

Young, R.C. 2007. Myocytes, myometrium, and uterine contractions. *Ann N Y Acad Sci*. 1101:72-84.

Young, R.C., and L. Herndon-Smith. 1991. Characterization of sodium channels in cultured human uterine smooth muscle cells. *Am J Obstet Gynecol*. 164:175-181.

Young, R.C., and R.O. Hession. 1997. Paracrine and intracellular signaling mechanisms of calcium waves in cultured human uterine myocytes. *Obstet Gynecol*. 90:928-932.

Young, R.C., and P. Zhang. 2001. The mechanism of propagation of intracellular calcium waves in cultured human uterine myocytes. *Am J Obstet Gynecol*. 184:1228-1234.

Yuan, X.J., J. Wang, M. Juhaszova, V.A. Golovina, and L.J. Rubin. 1998. Molecular basis and function of voltage-gated K+ channels in pulmonary arterial smooth muscle cells. *Am J Physiol*. 274:L621-635.

Zhao, F., F. Qiu, X. Zhang, S. Yu, H.S. Kim, H.D. Park, S. Takizawa, and P. Wang. 2012. Preparation of single-walled carbon nanotubes/polyvinylchloride membrane and its antibacterial property. *Water Sci Technol*. 66:2275-2283.

Zhong, X.Z., M.I. Harhun, S.P. Olesen, S. Ohya, J.D. Moffatt, W.C. Cole, and I.A. Greenwood. 2010. Participation of KCNQ (Kv7) potassium channels in myogenic control of cerebral arterial diameter. *J Physiol*. 588:3277-3293.

Zhou, M., Z. Diwu, N. Panchuk-Voloshina, and R.P. Haugland. 1997. A stable nonfluorescent derivative of resorufin for the fluorometric determination of trace hydrogen peroxide: applications in detecting the activity of phagocyte NADPH oxidase and other oxidases. *Anal Biochem*. 253:162-168.

Zhou, M., and N. Panchuk-Voloshina. 1997. A one-step fluorometric method for the continuous measurement of monoamine oxidase activity. *Anal Biochem*. 253:169-174.